DISS. ETH No. 20793

PERSISTENCE OF NUCLEIC ACID ALKYLATION AND SELENOPROTEIN INHIBITION BY MYCOTOXINS

A dissertation submitted to

ETH ZURICH

for the degree of

Doctor of Sciences (Dr. sc. ETH Zurich)

presented by

KATHRYN ELIZABETH PIETSCH

M.S. Medicinal Chemistry, University of Minnesota, Twin Cities

born on 26.01.1984

citizen of the United States of America

accepted on the recommendation of

Prof. Dr. Shana J. Sturla, examiner

Prof. Dr. Karl-Heinz Altmann, co-examiner

Prof. Dr. Muriel Cuendet, co-examiner

2012

Acknowledgements

I would first like to give heartfelt thanks to my advisor, Professor Shana J. Sturla for her support and guidance throughout my graduate studies. A move to Switzerland was something I certainly wasn't anticipating when I joined her group, but am grateful for the opportunity to join her in establishing her lab at ETH Zürich.

I thank Professors Karl-Heinz Altmann (ETH Zürich) and Muriel Cuendet (University of Geneva) for serving as co-examiners on my defense committee. I appreciate their feedback and suggestions regarding findings from my studies over the past three years.

I thank Dr. Paul van Midwoud for his collaboration on my projects. He has readily provided technical expertise and insight along the way.

I thank Dr. Pete Villalta for getting me excited about mass spectrometry. He has been a great mentor in this area and has provided valuable direction in my analytical endeavors.

I thank the "Minnesota" members of the Sturla lab. Dr. Xiaodan "Kathy" Liu oversaw my development as a bioanalytical chemist during my time at the University of Minnesota. Her willingness to always look over my shoulder has guaranteed proper pipetting over the past five years. Dr. Rahul Lad, Hailey Gahlon, Heidi Dahlmann, Dr. Marina Tanasova, and I were the "transplanted crew" from Minnesota, and moving one's personal and professional life overseas is a unique experience. I also thank Amy Doan, a classmate from the University of Minnesota. Amy, Hailey, and I were "three peas in a pod" during our first years of graduate school and had many memorable moments together including multiple all-nighters and annual Halloween shenanigans.

I thank the “Switzerland” members of the Sturla lab. Melanie Erzinger has been my neighbor in lab since I arrived in Zürich and has served as my translator and German teacher in times of need (e.g. weeks before I found out I would be getting married in German). In this regard, I must acknowledge her assistance in preparing my Zusammenfassung for this thesis. I have really enjoyed sharing my lab knowledge with her throughout her time as a Masters and PhD student, and we are now at the point where she is teaching me things. I thank my other “biochem lab” members: Claudia Otto, Dr. Katrin Hecht, Dr. Cédric Bovet, Dr. Mostafa Fekry, Peter Rast, Arman Nilforoushan, and Nathalie Ziegler. I also thank my “synthesis lab” counterparts: Dr. Todor Angelov, Alessia Stornetta, Laura Wyss, Manual Kradolfer, Lea von Moos, and Dr. Ioannis Trantakis.

I thank Teresa Probanowski-Angst for all she does to keep this lab running. She is an amazingly busy person but always has time for you when you visit her office. I also thank Ruth Bürkli for facilitating administrative aspects of everything ranging from matriculation to scheduling my final oral exam in such a speedy manner.

I thank Dr. Britt Peterson and Rachel Lundeen for their participation in beer sessions, and I wonder if we ever would have become such good friends if we hadn’t ended up in Zürich together?

Lastly, I thank my ever-optimistic cheerleader, my husband Philipp. His support and motivation are the reason I’m submitting this thesis today.

Table of Contents

Abbreviations

Chapter 1:

MMC	mitomyin C
CYP450	cytochrome P450
NQO1	NAD(P)H:quinone oxidoreductase 1
GST	glutathione *S*-transferase
AFs	acylfulvenes
HMAF	6-hydroxymethylacylfulvene
AF	acylfulvene
GSH	glutathione
PTGR1	prostaglandin reductase 1
AOR	alkenal/one oxidoreductase
ctDNA	calf thymus DNA

Chapter 2:

Se	selenium
Sec	selenocysteine
TrxR	thioredoxin reductase
Gpx	glutathione peroxidase
DTNB	5,5'-dithiobis(2-nitrobenzoic acid)
AF	acylfulvene
HMAF	hydroxymethylacylfulvene
GR	glutathione reductase
BIAM	biotin-conjugated iodoacetamide
DMEM	Dulbecco's modified Eagle's medium
DMSO	dimethyl sulfoxide

Trx	thioredoxin
BCA	bicinchoninic acid
TBS	Tris-buffered saline
CEES	2-chloroethyl ethyl sulfide
DNCB	1-chloro-2,4-dinitrobenzene
ROS	reactive oxygen species
MTS	3-(4,5-dimethylthiazol-2-yl)-5-(3-carboxymethoxyphenyl)-2-(4-sulfophenyl)-2H-tetrazolium
NMWL	nominal molecular weight limit
PVDF	polyvinylidene fluoride
TFA	trifluoroacetic acid
H_2O_2	hydrogen peroxide
IAA	iodoacetamide

Chapter 3:

NQO1	NAD(P)H:quinone oxidoreductase 1
AF	acylfulvene
PTGR1	prostaglandin reductase 1
PTGR1-480	SW-480 cells stably transfected to overexpress PTGR1
ctDNA	calf thymus DNA
DMSO	dimethylsulfoxide
CNL-MS^3	constant neutral loss scanning with triple stage mass spectrometry
dGuo	deoxyguanosine
ESI	electrospray ionization
CID	collision-induced dissociation
UPLC	ultra performance liquid chromatography
dAdo	deoxyadenosine

SRM	selected reaction monitoring
nano-ESI	nanoelectrospray ionization
iSRM	intelligent SRM
PVDF	polyvinylidene fluoride
MTS	3-(4,5-dimethylthiazol-2-yl)-5-(3-carboxymethoxyphenyl)-2-(4-sulfophenyl)-2*H*-tetrazolium
NTH	neutral thermal hydrolysis
t_R	retention time
TrxR1	thioredoxin reductase 1
APCI	atmospheric pressure chemical ionization
HMAF	6-hydroxymethylacylfulvene

Chapter 4:

AP site	abasic site, apurinic/apyrimidinic site
BER	base excision repair
NER	nucleotide excision repair
TLS	translesion synthesis
ARP	aldehyde reactive probe
NBHA	*O*-4-nitrobenzylhydroxylamine
ctDNA	calf thymus DNA
AF	acylfulvene
5'-dRp-NBHA	5'-deoxyribose monophosphate-NBHA
dAMP	deoxyadenosine monophosphate
dGuo	deoxyguanosine
ESI	electrospray ionization
SRM	selected reaction monitoring
UPLC	ultra performance liquid chromatography

PTGR1-480	SW-480 cells stably transfected to overexpress PTGR1
TC-NER	transcription-coupled NER
XP	xeroderma pigmentosum

Abstract

Alkylating agents are commonly used to treat cancers but suffer from lack of selectivity for target cells over healthy cells. The illudins and acylfulvenes (AFs) are a unique pair of structurally related compounds that display differences in selective toxicity toward cancer cells. AFs are derived from the sesquiterpene illudane natural products, some of which are mycotoxins produced by and isolated from *Omphalotus* basidiomycetes. Both AFs and illudins are alkylating agents that target important biomacromolecules, like DNA and proteins. While the differences in their chemical structures are apparently subtle, the differences in their cytotoxicity profiles are significant. With an overarching goal to better understand chemical and biochemical factors that dictate selectivity of cytotoxicity, illudin S and AFs were studied in terms of their reactivity with redox-regulating proteins and DNA, as a basis for this thesis.

The ability of illudin S and AFs to inhibit the selenocysteine-containing redox-regulating enzyme glutathione peroxidase was determined and contrasted with results concerning the interactions of these molecules with the analogous enzyme thioredoxin reductase. DNA alkylation by illudin S and AFs was studied in the context of whether cellular bioactivating capacity influences the toxicity of these compounds. It has been demonstrated previously that the cytotoxicity of AFs is correlated with levels of prostaglandin reductase 1 (PTGR1), an enzyme involved in the activation of AFs to cytotoxic reactive intermediates. However, the relative influence of PTGR1 on illudin S versus AF cytotoxicity or whether reductions in sensitivity are associated with a concomitant decrease in abasic site formation have not been determined. As part of a strategy to address these questions, depurinating DNA adducts resulting from treating cells with illudin S or AF were quantified in cancer cells engineered to overexpress

PTGR1, and correlated with cytotoxicity. Finally, the cellular by-products of adduct depurination are abasic sites, however, the relative importance of initial adduct formation versus abasic site accumulation in AF cytotoxicity is not understood. Research described in this thesis involves preliminary steps toward the development of a suitable analytical strategy for cell-based studies. These studies would aim to compare abasic site and alkylation adduct accumulation in mammalian cancer cells, potentially as a function of DNA repair capacity. Together, the studies described in this thesis provide further understanding of biochemical factors contributing to the selective toxicity of AFs, including redox-mediating cellular enzymes and the integrity of DNA.

Zusammenfassung

Alkylierende Stoffe werden häufig zur Behandlung von Krebs eingesetzt, obwohl ihre Selektivität bezüglich Krebszellen gegenüber gesunden Zellen gering ist. Illudine und Acylfulvene (AFs) sind ein einzigartiges Paar von strukturell verwandten Verbindungen mit deutlichen Unterschieden in selektiver Toxizität bezüglich Krebszellen. Illudine sind natürliche Sesquiterpene, die als Mykotoxine von *Omphalotus* Basidiomyceten produziert werden. Aus den isolierten Illudinen können dann AFs gewonnen werden. Sowohl AFs als auch Illudine sind alkylierende Stoffe, die wichtige Biomakromoleküle, wie DNA oder Proteine, angreifen. Während die strukturellen Unterschiede vordergründig gering erscheinen, sind die Unterschiede in ihren Zytotoxizität-Profilen signifikant. Mit dem übergreifenden Ziel, die chemischen und biochemischen Faktoren zu verstehen, welche die Selektivität der Zytotoxizität bestimmen, untersuchten wir Illudin S und AFs bezüglich ihrer Reaktivität mit Redox-regulierenden Proteinen und DNA.

Wir bestimmten die Fähigkeit von Illudin S und AFs die Redox-regulierenden Enzyme Glutathion Peroxidase und Thioredoxin Reduktase, welche beide eine Selenocystein enthalten, zu hemmen und verglichen die entsprechenden Resultate miteinander. Zudem wurde untersucht, ob die zelluläre Bioaktivierung von Illudin S und AFs einen Einfluss hat auf die Toxizität dieser Substanzen hat und ob dies die Kapazität DNA zu alkylieren verändert. Bereits in früheren Studien wurde gezeigt, dass die Zytotoxizität von AFs mit dem Gehalt der Prostaglandin Reduktase 1 (PTGR1) korreliert, einem Enzym, das AFs zu zytotoxisch reaktiven Zwischenprodukten aktiviert. Der relative Einfluss von PTGR 1 auf die Zytotoxizität von Illudin S verglichen mit AFs, oder ob die Sensitivitätsreduktion mit einer gleichzeitigen Abnahme der Bildung von abasic

sites in der DNA zusammenhängt wurde bis jetzt noch nicht untersucht. Um diese Fragen zu beantworten, wurden depurinierte DNA Addukte, welche auf Grund einer Behandlung mit Illudin S oder AF gebildet wurden, in Zellen quantifiziert, die genetisch so verändert wurden, dass sie PTGR1 überexprimieren. Die gemessenen Addukte wurden dann mit der entsprechenden Zytotoxizität korreliert. Zelluläre Nebenprodukte der Addukt-Depurinierung sind abasic sites, aber der relative Bedeutung der initialen Bildung von Addukten und der Akkumulierung von abasic sites in der DNA für die Zytotoxizität von AF konnte bis jetzt nicht bestimmt werden. Die vorliegende Forschungsarbeit beschreibt erste Schritte für die Entwicklung einer Analysestrategie, die zukünftige zellbasierte Studien ermöglicht, welche den obengenannten relativen Einfluss von abasic sites in der DNA und der Bildung von Addukten auf die Zytotoxizität untersuchen und zusätzlich einen möglichen Zusammenhang mit der Kapazität DNA zu reparieren herstellen zu können. Zusammenfassend liefert die vorliegende Doktorarbeit neue Erkenntnisse zu biochemischen Faktoren, wie Redox-regulierenden zellulären Enzymen und die Integrität der DNA, welche zu der selektiven Toxizität von AFs beitragen.

Preface

Parts of this thesis have been adapted from articles co-written by the author. The following articles were reproduced in part with permission from the American Chemical Society:

"Chemical and enzymatic reductive activation of acylfulvene to isomeric cytotoxic reactive intermediates." Pietsch, K. E.; Neels, J. F.; Yu, X.; Gong, J.; Sturla, S. J. *Chem. Res. Toxicol.* **2011**, *24*, 2044–2054.

"Susceptibility of the antioxidant selenoenzymes thioredoxin reductase and glutathione peroxidase to alkylation-mediated inhibition by anticancer acylfulvenes." Liu, X.; Pietsch, K. E.; Sturla, S. J. *Chem. Res. Toxicol.* **2011**, *24*, 726–736.

"Quantification of acylfulvene- and illudin S-DNA adducts in cells with variable bioactivation capacities." Pietsch, K. E.; Van Midwoud, P. M.; Villalta, P. W.; Sturla, S. J. *Chem. Res. Toxicol.* **2013**, *26*, 146–155.

Chapter One: Introduction[1]

[1] Portions reprinted with permission from Pietsch, K. E., Neels, J. F., Yu, X., Gong, J., Sturla, S. J. (2011) Chemical and enzymatic reductive activation of acylfulvene to isomeric cytotoxic reactive intermediates. *Chem. Res. Toxicol. 24*, 2044–2054. Copyright 2011 American Chemical Society.

1. Cancer and its treatment with alkylating agents

Cancer is a disease characterized by uncontrolled cell growth that starts from a single transformed cell. It can affect any part of the body and can spread from its initial site of development.[1,2] It is a devastating disease on a personal and global level, responsible for 13% of all deaths (7.6 million) in 2008 and projected to result in more than 13.1 million deaths in 2030.[2] While cancer prevention and early detection are priorities for decreasing the number of cancer victims, developing new and improving existing cancer treatments is still pertinent to managing and curing current and future cases.

Cancer treatment generally includes surgery, radiation therapy, and/or chemotherapy. Simply put, chemotherapy uses chemicals to kill cancer cells by targeting important cellular components, like DNA and protein, to trigger apoptosis.[1] The first and one of the most commonly used chemotherapy strategies involves alkylating agents, exemplified by mechlorethamine, the first FDA-approved alkylating agent (Scheme 1).

Scheme 1. Active alkylating species of mechlorethamine.

Mechlorethamine is a nitrogen mustard that has been used to treat leukemias, lymphoma, and lung cancers since 1949.[3] In general the mechanism of action of alkylating agents is to form covalent adducts with DNA and interfere with critical cellular processes like DNA repair and replication, ultimately leading to cell cycle arrest and apoptosis. While drugs like mechlorethamine are effective, they often lack selectivity, also targeting DNA in normal healthy cells. Understanding how such drugs can be engineered to target more

specifically malignant target cells is one of the most important goals for improving cancer therapy. Accomplishing this goal requires understanding combinations of chemical and biological factors that dictate cytotoxin selectivity.

2. Enzyme-mediated xenobiotic transformation

Amongst the potential strategies for achieving selectivity in chemotherapy is that drugs require bioactivation within a cancer cell.[4] Drug bioactivation is catalyzed by cellular enzymes and involves the transformation of less active pro-drugs to biologically reactive intermediates. These reactive intermediates are capable of interacting with, and in the case of alkylating agents, covalently modifying biological targets such as proteins and DNA.[5] In the case of a chemotherapy pro-drug, this can lead to a desirable outcome like cancer cell death. Two examples of chemotherapy pro-drugs that are activated by phase I xenobiotic transformations are cyclophosphamide and mitomycin C (MMC). Cyclophosphamide, indicated in leukemias, lymphoma, breast, and ovarian cancers, is oxidatively bioactivated by cytochrome P450s (CYP450) to unveil a phosphoramide mustard after α-hydroxylation (Scheme 2).[3] MMC, on the other hand, undergoes a two-electron reduction mediated by NAD(P)H:quinone oxidoreductase 1 (NQO1), and is used to treat a variety of cancers, including breast, lung, prostate, gastric and pancreatic

Scheme 2. Oxidative bioactivation of cyclophosphamide by CYP450.

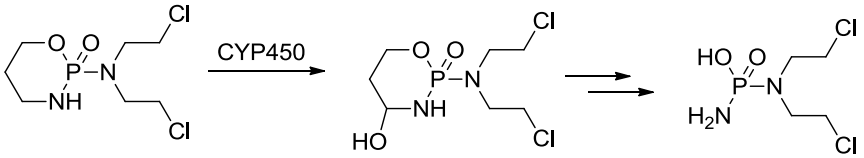

Cyclophosphamide

tumors.[3,6] Hypoxic environments in tumors, along with the fact that NQO1 is overexpressed in some cancers, like colon and non-small-cell lung cancers, provide

further degrees of selectivity for MMC to target cancer cells.[6] Shown in Scheme 3, activated MMC is capable of alkylating DNA twice to form interstrand crosslinks.

Scheme 3. Reductive bioactivation of MMC by NQO1 and resulting covalent DNA adduct.

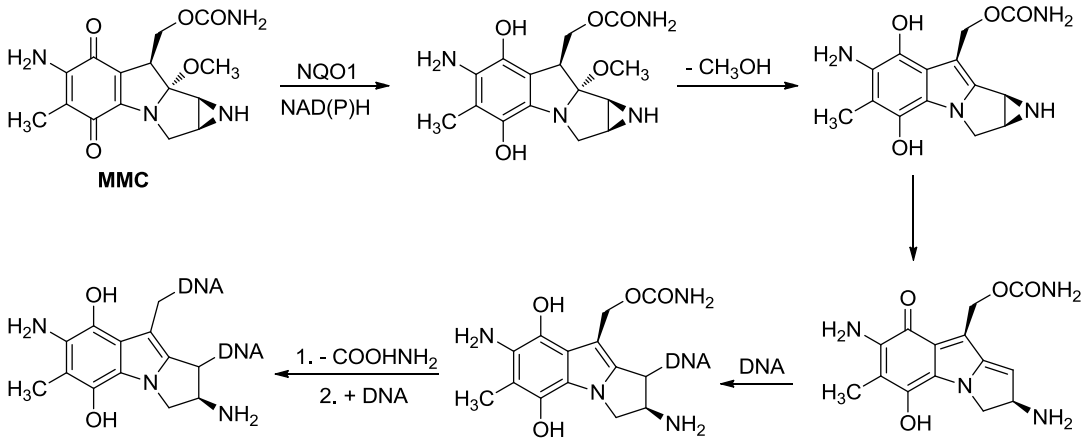

Enzymes that catalyze phase II transformations are also implicated in bioactivation, as is the case with TLK-286, which has progressed through phase 3 clinical trials for platinum-resistant ovarian cancer.[7] TLK-286 is a conjugate pro-drug that releases a tetra-functional nitrogen mustard upon cleavage by a glutathione *S*-transferase (GST) isozyme, GST-π (Scheme 4).[8] GST-π is known to be overexpressed in tumors and in this case, TLK-286 was designed to target this abundant isozyme for enhanced selectivity.[8]

Scheme 4. GST-mediated bioactivation of TLK-286 to a nitrogen mustard.

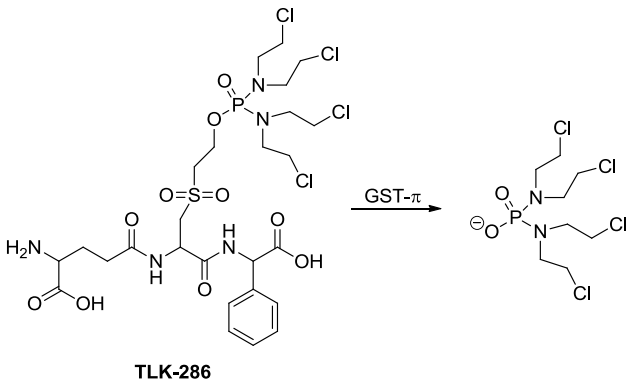

Other potential outcomes of metabolism could include inactivation, i.e. detoxification, which is most often mediated by phase II enzymes. Since phase II processes tend to be more protective compared to phase I transformations, it is not surprising that conjugating enzymes are implicated in undesired chemotherapy inactivation. Looking at GST again as an example, there is convincing data that GST inactivates nitrogen mustards including the reactive phosphoramide mustard of cyclophosphamide. While detoxification is a liability in the context of a cancer drug in a cancer cell, from the perspective of toxic chemicals in the environment and/or diet, inactivation is a favored outcome of metabolism. Possibilities discussed here demonstrate why bioactivation is considered a double-edged sword; enzymes can mediate chemical bioactivation to, for example, DNA-reactive species that may induce carcinogenic mutations.[9]

3. Illudins and AFs

A unique situation where cytotoxic selectivity has a potential relationship with reductive bioactivation involves acylfulvenes (AFs), which are semisynthetic derivatives of the illudin natural products. Illudins M and S (Chart 1) are toxic fungal metabolites with antibacterial and anticancer properties, produced by the *Omphalotus* species of basidiomycetes.[10–13] Unfortunately, the illudins exhibit low therapeutic indices, meaning that the therapeutic dose is very close to the toxic dose of the drug[14,15] and they are

Chart 1. Natural product illudins and semi-synthetic analogues AF and HMAF.

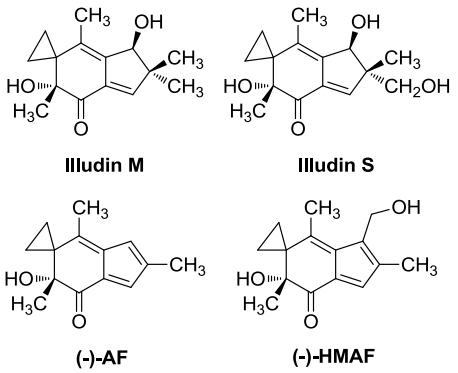

therefore, not clinically useful as cancer chemotherapeutics. AFs [16–19] (Chart 1) were subsequently developed to overcome toxicity issues and were indeed found to have superior therapeutic indices.[18, 20–22] Clinical trials involving 6-hydroxymethylacylfulvene (HMAF) started in 2000 and progressed through phase 3, but are no longer active.[19] Amongst various contributing factors, a question that remained unaddressed at the time was origin of selectivity. A better understanding of this property could potentially resolve unwanted toxicity aspects in normal cells.

The fact that illudin S is non-selective and AFs are more selective makes these a unique set of chemical probes to understand the chemical and biochemical basis of

selective toxicity of small molecules toward tumor cells. Both illudin S and acylfulvene (AF) are alkylating agents with unique structures, and the main components required for potent activity include the α,β-unsaturated ketone and strained cyclopropyl ring. They exhibit slight differences in chemical structure, mainly on the five membered ring, and a goal is to understand how these chemical differences account for their differential toxicity profiles.

Illudin S is capable of reacting directly with important thiol-containing nucleophiles like glutathione (GSH) directly via Michael addition at its α,β-unsaturated ketone (Scheme 5).[23,24] This reaction is considered detoxifying, as elevated levels of GSH

Scheme 5. Proposed pathway for Michael-addition of GSH to illudin S.

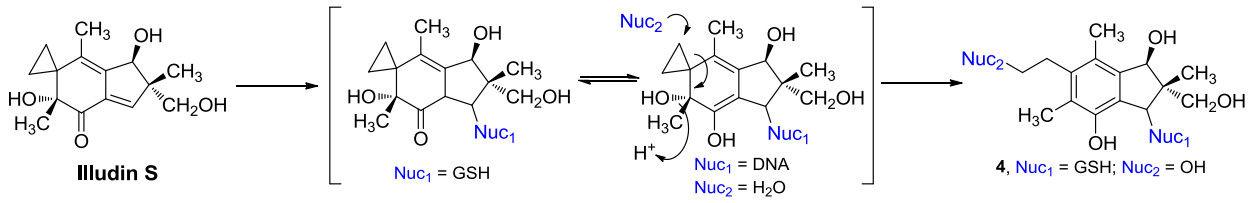

reduced illudin S toxicity in cells.[23] AFs, on the other hand, are less likely to react directly with cellular nucleophiles at the α,β-unsaturated ketone. Instead, enzymatic activation at this position yields a reactive intermediate that can alkylate cellular macromolecules. On the basis of the chemical structure of the major cytosolic metabolite **2** (Scheme 6), a pathway for AF bioactivation was put forth by McMorris and co-workers over 20 years ago. Much like the reaction of illudin S with GSH (Scheme 5), it involved conjugate addition to the α,β-unsaturated ketone, keto-enol tautomerism, and nucleophilic opening of the cyclopropyl ring. It was hypothesized that hydride delivery from NADPH to the α,β-unsaturated ketone gives rise to an electrophilic intermediate capable of alkylating

cellular nucleophiles, thus yielding metabolites or adducts (Scheme 6).[16] Previous studies demonstrated that this bioactivation is mediated by an enzyme or enzymes primarily located in the cytosol of drug-sensitive cells and requires NADPH as a cofactor.[21,25,26]

Scheme 6. Proposed pathways for the formation of AF DNA adducts via direct alkylation and bioreductive alkylation.

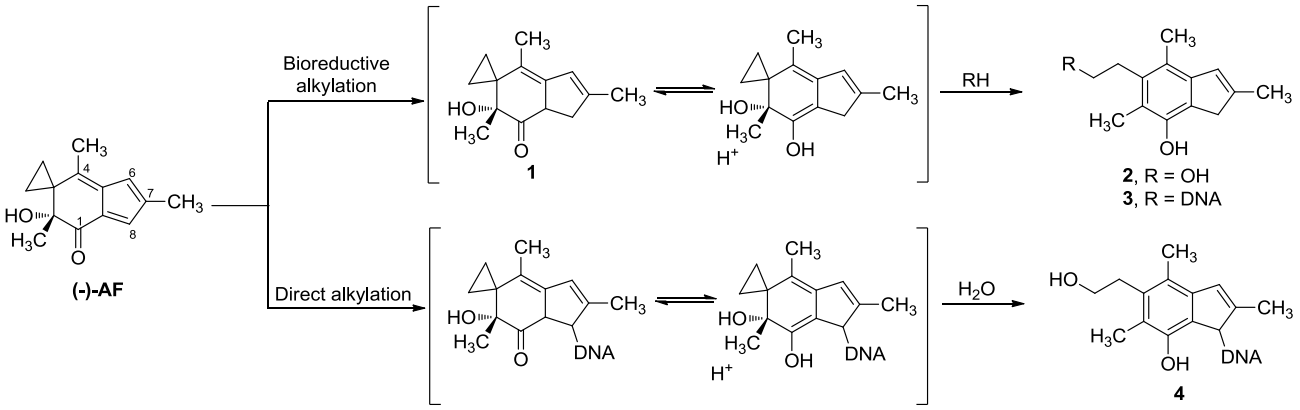

4. PTGR1 in illudin and AF bioactivation

AFs and illudins are substrates for the inducible cytosolic NADPH-dependent enzyme prostaglandin reductase 1 (PTGR1).[27–30] PTGR1, also known as alkenal/one oxidoreductase (AOR), a cytosolic medium chain reductase is invoked in the detoxification of electrophiles, such as lipid peroxidation products, and prevents biological adduct formation.[29] The cytotoxicity of AFs can be attributed to reductive biotransformation-coupled alkylation of critical biomolecules, including DNA,[20,31–34] and a positive correlation exists between cellular PTGR1 levels, cell sensitivities, and DNA adduct levels,[27,28,35,36] such that cells with high levels of PTGR1 are more capable of activating AFs to a reactive species that alkylates DNA and induces toxicity. The bioactivation of illudin S, however, is not implicated in differentiating sensitive from resistant cells, and AFs offer, therefore, unique chemical tools for probing the role of bioactivation in cytotoxic selectivity.[27,28]

The ability to isolate the intermediate that reacts with biomolecules, or a chemical surrogate, would enable mechanistic studies of chemical toxicity. The reduced species presumably is extremely unstable and reactive and has, therefore, not been isolated. Considering the important contributions of PTGR1-mediated activation and the reactivity of the reduced form of AF in dictating the activity and selectivity of the drug, it was of interest to characterize the chemical and biochemical aspects of the mechanism of AF reduction and nature of its activated intermediate.

A previous study demonstrated that the reduction of illudin M by PTGR1 occurred via addition to α,β-unsaturated ketone at the 8 position of the compound.[30] The regiochemistry of AF reduction catalyzed by PTGR1 was evaluated in a similar manner by carrying out enzyme-mediated reduction reactions with isolated enzyme and deuterium-labeled cofactor NADPD (Scheme 7).[37] The resulting product **2** had *m/z* 220, consistent with a 1,4- or 1,6-reduction. The 1,4-reduction mechanism has precedent in previous data[29] indicating that PTGR1 catalyzes the reduction of α,β-unsaturated ketones or aldehydes via hydride addition to the β-carbon. However, on the basis of data available in this and previous studies, a potential 1,6-pathway cannot be strictly excluded.[37]

Scheme 7. Strategy for probing the AF bioactivation mechanism using HPLC-ESI-MS.

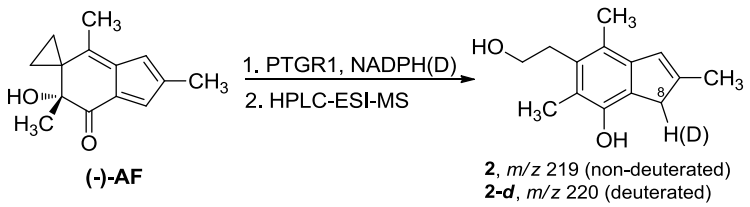

In an effort to obtain an isolable reductively activated form of AF, and to further probe the activated AF structure and reactivity, we found that the $NaBH_4$- mediated reduction of AF in pyridine[38] yielded a stable product, **5**, assigned on the basis of diagnostic ^1H NMR and MS signals (Scheme 8).[37] Collectively, these data suggest that **5** results from chemically-mediated hydride addition to C4, the exocyclic fulvene double bond of AF. The regiochemistry of borohydride-mediated AF reduction was confirmed by carrying out the reaction with $NaBD_4$. The resulting product was characterized by ^1H and ^{13}C NMR, and these data are consistent with deuteration at C4, and more generally support the assertion that the hydride (deuteride) is delivered to C4.[37]

Scheme 8. Chemical reduction of AF with $NaBH_4$.

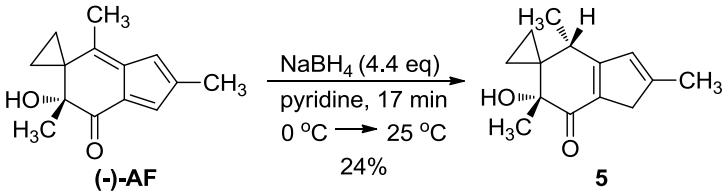

The enzymatic (PTGR1-mediated) and chemical ($NaBH_4$-mediated) activation processes give rise to different isomeric intermediates. PTGR1 catalyzes hydride addition to C8 yielding **1** in the case of the 1,4-pathway, while $NaBH_4$ delivers the hydride to C4 yielding **5**.[37] Compound **5** is an isomer of the proposed bioactivation product. Further, the regiochemistry of the $NaBH_4$-mediated reduction is different than previous reactions with simple α,β-unsaturated ketone substrates, which undergo $NaBH_4$-mediated 1,4-addition in pyridine.[38] Literature examples demonstrate that strong hydride reducing agents, like alkyllithium reagents[39] and lithium triethylborohydride[40] are generally required to reduce fulvenes, but here we demonstrate fulvene reduction with the mild reducing agent $NaBH_4$.[37] The regioselectivity of the chemical reduction can be rationalized on the basis of a dipolar resonance structure with an aromatic

cyclopentadiene ring, suggested earlier by McMorris et al[16,18] (Scheme 9) where positive charge is localized at C4 and negative charge is delocalized in the cyclopentadiene ring. In addition, it is possible that the adjacent carbonyl may tune the reduction potential of the fulvene, suggesting a possible means for modifying the reactivity of the molecule, thus enabling the reduction with $NaBH_4$.[37]

Since reduced AF analogue **5** is an isomer of the proposed bioactivation

Scheme 9. Reduction of AF to yield **5** and instructive dipolar resonance precursor structure.

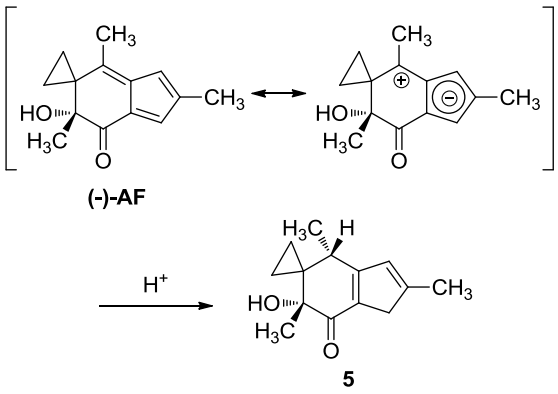

intermediate, it was anticipated that this chemically activated species would be capable of being converted to metabolite **2**. A consistent chemical mechanism therefore involves tautomerization to **1-enol** followed by hydrolytic cyclopropane cleavage (Scheme 10). We demonstrated that this reaction takes place in the presence of acid, and this reactivity profile suggests that **5** is a competent chemical model for enzymatically reduced AF. Under the same conditions **6** is also converted to **2**, which further supports the putative reaction mechanism illustrated in Scheme 10.[37]

Scheme 10. Proposed mechanism for the conversion of **5** to **2** in aqueous acid.

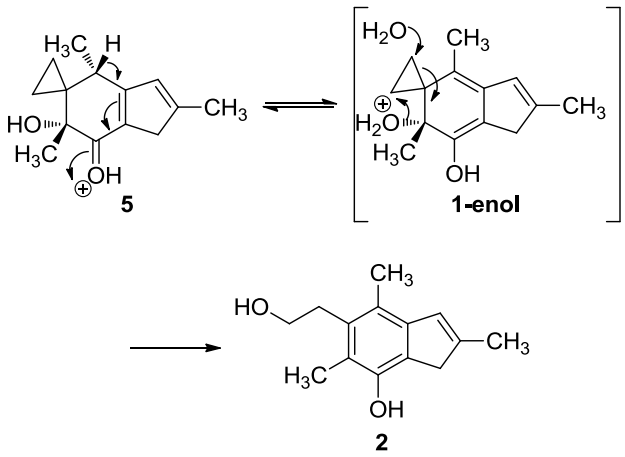

In a cell-free system, **5** alkylates nucleic acids less efficiently than bioactivated AF. For reactions with monomeric nucleosides, 7-AF-Gua and 3-AF-Ade adducts arising from **5** were on average 400- and 50-fold less abundant, respectively, than adducts resulting from covalent modification by bioactivated AF. Adducts formed in calf thymus DNA (ctDNA) from **5** were less abundant than those resulting from bioactivated AF, but were similar in scale (both adducts were on average 300-fold less abundant compared to adducts resulting from bioactivated AF).[37] Compound **5** is stable despite being chemically activated, as demonstrated by testing its stability in cell media. While this observation fails to explain the difference in adduct abundance resulting from treatments with **5** vs. bioactivated AF, such reduced reactivity of chemically vs. biologically activated intermediates has been observed previously. Examples include leinamycin[41] and a small molecule leinamycin analogue.[42] Leinamycin primarily relies on thiol-dependent activation in order to alkylate DNA, however it was discovered that thiol-independent activation results in the same DNA damage, but at a slower rate and lower abundance,[41]

which is also the case for its analogue.[42] The observation that these two activation pathways yield the same products suggests that they share a common intermediate. Thus, by analogy, the conversion of AF and **5** under acidic conditions to metabolite **2** also suggests a common intermediate such that the compound is an effective model on a pharmacodynamics basis, but not a pharmacokinetic basis. On the basis of MS data, reactions of **5** with ctDNA appeared to proceed with fewer additional/unknown products than those with individual nucleosides, especially when comparing the chromatograms corresponding to 3-AF-Ade adduct fragments.[37] AF is planar, similar to nucleobases, and it is possible that AF and **5** are capable of non-covalently associating with DNA, possibly intercalating within the duplex, prior to alkylation. Analogous non-covalent pre-associations have been suggested for a number of alkylating agents, such as aflatoxin-B_1,[43] CC-1065,[44] and benzo(a)pyrene's metabolically activated *anti*-BP-diol epoxide.[45–47] It is also interesting to note that **5** has an extra stereocenter relative to bioactivated AF. Knowing that the (+)-enantiomers of AFs are less potent than their (-)-counterparts,[28] it is interesting to consider how the additional stereocenter in **5** may influence its reactivity with chiral biomolecules, and ultimately its activity in cells.

Transiently transfected cells are a convenient and generally informative model, however there is typically wide variability in enzyme overexpression levels and cells stop overexpressing the enzyme— PTGR1 in this case—over time. Consequently, the data obtained with this model should be interpreted with these caveats in mind and only relative comparisons within a given experiment seem informative. The data obtained here suggests that **5** is toxic to cells with little dependence on bioactivation capacity.[37] Yet, there is a small but statistically significant difference between the cells with high and low levels of PTGR1 expression. However, compared to the 20- to 100-fold-differences of

drug potencies for AF or HMAF that have been observed in the same model in the current and previous studies,[27,28] the approximate 3-fold difference for compound **5** is relatively minor and cannot be interpreted as contributing to toxicity to a similar extent as for AF or HMAF. Further studies in stable cell lines may suggest possible factors that contribute to susceptibility differences toward **5**, such as transport or metabolism.

5. Overview of the thesis work

The work presented in this thesis contributes to the understanding of the role of bioreductive activation in AF and illudin S and how their alkylation profiles influence cytotoxic outcomes. In **Chapter 2**, inhibition of important redox-regulating enzymes by AFs and illudin S are studied. Specifically, the reactivity of selenocysteine active sites in thioredoxin reductase and glutathione peroxidase are investigated. AFs and illudin S are found to inhibit thioredoxin reductase activity and alkylate active site residues, while glutathione peroxidase is not affected. The work described in **Chapter 3** determines the influence of PTGR1 levels on AF- and illudin S-DNA adduct formation and cytotoxicity in cells engineered to stably overexpress PTGR1. A relationship between PTGR1 levels and AF cytotoxicity and DNA adduct quantities is established; this relationship does not hold true in the case of illudin S. **Chapter 4** contains preliminary data concerning the application of a quantitative method for measuring abasic sites in drug-treated cells. A proposal for applying this method to AF- and illudin S-treated cells to examine abasic site abundance and persistence resulting from depurinated DNA adducts is presented. Overall, this work provides further understanding of AFs selective toxicity in terms of redox proteins alkylation and DNA damage.

References

1. Pecorino, L., *Molecular Biology of Cancer*. Oxford University Press: New York, 2005.
2. Cancer. http://www.who.int/mediacentre/factsheets/fs297/en/index.html (accessed October 3, 2012).
3. Callery, P., and Gannett, P., Cancer and Cancer Chemotherapy. In *Foye's Principles of Medicinal Chemistry*, fifth ed.; Troy, D., Ed. Lippincott Williams & Wilkins: Philadelphia, 2002; pp 924-951.
4. Hurley, L. H. (2002) DNA and its associated processes as targets for cancer therapy. *Nat. Rev. Cancer 2,* 188-200.
5. Moore, H. W. (1977) Bioactivation as a model for drug design bioreductive alkylation. *Science 197,* 527-532.
6. Alcaín, F. J., and Villalba, J. M. (2007) NQO1-directed antitumour quinones. *Expert Opin. Ther. Patents 17,* 649-665.
7. Vergote, I., Finkler, N., del Campo, J., Lohr, A., Hunter, J., Matei, D., Kavanagh, J., Vermorken, J. B., Meng, L., Jones, M., Brown, G., and Kaye, S. (2009) Phase 3 randomised study of canfosfamide (Telcyta®, TLK286) versus pegylated liposomal doxorubicin or topotecan as third-line therapy in patients with platinum-refractory or -resistant ovarian cancer. *Eur. J. Cancer 45,* 2324-2332.
8. Tew, K. D. (2005) TLK-286: a novel glutathione S-transferase-activated prodrug. *Expert Opin. Investig. Drugs 14,* 1047-1054.
9. Klaassen, C. D., *Casarett and Doull's Toxicology*. seventh ed.; The McGraw-Hill Companies: New York, 2008.
10. Anchel, M., Hervey, A., and Robbins, W. J. (1950) Antibiotic substances from basidiomycetes. VII. Clitocybe illudens. *Proc. Natl. Acad. Sci. U.S.A. 36,* 300-305.
11. McMorris, T. C., and Anchel, M. (1963) The structures of the basidiomycete metabolites illudin S and illudin M. *J. Am. Chem. Soc. 85,* 831-832.
12. McMorris, T. C., and Anchel, M. (1965) Fungal metabolites: the structures of the novel sesquiterpenoids illudin-S and -M. *J. Am. Chem. Soc. 87,* 1594-1600.
13. Schobert, R., Knauer, S., Seibt, S., and Biersack, B. (2011) Anticancer active illudins: recent developments of a potent alkylating compound class. *Curr. Med. Chem. 18,* 790-807.
14. Kelner, M. J., McMorris, T. C., and Taetle, R. (1990) Preclinical evaluation of illudins as anticancer agents: basis for selective cytotoxicity. *J. Natl. Cancer Inst. 82,* 1562-1565.
15. Kelner, M. J., McMorris, T. C., Beck, W. T., Zamora, J. M., and Taetle, R. (1987) Preclinical evaluation of illudins as anticancer agents. *Cancer Res. 47,* 3186-3189.
16. McMorris, T. C., Kelner, M. J., Wang, W., Diaz, M. A., Estes, L. A., and Taetle, R. (1996) Acylfulvenes, a new class of potent antitumor agents. *Experientia 52,* 75-80.
17. McMorris, T. C., Yu, J., Hu, Y., Estes, L. A., and Kelner, M. J. (1997) Design and synthesis of antitumor acylfulvenes. *J. Org. Chem. 62,* 3015-3018.
18. McMorris, T. C. (1999) Discovery and development of sesquiterpenoid derived hydroxymethylacylfulvene: a new anticancer drug. *Bioorg. Med. Chem. 7,* 881-886.

19. Tanasova, M., and Sturla, S. J. (2012) Chemistry and biology of acylfulvenes: sesquiterpene-derived antitumor agents. *Chem. Rev. 112,* 3578-3610.
20. Woynarowska, B. A., Woynarowski, J. M., Herzig, M. C., Roberts, K., Higdon, A. L., and MacDonald, J. R. (2000) Differential cytotoxicity and induction of apoptosis in tumor and normal cells by hydroxymethylacylfulvene (HMAF). *Biochem. Pharmacol. 59,* 1217-1226.
21. McMorris, T. C., Kelner, M. J., Wang, W., Yu, J., Estes, L. A., and Taetle, R. (1996) (Hydroxymethyl)acylfulvene: an illudin derivative with superior antitumor properties. *J. Nat. Prod. 59,* 896-899.
22. MacDonald, J. R., Muscoplat, C. C., Dexter, D. L., Mangold, G. L., Chen, S. F., Kelner, M. J., McMorris, T. C., and Von Hoff, D. D. (1997) Preclinical antitumor activity of 6-hydroxymethylacylfulvene, a semisynthetic derivative of the mushroom toxin illudin S. *Cancer Res. 57,* 279-283.
23. McMorris, T. C., Kelner, M. J., Wang, W., Moon, S., and Taetle, R. (1990) On the mechanism of toxicity of illudins: the role of glutathione. *Chem. Res. Toxicol. 3,* 574-579.
24. Tanaka, K., Inoue, T., Tezuka, Y., and Kikuchi, T. (1996) Michael-type addition of illudin S, a toxic substance from Lampteromyces japonicus, with cysteine and cysteine-containing peptides in vitro. *Chem. Pharm. Bull. (Tokyo) 44,* 273-279.
25. McMorris, T. C., Elayadi, A. N., Yu, J., Hu, Y., and Kelner, M. J. (1999) Metabolism of antitumor hydroxymethylacylfulvene by rat liver cytosol. *Drug Metab. Dispos. 27,* 983-985.
26. McMorris, T. C., Elayadi, A. N., Yu, J., and Kelner, M. J. (1999) Metabolism of antitumor acylfulvene by rat liver cytosol. *Biochem. Pharmacol. 57,* 83-88.
27. Dick, R. A., Yu, X., and Kensler, T. W. (2004) NADPH alkenal/one oxidoreductase activity determines sensitivity of cancer cells to the chemotherapeutic alkylating agent irofulven. *Clin. Cancer Res. 10,* 1492-1499.
28. Gong, J., Neels, J. F., Yu, X., Kensler, T. W., Peterson, L. A., and Sturla, S. J. (2006) Investigating the role of stereochemistry in the activity of anticancer acylfulvenes: synthesis, reductase-mediated bioactivation, and cellular toxicity. *J. Med. Chem. 49,* 2593-2599.
29. Dick, R. A., Kwak, M. K., Sutter, T. R., and Kensler, T. W. (2001) Antioxidative function and substrate specificity of NAD(P)H-dependent alkenal/one oxidoreductase. A new role for leukotriene B4 12-hydroxydehydrogenase/15-oxoprostaglandin 13-reductase. *J. Biol. Chem. 276,* 40803-40810.
30. Dick, R. A., and Kensler, T. W. (2004) The catalytic and kinetic mechanisms of NADPH-dependent alkenal/one oxidoreductase. *J. Biol. Chem. 279,* 17269-17277.
31. Kelner, M. J., McMorris, T. C., Montoya, M. A., Estes, L., Uglik, S. F., Rutherford, M., Samson, K. M., Bagnell, R. D., and Taetle, R. (1998) Characterization of acylfulvene histiospecific toxicity in human tumor cell lines. *Cancer Chemother. Pharmacol. 41,* 237-242.
32. Kelner, M. J., McMorris, T. C., Montoya, M. A., Estes, L., Uglik, S. F., Rutherford, M., Samson, K. M., Bagnell, R. D., and Taetle, R. (1999) Characterization of MGI 114 (HMAF) histiospecific toxicity in human tumor cell lines. *Cancer Chemother. Pharmacol. 44,* 235-240.
33. Herzig, M. C. S., Arnett, B., MacDonald, J. R., and Woynarowski, J. M. (1999) Drug uptake and cellular targets of hydroxymethylacylfulvene (HMAF). *Biochem. Pharmacol. 58,* 217-225.

34. Woynarowski, J. M., Napier, C., Koester, S. K., Chen, S.-F., Troyer, D., Chapman, W., and MacDonald, J. R. (1997) Effects on DNA integrity and apoptosis induction by a novel antitumor sesquiterpene drug, 6-hydroxymethylacylfulvene (HMAF, MGI 114). *Biochem. Pharmacol.54,* 1181-1193.
35. Neels, J. F., Gong, J., Yu, X., and Sturla, S. J. (2007) Quantitative correlation of drug bioactivation and deoxyadenosine alkylation by acylfulvene. *Chem. Res. Toxicol. 20,* 1513-1519.
36. Gong, J., Vaidyanathan, V. G., Yu, X., Kensler, T. W., Peterson, L. A., and Sturla, S. J. (2007) Depurinating acylfulvene-DNA adducts: characterizing cellular chemical reactions of a selective antitumor agent. *J. Am. Chem. Soc. 129,* 2101-2111.
37. Pietsch, K. E., Neels, J. F., Yu, X., Gong, J., and Sturla, S. J. (2011) Chemical and Enzymatic Reductive Activation of Acylfulvene to Isomeric Cytotoxic Reactive Intermediates. *Chem. Res. Toxicol.24,* 2044-2054.
38. Jackson, W. R., and Zurqiyah, A. (1965) The occurrence of 1,2- or 1,4-addition in the reduction of some α,β-unsaturated ketones with metal hydrides. *J. Chem. Soc.* 5280-5287.
39. Erker, G., Nolte, R., Aul, R., Wilker, S., Krueger, C., and Noe, R. (1991) Cp-substituent additivity effects controlling the stereochemistry of the propene polymerization reaction at conformationally unrestricted (Cp-CHR1R2)2ZrCl2/methylalumoxane catalysts. *J.Am. Chem. Soc. 113,* 7594-7602.
40. Sweeney, N. J., Mendoza, O., Müller-Bunz, H., Pampillón, C., Rehmann, F.-J. K., Strohfeldt, K., and Tacke, M. (2005) Novel benzyl substituted titanocene anti-cancer drugs. *J. Organomet. Chem. 690,* 4537-4544.
41. Breydo, L., Zang, H., Mitra, K., and Gates, K. S. (2001) Thiol-independent DNA alkylation by leinamycin. *J. Am. Chem. Soc. 123,* 2060-2061.
42. Chatterji, T., Kizil, M., Keerthi, K., Chowdhury, G., Pospísil, T., and Gates, K. S. (2003) Small molecules that mimic the thiol-triggered alkylating properties seen in the natural product leinamycin. *J. Am. Chem. Soc. 125,* 4996-4997.
43. Gopalakrishnan, S., Byrd, S., Stone, M. P., and Harris, T. M. (1989) Carcinogen-nucleic acid interactions: equilibrium binding studies of aflatoxin B1 with the oligodeoxynucleotide d(ATGCAT)2 and with plasmid pBR322 support intercalative association with the B-DNA helix. *Biochemistry 28,* 726-734.
44. Boger, D. L., Invergo, B. J., Coleman, R. S., Zarrinmayeh, H., Kitos, P. A., Thompson, S. C., Leong, T., and McLaughlin, L. W. (1990) A demonstration of the intrinsic importance of stabilizing hydrophobic binding and non-convalent van der waals contacts dominant in the non-covalent CC-1065/B-DNA binding. *Chem.-Biol. Interact. 73,* 29-52.
45. Geacintov, N. E., Yoshida, H., Ibanez, V., and Harvey, R. G. (1981) Non-covalent intercalative binding of 7,8-dihydroxy-9,10-epoxybenzo(a)pyrene to DNA. *Biochem. Biophys. Res. Commun. 100,* 1569-1577.
46. Boger, D. L., and Garbaccio, R. M. (1999) Shape-Dependent Catalysis: Insights into the Source of Catalysis for the CC-1065 and Duocarmycin DNA Alkylation Reaction. *Acc. Chem. Res. 32,* 1043-1052.
47. Guza, R., Kotandeniya, D., Murphy, K., Dissanayake, T., Lin, C., Giambasu, G. M., Lad, R. R., Wojciechowski, F., Amin, S., Sturla, S. J., Hudson, R. H. E., York, D. M., Jankowiak, R., Jones, R., and Tretyakova, N. Y. (2011) Influence of C-5 substituted cytosine and related nucleoside analogs on the formation of

benzo[a]pyrene diol epoxide-dG adducts at CG base pairs of DNA. *Nucleic Acids Res. 39*, 3988-4006.

Chapter Two:

Susceptibility of glutathione peroxidase to alkylation-mediated inhibition by anticancer acylfulvenes and comparison with thioredoxin reductase responses[1]

[1] Portions reprinted with permission from Liu, X., Pietsch, K. E., Sturla, S. J. (2011) Susceptibility of the antioxidant selenoenzymes thioredoxin reductase and glutathione peroxidase to alkylation-mediated inhibition by anticancer acylfulvenes. *Chem. Res. Toxicol. 24*, 726–736. Copyright 2011 American Chemical Society.

1. Introduction

Selenium (Se) is a biologically important trace element; low levels are required for cell growth and high concentrations are cytotoxic.[1] Human blood Se levels are low to submicromolar and vary with regional dietary Se content, as well as health status. Se homeostasis can inhibit tumor cell invasion and decrease the risk of some human cancers, such as prostate, lung, and colon cancer.[2,3] Se is incorporated into proteins in the form of selenocysteine (Sec), the naturally occurring selenium analog of cysteine (Cys), regarded as the 21st amino acid.[4,5] As such, Se acts as an antioxidant,[6] and changes in selenoenzyme levels may be an underlying mechanism for Se's chemopreventive and chemotherapeutic effects.[3,7] Similarly, if the action of a drug is dictated even in part by selenoenzymes, its supplementation may impact drug effectiveness or toxicity.

The cellular antioxidant enzymes thioredoxin reductase (TrxR) and glutathione peroxidase (Gpx) rely on Sec residues, and have both been found to be deregulated in tumor cells, such that TrxR levels are high and Gpx levels are low in tested cancer cell lines and human tumor tissue.[8–10] TrxR has a broad range of substrates, including disulfide-containing proteins, such as thioredoxin (Trx), many small molecule thiols, such as 5,5'-dithiobis(2-nitrobenzoic acid) (DTNB),[11] and even non-disulfide compounds such as dehydroascorbic acid.[12] The Gpxs are a family of peroxidases that contain one essential active site Sec and require glutathione (GSH) as a co-substrate. Gpx 1 is the predominant Gpx isoform. It is found in the cytoplasm of all mammalian tissues and it catalyzes the cellular reduction of inorganic hydrogen peroxide or organic lipid hydrogen peroxides to water or corresponding alcohols.[13] The active site Sec of Gpx is highly sensitive to oxidative modification, and nitric oxide-mediated modifications of the Gpx Sec has been shown to inactivate the enzyme.[14] In TrxR, the Sec residue is located at the C-terminus active site as part of the tetrapeptide Gly-Cys-Sec-Gly motif.[5] The flexible C-terminus of

the TrxR active site is exposed to the protein surface and is accessible to substrates and inhibitors. In addition, the Sec residue is more reactive than Cys towards electrophiles due to its lower pK_a (5.24 vs 8.25).[15] These features make TrxR highly susceptible to reactions with electrophilic compounds, and previous studies show that some alkylating agents such as the nitrogen mustard compounds chlorambucil and melphalan inhibit TrxR with micromolar IC_{50}s.[16,17] However, the potential role of selenoenzyme inhibition by more selectively toxic non-traditional anticancer agents, such as acylfulvene (AF), in cytotoxicity has not been tested.

Acylfulvenes (AFs) are a class of semisynthetic antitumor agents derived from the natural sesquiterpene cytotoxin illudin S, isolated from the Jack O'Lantern mushroom (Chart 1).[18–21] Illudin S kills various drug-resistant cancer cells, but exhibits low

Chart 1. Structure of illudin S and acylfulvene derivatives AF and HMAF.

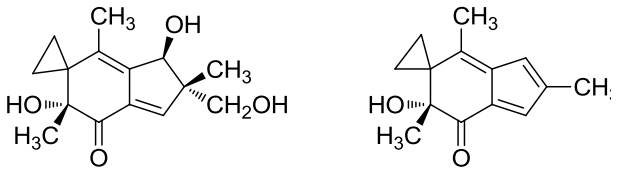

Illudin S

Acylfulvene (AF)

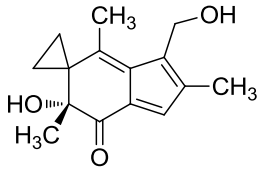

6-Hydroxymethylacylfulvene (HMAF)

malignant cell versus normal cell selectivity and therefore has no practical potential in cancer therapy.[22] On the other hand, newer semisynthetic AF analogues, including 6-hydroxymethylacylfulvene (HMAF), have improved cancer cell selectivity.[23,24] Studies regarding their cellular accumulation suggest that illudin S and AFs covalently bind to cellular DNA, RNA, and protein.[25,26] There is evidence that cytotoxicity is associated

with bioactivation to an unstable cyclohexadiene intermediate that more potently reacts with DNA compared to and interrupts DNA synthesis/repair.[27–32] The specificity and efficiency with which tumor-associated reductase enzymes activate AFs versus illudins appear to contribute in part to the selectivity of AF analogs compared to illudin S. However, this process does not account for the full magnitude of cytotoxicity differences between these structurally related small molecules.

Differences in amino acid alkylation proficiencies between the illudin and AF analogs, presumed to extend to the protein alkylation, have been hypothesized to additionally contribute to toxicity. Thus, illudin S reacts with cysteine under mild conditions (aqueous buffer at pH 6) more readily than AFs; no data is available for Sec reactivity, but we hypothesized it to be more reactive toward the electrophilic compounds.[20,33–35] Despite the increased reactivity of illudin S toward Cys, however, we have previously found that for glutathione reductase (GR), an enzyme with a redox-active disulfide at its active site, AFs are more reactive as inhibitors. They disrupt enzyme structure and inhibit GSSG reductase activity, and in particular, HMAF covalently binds active site Cys residues.[17]

In a continued effort to understand potential contributions of reactive redox enzyme-drug interactions in dictating selective toxicities of alkylating agents, in this study, we aimed to test the hypothesis that the high nucleophilicity and accessibility of the Sec-containing enzymes TrxR and Gpx may render them susceptible to illudin S and/or AFs. If so, we wished to determine whether there could be any basis for chemical selection in this process. Thus, we have characterized the reactivities of illudin S and AFs toward isolated TrxR and Gpx enzymes, and the results reveal differences in inhibition potencies and enzyme alkylation profiles as a function of active site residue/accessibility

and drug structure. A further compelling finding is that in cancer cells there exists a positive correlation between selenium availability and drug sensitivity. These data suggest that the more selectively cytotoxic AF derivatives may act in part by interacting with reactive Sec or Cys protein residues more abundant in sensitive cells, and inhibit these cellular redox enzymes.

2. Experimental procedures

2.1. Chemicals and enzymes

Illudin S from the mature fungal *Omphalotus* species was provided by MGI Pharma.[36] AF and HMAF were synthesized according to the published procedure with illudin S as the starting material.[20,21] Purified rat TrxR, Gpx from bovine erythrocytes, Tris base, 5,5'-Dithiobis(2-nitrobenzoic acid) (DTNB), hydrogen peroxide (H_2O_2), reduced glutathione (GSH), iodoacetamide, and EDTA were obtained from Sigma Chemical. Biotin-conjugated iodoacetamide (BIAM) was purchased from Invitrogen. Reduced nicotinamide adenine dinucleotide phosphate (NADPH) was purchase from EMD chemicals. Dulbecco's modified Eagle's medium (DMEM) was purchased from Mediatech (Herndon, VA). Fetal bovine serum (FBS) was purchased from Atlanta Biologicals (Lawrenceville, GA). Phosphate-buffered saline (PBS), 0.25% trypsin-EDTA, penicillin-streptomycin were obtained from Invitrogen. Tris-buffered saline was purchased from Bio-Rad. Glutathione reductase was purchased from MP Biomedicals (Solon, OH). Drug stock solutions were prepared in DMSO.

2.2. Instrumentation

LC/MS analysis of drug-treated enzymes were performed on an Agilent 1100 capillary HPLC in line with an Agilent 1100 ion trap mass spectrometer (Agilent Technologies, Santa Clara, CA) operated in positive ion mode. For drug-treated TrxR

peptide mixtures, an Agilent Zorbax SB-C_{18} column (150 mm×0.5 mm, 5 µm) was used. Analytes were eluted with a gradient of solvent A (0.5% formic acid/0.01% TFA in water (v/v)) and solvent B (0.5% formic acid/0.01% TFA in acetonitrile (v/v)) at a flow rate of 15 µL/min: initial conditions, 3:97 B:A, were held constant for 3 min, and then increased to 5:95 B:A in 7 min and held for 10 min followed by linear increase to 35:65 B:A over a course of 95 min, and finally to 75:25 B:A in 10 min. For drug-treated Gpx, a Zorbax 300 SB-C_3 column (150 mm×0.5 mm, 5 µm) was used for chromatography. Analytes were eluted with a solvent gradient of 0.05% TFA in water (A) and 0.05% TFA in acetonitrile (B), at a flow rate of 15 µL/min: initial conditions, 30:70 B:A, were held 3 min followed by a linear increase to 80:20 B:A over a course of 20 min. Absorbance measurements for enzyme assays were determined using a Varian Cary UV 100 UV/visible spectrophotometer (Varian, Inc., Palo Alto, CA).

2.3. Gpx enzyme activity assay

The influence of test compounds on Gpx was evaluated by adaptation of a published assay.[37] In a microcentrifuge tube (1.5 mL), 0.02 U Gpx (5 µL, 80 nM in phosphate buffer) was allowed to react with varying concentrations of test compound in a total volume of 0.5 mL phosphate buffer (0.1 M, 1 mM EDTA, pH 7.0) at 37 ^{o}C. After 40 min, GSH (0.1 mL, 10 mM aqueous) and glutathione reductase (0.1 mL, 0.33 µM in phosphate buffer) were added and vortex mixed. The resulting mixture was allowed to react at 37 ^{o}C for an additional 10 min, and then transferred to a disposable cuvette. NADPH (0.1 mL, 1.5 mM in 0.1% $NaHCO_3$ (w/v)) was added to the cuvette. The H_2O_2-independent consumption of NADPH was determined by monitoring the change in UV absorption of the sample at 340 nm, at 25 ^{o}C. After 2-3 minutes, H_2O_2 (0.1 mL, 1.5 mM aqueous) was added to the cuvette to initiate the H_2O_2-dependent reaction. The change in UV absorbance was monitored for an additional 7 min, and the slope of the plot of

absorption vs. time was normalized to 100% activity as determined by the blank (10 µL DMSO) control. As positive control, Gpx was treated with 1.87 mM iodoacetamide. Data was fit to a linear model for the first 5 data points.

2.4. TrxR enzyme activity assay[2]

Drug stock solutions were prepared in DMSO. All other solutions used in the assay were prepared in TE buffer (50 mM Tris-Cl, 1 mM EDTA) at pH 7.2. TrxR activity was determined at 25 ^{o}C with a UV/visible spectrophotometer (Varian Cary-100). TrxR (80 nM) was first reduced by addition of excess NADPH (100 µM) to result in a total volume of 0.1 mL. After 10 min at 25 ^{o}C, varying amounts of drug were added to the pre-reduced TrxR followed by incubating at 25 ^{o}C for the time indicated. Negative control runs were conducted by adding the same amounts of DMSO. The enzyme activities were measured by DTNB reducing assay in which at the end of incubation, 0.4 mL of assay solution (2 mM DTNB and 200 µM NADPH in TE buffer) was added and the absorbance at 420 nm was monitored for 3 min. Initial data points were fit to a straight line to obtain relative inhibition concentrations under the conditions of each experiment. To determine the reversibility of inhibition, TrxR was allowed to react with AFs as described above. After the 2 h reaction period, unbound drug was removed by gel-filtration with a size-exclusion Micro Bio-Spin™ P-6 pre-packed column (containing 10 mM Tris-HCl buffer, pH 7.4, with 0.02% sodium azide (w/v)) according to the Bio-Rad's protocols. Briefly, the column was placed in 2 mL centrifuge tube to drain the excess packing buffer by gravity. After discarding the drained buffer, the column was placed back into the tube and centrifuged to remove any remaining packing buffer (2 min, 1000*g*). Afterwards, the column was placed in a clean 1.5 mL centrifuge tube, and the

[2] These experiments, performed by Xiaodan Liu and published previously, are included here for completeness.

reaction solution was loaded into two columns (100 µL/each) followed by centrifugation for 4 min at 1000*g*. The resulting solutions were combined, and the activity was determined following the procedure for the DTNB reducing assay described above. Each data point represents an average of at least three measurements.

2.5. Cell culture[3]

HeLa cells were maintained as monolayers in Dulbecco's Modified Eagle Medium (DMEM) medium supplemented with 10% Fetal Bovine Serum (FBS) and 1% penicillin-streptomycin in a humidified, 5% CO_2 atmosphere at 37 °C. HeLa cells were subcultured in the medium described above for three days to reach 80% confluence (100 mm^2 plate, 2×10^6 cells/plate) evaluated with microscope. Cells were treated with test compounds diluted with medium (0.1% final concentration of DMSO) for 4 h. After treatment cells were washed with 5 mL phosphate buffered saline (PBS) twice. Cells were collected as follows: 2 mL of 0.25% trypsin-ethylenediaminetetraacetic acid (EDTA) was added and the cells were incubated for 5 min at 25 °C. Cells were scratched off from the plates and divided evenly into three centrifuge tubes (1.5 mL), and centrifuged (5 min, 1000g). The supernatant was removed by pipette. Cells were resuspended in 0.2 mL of lysis buffer (50 mM Tris-HCl, pH 7.5; 1 mM EDTA; 0.1% Triton X-100; 1 mM phenylmethanesulfonyl fluoride; 1 mM benzamidine; 1.4 µM pepstatin A; and 2.0 µM leupeptin) and sonicated at 4 °C (5 s bursts). The resulting cell lysate was centrifuged for 10 min (8000 g, 4 °C), and the supernatant was withdrawn for analysis. Cell cytosol containing 50 µg protein as determined by the bicinchoninic acid (BCA) protein assay reagent (Pierce, Rockford, IL) was incubated with an 80 µL mixture of insulin (1 mg/mL) and NADPH (200 µM) in TE buffer at 25 °C for 10 min. Trx (50 µL, 1 mg/mL) was added, and the rate of NADPH

[3] These experiments, performed by Xiaodan Liu and published previously, are included here for completeness.

consumption was determined by monitoring changes in absorbance at 340 nm for 5 min at 25 °C.

2.6. Immunoassay of TrxR levels in HeLa cells[4]

Cell cytosol containing 50 μg protein was separated by 4-12% SDS-PAGE (Invitrogen) and transferred onto a PVDF membrane (Invitrogen) for 1 h at 33 V, 4 °C. Membranes were blocked with 5% (w/v) nonfat milk powder in tris-buffered saline (TBS)/Tween 20 (0.05%) overnight at 4 °C. The membrane was incubated with primary anti-TrxR (ABR, Rockford, IL) and anti-actin (Invitrogen) antibodies diluted 2000 times in TBS/Tween 20 (5 mL) for 1 h. The membrane was washed three times with TBS/Tween 20 (5 mL, 5 min) and subject to incubation with 5 mL of secondary conjugated antibody (goat anti-rabbit IgG horseradish peroxidase, Bio-Rad, 1:2000 dilution in TBS/Tween 20,) for 1 h. After four 5 min washes with TBS/Tween 20 (5 mL/each), the Peroxide Solution and the Luminol Enhancer Solution from the ECL Western Blotting Substrate analysis system (Pierce, Rockford, IL) were mixed in a 1:1 ratio in a tray and rinsed over the membrane. The membrane was exposed to a film, developed, and the chemiluminescence was quantified.

2.7. Cell viability assay[4]

Drug cytotoxicity toward HeLa cells was determined by Promega CellTiter 96 Aqueous One Solution Cell Proliferation Assay, where viable cells yield a colored, quantifiable product via bioreduction of 3-(4,5-dimethylthiazol-2-yl)-5-(3-carboxymethoxyphenyl)-2-(4-sulfophenyl)-2H-tetrazolium, inner salt (MTS).[38] Briefly, cells were seeded on 96-well plate with a starting density of 1000 cells/well in either

[4] These experiments, performed by Xiaodan Liu and published previously, are included here for completeness.

regular medium or medium containing 1 µM sodium selenite for 3 days. The exponentially growing cells were then exposed to drugs in varying concentrations for 12 h. The drug-containing medium was exchanged with fresh regular medium. Cell viability was determined by exposing cells to an MTS-containing solution for 2 h at 37 °C, and measuring formazan formation, i.e. absorbance at 490 nm, with a microplate reader. All experiments were carried out in triplicate.

2.8. Chemical labeling and assay of AF-modified TrxR[5]

NADPH-reduced TrxR (0.9 µM, prepared as described above) and AFs at varying concentrations in DMSO were allowed to react at 37 °C for 2 h. The samples containing equivalent amounts of DMSO only were used for control experiments. After incubation, 1 µl of the reaction mixture was taken out and added to new tubes containing 19 µL of BIAM (100 mM, pH 6.5 and 8.5 in TE buffer) further incubated at 37 °C for another 30 min to allow the alkylation at the remaining free –SeH and –SH groups in the enzyme. Fifteen microliters of BIAM-modified enzyme were mixed with 5 µL of loading buffer (Invitrogen), 20 µL of the samples were subjected to SDS-PAGE on a 4-12% gel, and the separated proteins were transferred to nitrocellulose membrane. Proteins labeled with BIAM were detected with horseradish peroxidase-conjugated streptavidin and enhanced chemiluminescence detection.

2.9. Trypsin-mediated digestion and LC/MS analysis of AF-treated TrxR[5]

TrxR (50 µg, 1 nmol) was allowed to react with AFs (2 µL, 125 mM) or 2 µL of DMSO as control in a total volume of 0.2 mL TE buffer containing NADPH (1 mM) for 2 h at 25 °C with reaction with 10 µL of DMSO as control. An aliquot (1 µL) of reaction

[5] These experiments, performed by Xiaodan Liu and published previously, are included here for completeness.

solution was withdrawn and diluted to a total volume of 300 µL; enzyme activity was determined as described above for measurement of TrxR activity. After 2 h, TrxR activity was inhibited by AFs completely. The resulting solutions were diluted to a volume of 1 mL by adding 0.8 mL TE buffer followed by trypsin (0.2 µg/µL, 10 µL) in 0.1 M HCl. Proteolytic digestion was allowed to occur at 37 °C for 24 h. The resulting mixture was divided into two equal portions, placed into centrifuge tubes, concentrated to dryness on a centrifugal vacuum concentrator, and reconstituted by adding 20 µL of solvent A (0.5% formic acid/0.01% TFA in water (v/v)) to each tube. The resulting samples were analyzed by LC/MS.

2.10. Mass analysis of Gpx modification by AFs[6]

Gpx (50 µg, 1.6 nmol) was allowed to react with AFs (10 µL, 125 mM) or 10 µL of DMSO as control in a total volume of 1 mL TE buffer for 2 h at 25 °C. A Microcon® Y-10 centrifuge filter (NMWL 10,000) was used to remove unbound compound and concentrate Gpx to a final volume of 30 µL. Samples (8 µL) were analyzed by LC/MS with the general analytical protocol. Spectra were obtained by full scan data acquisition performed within *m/z* 100-1500. Mass deconvolution was performed with the Agilent ion trap analysis software (Charge Deconvolution for Data Analysis for LC/MSD Trap, version 3.2).

3. Results and discussion

3.1. AFs do not impact Gpx activity

The test compounds were evaluated as potential Gpx inhibitors. Thus, Gpx was treated with varying concentrations of AFs and illudin S and residual enzyme activity was measured by a GR-coupled assay, however none of the tested drugs caused a decrease in

[6] These experiments, performed by Xiaodan Liu and published previously, are included here for completeness.

enzyme activity (Table 1).[7] The apparent increase in Gpx activity may result from the absorbance of the drugs, as AFs absorb around 330 nm, so higher drug concentrations results in higher absorption and translates to a higher calculated activity. By contrast, and as a positive control, Gpx was treated with iodoacetamide (IAA), and under the conditions of the general assay IAA inhibited Gpx activity with an IC_{50} of 2.4 mM.[39] While IAA has not been characterized explicitly as a Gpx inhibitor previously, it is a common alkylating agent known to efficiently modify free cysteine and selenocysteine residues, and it was found to be an effective positive control for monitoring loss of Gpx activity. Furthermore, after Gpx was incubated with AFs for 3 h and unbound compound removed with a Microcon® Y-10 centrifuge filter (NMWL 10,000), whole protein mass spectrometry analysis indicated only the intact Gpx peak.[40] These data suggest that neither AFs nor illudin S impact Gpx activity, and do not modify or interact with the enzyme active site.

[7] As a control for potential drug interactions with the GR-coupled portion of the assay, experiments without Gpx were performed and results showed that the drugs do not interfere with this background reaction.

Table 1. Effect of a wide range of illudin S, AF, and HMAF concentrations on Gpx activity. Each activity value is the average of at least two trials expressed as a percentage (± standard deviation).

Illudin S (μM)	Average Activity (%)
0	100 ± 31
0.5	119 ± 41
2	125 ± 34
20	128 ± 36
200	110 ± 24
1000	160 ± 10
AF (μM)	Average Activity (%)
0	99 ± 14
0.5	102 ± 6
2	102 ± 17
20	144 ± 12
200	198 ± 25
1000	196 ± 34
HMAF (μM)	Average Activity (%)
0	100 ± 59
0.25	111 ± 46
0.5	129 ± 58
2	162 ± 12
200	155 ± 22

3.2. Interaction of TrxR with AFs

A number of experiments were carried out to study the reactivity of AFs and illudin S with the selenoenzyme TrxR.[41] This aspect of the project was carried out as a collaboration with Xiaodan Liu, another PhD student in our lab. Results from experiments with isolated enzyme demonstrated that TrxR inhibition by illudin S and AFs was dose-dependent, time-dependent, and irreversible. When NADPH-reduced TrxR was treated with illudin S and AFs, its DTNB reduction activity was inhibited in a dose-dependent manner (Figure 1). The IC_{50} values were determined to be 260 μM for illudin S, 7.3 μM for AF, and 0.38 μM for HMAF respectively.

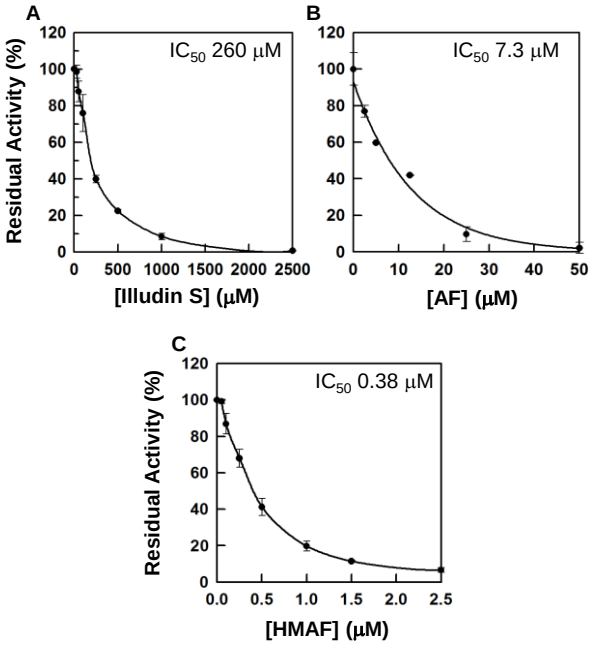

Figure 1. Dose-dependent inhibition of prereduced TrxR by illudin S and AFs. TrxR (80 nM) was first incubated with NADPH (100 μM) at 25 °C for 10 min, followed by the addition of test compounds, and further incubated for 2 h at 25 °C. The residual activity was measured with the DTNB assay. Each data point represents an average of at least three measurements.

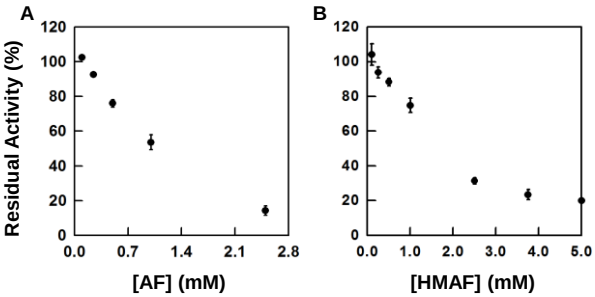

Figure 2. Inhibition of nonreduced TrxR by AF and HMAF. TrxR (80 nM) was incubated with the test compounds for 2 h at 25 °C. The residual activity was measured with the DTNB assay. Each data point represents an average of at least three measurements.

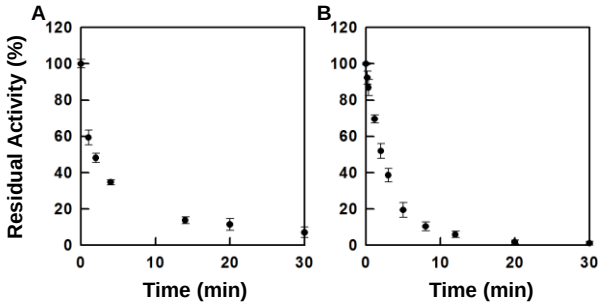

Figure 3. Time-dependent inhibition of prereduced TrxR by AFs. TrxR (80 nM) was first incubated with NADPH (100 μM) at 25 ^{o}C for 10 min, followed by the addition of test compounds at concentrations that would completely inhibit TrxR upon 30 min of treatment (A, 50 μM AF; B, 7.5 μM HMAF) at 25 ^{o}C. To assay the enzyme activity, 100 μL of the incubation solution was taken out at different time intervals, and the residual activity was measured with the DTNB assay. Each data point represents an average of at least three measurements.

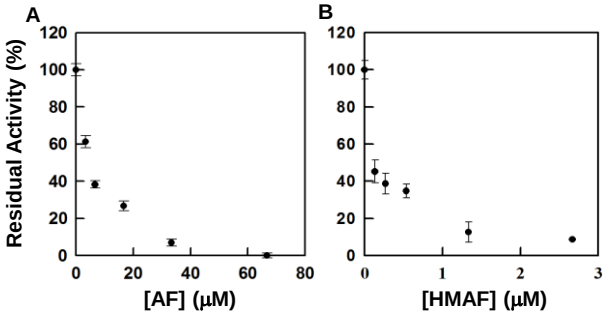

Figure 4. Gel-filtration analysis of AF and HMAF-inactivated TrxR. TrxR (80 nM) was first incubated with NADPH (100 μM) at 25 ^{o}C for 10 min, followed by the addition of test compounds, and further incubation for 2 h at 25 ^{o}C. Unbound compound was removed by Micro Bio-Spin P-6 prepacked size exclusion columns. The residual activity was measured with the DTNB assay. Each data point represents an average of at least three measurements.

Without pre-reducing TrxR, no inhibition was observed by illudin S, and the IC_{50} values for AFs increase to millimolar ranges (Figure 2). The inhibition of TrxR by AFs was time-dependent; within five minutes, over 60% of TrxR activity was inhibited by 50 μM AF and 7.5 μM HMAF respectively (Figure 3), suggesting a rapid reaction between TrxR and AFs. On the basis of gel-filtration studies, TrxR inhibition by AFs was determined to be irreversible. TrxR was allowed to react with AFs in the same manner as described for studies carried out to determine the concentration-dependence of inhibition. The resulting inactivated TrxR was filtered through a size exclusion column with molecular weight cut-off 6000 to remove non-covalently bound drug and the re-isolated enzyme was assayed for DTNB reduction capacity. The native TrxR activity was not recovered (Figure 4), suggesting AFs are irreversible inhibitors of TrxR. The relative potencies of the three compounds for reducing cellular TrxR activity (Figure 5) in HeLa cells were, at equitoxic levels, in the same order (HMAF > AF > illudin S) as TrxR inhibition potencies in a cell-free system (Figure 1). Cells were treated with illudin S, AF, or HMAF at concentrations that maintain 80% cell viability upon 12 h treatment. After washing and cell lysis, residual TrxR activity was determined. A dose-dependent loss of TrxR activity resulted from each of the compounds tested (Figure 5).

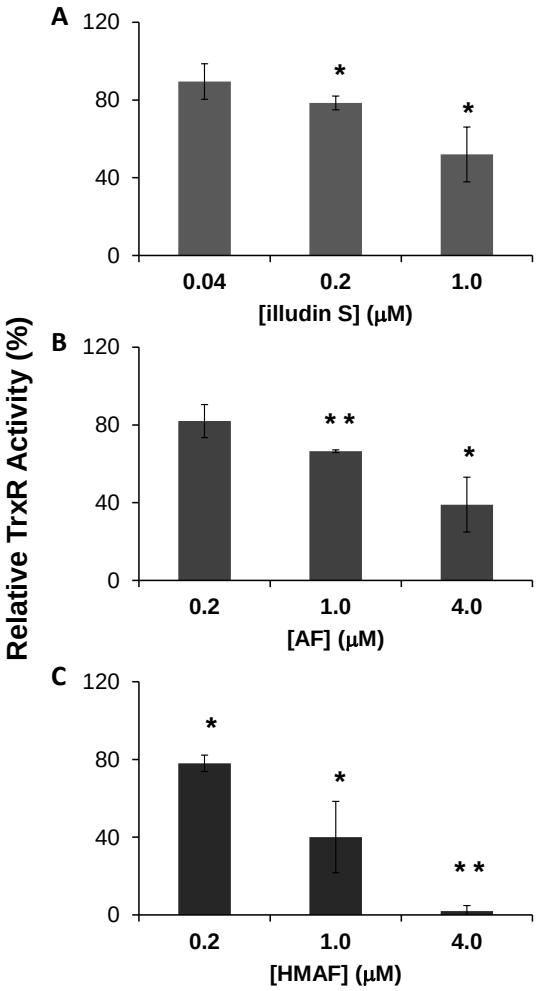

Figure 5. Inhibition of the TrxR activity in HeLa cells by illudin S and AFs. HeLa cells were exposed to the individual compound for 12 h, and then cellular TrxR activity was measured. Asterisks represent a significant difference relative to controls: * $p < 0.05$ and ** $p < 0.01$.

Alkylation at the active site of TrxR was further characterized using an affinity assay and mass spectrometry. The assay involves pH-selective BIAM-alkylation of free Cys vs. Sec residues, and was carried out for the inactivated protein resulting from treatment with AFs. The purpose of the experiment was to determine whether active site Sec and Cys in TrxR were chemically modified by AFs. The pH- and time-dependent selective alkylation of TrxR active site residues by BIAM has been optimized and established previously, and applied to other TrxR-alkylating compounds.[42–44] Per the

published procedures, the enzyme was allowed to react with varying concentrations of AFs, then labeled with BIAM. Due to the pK_a difference of active site residues Cys 497 (pK_a 8.3) and Sec 498 (pK_a 5.2),[15] only the free selenol of Sec is modified at pH 6.5 and both active site residues are modified at pH 8.5. The results of the experiment were that at pH 6.5, the intensity of the BIAM label was diminished in intensity for low micromolar AF and HMAF (25 µM and 5 µM, respectively). The same trend was observed with increasing concentrations of AFs, suggesting selective modification of the free selenol of Sec by AFs (Figure 6). Likewise, at pH 8.5 and for the highest levels of AFs (125 µM AF and 25 µM HMAF), BIAM labeling was almost abolished as compared to that at pH 6.5. These data suggest that both active site Cys and Sec residues were modified by both AF and HMAF. Since AF irreversibly inhibited the DTNB reduction activity by TrxR, and

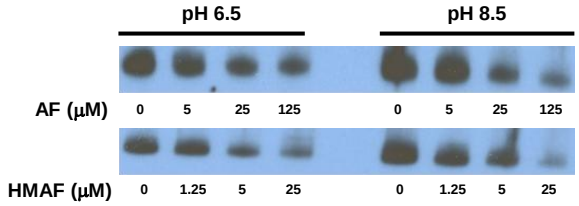

Figure 6. Free C-terminus redox-active sites Sec and Cys of TrxR were detected by biotin-conjugated iodoacetamide. Different concentrations of AFs were added to NADPH (200 µM) prereduced TrxR (0.9 µM) and incubated at 25 ^{o}C for 2 h. BIAM was added to label the active site free Sec at pH 6.5 and free Cys and Sec at pH 8.5. Results are representative of three independent experiments.

the modification appears to occur at the C-terminus active site, we analyzed the trypsin digest of the covalently modified TrxR by LC/MS to evaluate the chemical pathway involved. A singly charged ion corresponding to the active site peptide product of the tryptic digest was observed by ion trap MS analysis (*m/z* 1142.4, Figure 7A). Due to the presence of selenium in the peptide sequence (SGGDILQSGCysSecG), the isotope envelope is uniquely diagnostic. A singly charged ion corresponding to AF-mediated mono-alkylation of the active site tryptic peptide was observed (*m/z* 1358.6, Figure 7B),

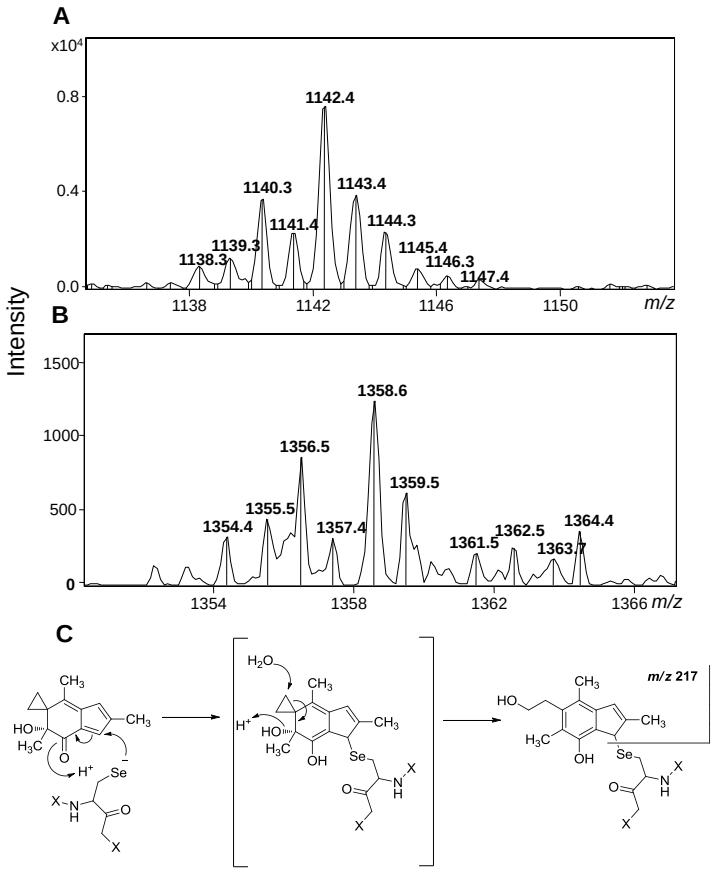

Figure 7. LC/MS analysis of AF-modified TrxR active-site peptide (SGGDILQSGCysSecG). (A) Average mass for the unmodified peptide (*m/z* 1142.4) from an untreated sample of enzyme as a blank control; (B) average mass for the AF-modified peptide (*m/z* 1358.6) from a treated sample; (C) proposed mechanism of reaction of AF with Sec at the TrxR active site.

and the associated mass change (*m/z* 216) is consistent with formation of an adduct via direct conjugate addition at the α,β-unsaturated carbonyl.

Studies carried out here to test the potential influence of TrxR induction on cytotoxicity demonstrated that cells could be favorably sensitized by selenite preconditioning. It is known that culture medium supplemented with sodium selenite (Na_2SeO_3) will induce TrxR expression in breast cancer MCF-7 cells and liver cancer HepG2 cells.[45,46] In the present study, HeLa cells were cultured in media containing 1 μM sodium selenite for three consecutive days. 1 μM of selenite is also close to physiological Se concentration, and higher concentrations of added selenite (2 and 3 μM) caused cytotoxicity (observed as cells significantly detached from culture dish). A

saturated level of TrxR was observed after three day induction by selenite. By Western blotting analysis and measurement of cellular TrxR activity after selenite supplementation, cellular TrxR protein levels and TrxR activity increased four-fold.[47] We then investigated whether changes in sensitivity toward illudin S and AFs were associated with the increased protein levels and activities. Results indicated that increasing the cellular level of TrxR makes cells more sensitive toward AFs, but not towards illudin S (Figure 8), which is consistent with the inhibition potency of these compounds with purified TrxR. After induction by 1 μM selenite for three continuous days, HeLa cell sensitivity towards 100 μM AFs was increased about 50% compared to the cell sensitivity without selenite induction.

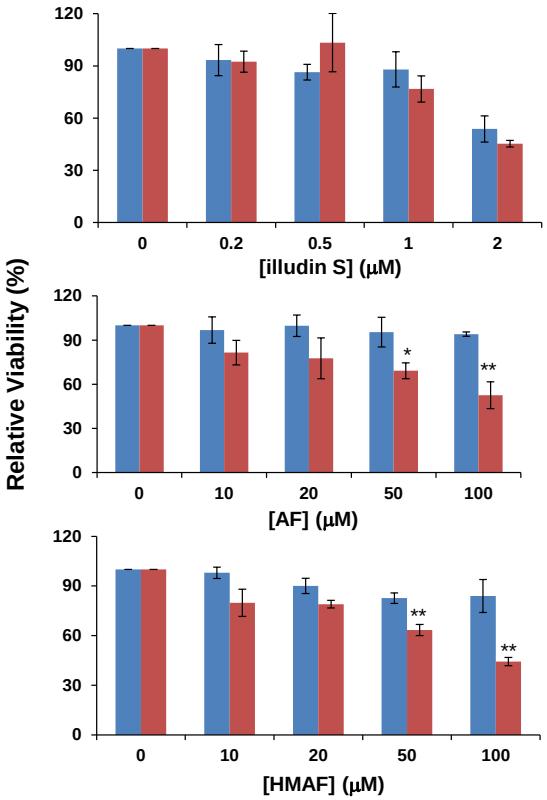

Figure 8. Differential sensitivity of HeLa cells toward illudin S and AFs. HeLa cells were seeded on 96-well plates (1000 cells/well) and cultured in medium with (red/right) or without (blue/left) the addition of sodium selenite (1 µM) for three continuous days and then changed with medium containing test compounds for 12 h. Cytotoxicity was measured with the MTS assay (Promega). Asterisks represent a significant difference between cytotoxicities resulting from no selenite and 1 µM selenite medium: * $p < 0.05$ and ** $p < 0.01$.

4. Discussion

The cellular function of Se has been attributed mainly to its presence in selenoproteins and the correlation of selenium administration and level of selenoenzymes has been extensively studied.[2,9,48–53] Se is incorporated into selenoproteins in the form of selenocysteine either during protein synthesis or through post-translational processes.[53–55] Selenoproteins such as TrxR and Gpx are involved in cellular antioxidant defense and redox signaling. The active site Sec residue of these proteins has a higher propensity to react with electrophiles compared to its Cys counterpart[15] and therefore, the potential to be more easily inactivated by alkylating agents. Key electrophilic features of illudin S and AFs include a cyclopropane ring and an α,β-unsaturated ketone, which may react by direct addition or coupled with reductive bioactivation.[27–31] Increased reductase-mediated bioactivation by NADPH-dependent enzyme or enzymes, and subsequent nucleophilic attack at the cyclopropane ring by DNA is thought to be an important process contributing to AF toxicity, but does not fully account for differences in cytotoxicity profiles,[26,56–58] and their potential for inactivating key cellular proteins as a contributing factor is a hypothesis under investigation.[17,26] In correlation with their reactivity with small thiols, illudin S and AFs were expected to have the same relative reactivities toward thiol-containing enzymes,[34,59] but in a previous study a surprising finding was that AFs are much more reactive than illudin S toward the cellular redox-regulating enzyme GR.[17]

The thioredoxin system comprising TrxR, its protein substrate Trx and NADPH, together with its homologous glutathione system comprising GR, NADPH and GSH, is the major regulator of intracellular redox balance, exerting a wide range of activities in oxidant defense, cell viability, and proliferation. Patterns of GR inhibition by illudin S and AF have been defined, but the potential influence of the more reactive Sec residue within TrxR, and similarly Gpx, is unknown. Elevated levels of TrxR were found in many

types of cancer cell lines, especially ovarian and prostate cancer which are both very sensitive to HMAF.[8] TrxR is very similar in both structure and mechanism to GR.[60] They both use NADPH as a cofactor to reduce the conserved internal disulfide center. TrxR is distinct from GR by the presence of a C-terminus redox center (Gly-Cys-Sec-Cys) which is functionally equal to GR's substrate GSSG.[61,62] The flexibility of the C-terminus redox center not only allows TrxR to have a broad range of substrates, but also makes it extraordinarily reactive towards electrophiles due to the reactive and solvent accessible Sec. The Sec was reported to be targeted by many anti-cancer compounds, such as curcumin, motexafin gadolinium, flavonoids, and quinones.[42,63] TrxR regulates cell proliferation by controlling DNA synthesis and antioxidant defense with reduced Trx. In normal cells, TrxR is critical for maintaining intracellular proteins in their reduced states and defending against oxidative stress. In malignant cells, however, TrxR supports tumor growth and progression, and inactivation may induce or promote cell death. Here we find that NADPH-reduced TrxR is inhibited by AFs with low micromolar IC_{50}s, which has similar potency as TrxR inhibitors characterized to date. Examples include curcumin,[64] carmustine,[65] gold complexes,[66] platinum compounds,[65,67] and 2-chloroethyl ethyl sulfide (CEES).[44] The IC_{50} of illudin S toward TrxR determined in this study was 100-fold higher than that of the AFs. This trend is reverse in order relative to cytotoxicity, but is consistent with the diminished ability of illudin S to inhibit GR.[17]

The related homotetrametic enzyme Gpx is comprised of two asymmetric units containing two dimers, each with two selenocysteines at the active sites in the form of Se^- in the resting state and that directly participate in the process of hydroperoxide reduction of Gpx. There was no data obtained in this study to suggest any chemical reactivity of the drugs toward the active site of the protein resulting in inhibition of activity. Unlike the flexible C-terminus active site of TrxR, the active site of Gpx locates at the N-terminal

ends of long α-helices, surrounded by aromatic side-chains. This structural context may therefore protect Sec from AFs.[68] For relatively high concentrations of drug (≥ 1000 μM illudin S, ≥ 20 μM AF, ≥ 2 μM HMAF) we observed an increase in Gpx activity (Table 1) that could not be explained on the basis of our experiments. To our knowledge there is no precedent or good rationale for this unusual observation, yet the data for lower concentrations show no change in activity and offer no suggestion that these compounds are Gpx inhibitors.

AF and HMAF are both irreversible TrxR inhibitors, however, only HMAF is an irreversible GR inhibitor. TrxR and GR are homodimeric flavoproteins of the same family and are similar in primary sequence and structure, but GR lacks the Sec residue in the C-terminal active site. A possible rationale for the difference in AFs reactivity is that Sec that may undergo a hindered conjugate addition reaction (Scheme 7C) with the α,β-unsaturated ketone that is common to AFs. Therefore, TrxR is capable of reacting with both AF and HMAF. In the case of GR inhibition by HMAF,[17] however, evidence suggests that a substitution reaction occurs with the methylenehydroxy substituent that is specific to HMAF. Thus, the differences in the chemical reaction mediating the modification may account for the combined observations.

On the basis of the BIAM labeling experiment performed here (Figure 6), both active site residues are alkylated at low micromolar concentrations of AF and HMAF. This affinity assay provides mechanistic information regarding how AFs compare to other TrxR inhibitors. AFs irreversibly inhibit TrxR to a similar degree as previously characterized inhibitors, but the manner in which they modify important active site residues differs. Our results demonstrate that like curcumin (polyphenol), carmustine (nitrosourea), and 1-chloro-2,4-dinitrobenzene (DNCB, nitroaromatic), AFs modify Sec

and Cys. In contrast, CEES (half-mustard)[44] and 5-iodoacetamidofluorescein (iodoacetamide conjugate)[69] inhibit TrxR by only modifying the Sec residue. Whether there is medicinal relevance in selectively targeting Sec vs. both active site residues is not understood, however existing data suggests possible differences in triggering molecular pathways. For example, alkylation of Sec and Cys by curcumin[42] and DNCB[70] results in irreversible inhibition and high induction of NADPH oxidase, which produces reactive oxygen species (ROS). Cisplatin-derivatization of TrxR inhibits enzyme activity but does not induce NADPH oxidase activity,[71] and Sec-targeting CEES is capable of producing (ROS),[44] but it has not been demonstrated whether the generation of ROS also occurs via induction of NADPH oxidase. Interestingly, it has been shown that alkylated TrxR (with DNCB or cisplatin) promotes apoptosis to a similar extent as truncated TrxR lacking its two C-terminal residues,[72] but ROS can be generated as long as a functional N-terminal redox active motif remains.[73]

Mass spectrometry analysis suggests the adduct was formed following a direct alkylation pathway with a mass change of *m/z* 216, which is also consistent with our proposed HMAF-GR adduct formed by direct attack at the α,β-unsaturated ketone followed by opening the cyclopropane ring by water molecule. Although blotting results suggest that the neighboring cysteine was also modified by higher concentration of AFs, no ions corresponding to the bis-adducts were observed, possibly due to the poor ionization efficiency of the alkylated peptides as previously discussed for GR-HMAF.[17] Because of the unique Se isotope envelope, it is easy to confirm the identity of corresponding peptide modifications. We only observed singly charged ions corresponding to the unmodified active peptide (SGGDILQSCysSecG, *m/z* 1142.4) and a mono-adduct of AF. Significant reduction (> 60%) on the extracted ion intensity corresponding to the active site tryptic peptide (*m/z* 1142.4) was observed for the AFs-

treated TrxR compared to the control,[74] suggesting that the reaction between TrxR and AFs occurred at the active site, which is consistent to the BIAM-labeling experiment. Similar results have been reported for 4-hydroxynonenal modification of the TrxR active site, in which also only a singly charged modified peptide mass peak was identified with the Se-specific isotopic mass distribution.[75]

In cancer cells, TrxR expression is up to 10-fold higher compared with normal cells.[5,76] Addition of Se to cell media has been reported to induce TrxR expression 10–30 fold by itself or in combination with sulforaphane.[45,46] An approximately 3.6-fold induction of TrxR protein levels in HeLa cells supplemented with 1 μM selenite is associated with a 4.2-fold increase in activity.[47] Preliminary tests for potential synergies of Se plus sulforaphane co-induction suggested that no significant additional increases resulted, and that sulforaphane displayed potentially confounding direct inhibitory properties (data not shown). Therefore, we used Se alone to induce TrxR and test the impact on drug sensitivity.[77]

After selenite-mediated TrxR induction, HeLa cells become more sensitive to AFs, but not to illudin S. AFs may be selectively toxic in part because TrxR inhibition contributes to toxicity more significantly in the case of high TrxR cancer cells than low TrxR normal cells. Thinking about the underlying mechanism, the high levels of TrxR in cancer cells will influence the redox state of its substrates, i.e. there will be more reduced Trx compared to normal cells with lower levels of TrxR. The increased levels of reduced Trx will influence gene expression activity by reducing transcription factors. Upregulation of these pathways in cancer cells compared to the basal levels in normal cells will make the cancer cells more susceptible to alkylating agents that can react with many targets. Enhanced antitumor activity has been observed for the combination therapy

of Se compounds and anticancer drugs such as taxol, doxorubincin, irinotecan, platinum agents, 5-fluorouracil and campthotecin.[78–80] Further, cisplatin and doxorubincin[16] have been characterized as TrxR inhibitors, suggesting increasing TrxR levels with Se may enhance cell sensitivity towards anticancer drugs.

5. Conclusion

In this study we evaluated potential interactions between the natural product illudin S and its AF analogues toward the Se-dependent cellular redox-regulating enzymes Gpx and TrxR as isolated enzymes, and in cell-based models. The inhibition potencies of illudin S and AFs are in the same order for TrxR as what has been previously observed for the thiol-based redox-regulating enzyme GR, i.e., HMAF > AF > illudin S. However, AF and HMAF irreversibly target the TrxR active site Sec and Cys residues more efficiently than the GR active site Cys residues, which is consistent with the existence of the more reactive Sec in the TrxR active site. In contrast, Gpx is not inhibited by AFs, suggesting that the TrxR active site is more accessible and reactive.[17] For both TrxR and GR, illudin S was a weaker inhibitor than AFs, which is opposite to their reactivity toward small molecule thiols, suggesting that the polar substituents (illudin S > HMAF > AF) that decorate the five membered ring may interfere with enzyme binding, and that the flat fulvene structure binds efficiently. Furthermore, AFs abrogate cellular TrxR activity and, for HeLa cells, are more potent cytotoxins after selenite-induced TrxR overexpression. The data obtained in this study contributes to a broader understanding of chemical and biochemical factors involved in regulating cancer cell susceptibility toward alkylating agents, specifically the potential for selectively targeting Se-dependent TrxR expression to enhance cytotoxicity.

References

1. Selenius, M., Rundlöf, A.-K., Olm, E., Fernandes, A. P., and Björnstedt, M. (2010) Selenium and the Selenoprotein Thioredoxin Reductase in the Prevention, Treatment and Diagnostics of Cancer. *Antioxid. Redox Signaling 12,* 867-880.
2. Rayman, M. P. (2005) Selenium in cancer prevention: a review of the evidence and mechanism of action. *Proc. Nutr. Biochem. 64,* 527-542.
3. Zeng, H., and Combs, G. F., Jr. (2008) Selenium as an anticancer nutrient: roles in cell proliferation and tumor cell invasion. *J. Nutr. Biochem. 19,* 1-7.
4. Forstrom, J. W., Zakowski, J. J., and Tappel, A. L. (1978) Identification of the catalytic site of rat liver glutathione peroxidase as selenocysteine. *Biochemistry 17,* 2639-2644.
5. Gladyshev, V. N., Jeang, K. T., and Stadtman, T. C. (1996) Selenocysteine, identified as the penultimate C-terminal residue in human T-cell thioredoxin reductase, corresponds to TGA in the human placental gene. *Proc. Natl. Acad. Sci. U.S.A. 93,* 6146-6151.
6. Bellinger, F. P., Raman, A. V., Reeves, M. A., and Berry, M. J. (2009) Regulation and function of selenoproteins in human disease. *Biochem. J. 422,* 11-22.
7. Lu, J., and Jiang, C. (2005) Selenium and cancer chemoprevention: hypotheses integrating the actions of selenoproteins and selenium metabolites in epithelial and non-epithelial target cells. *Antioxid. Redox Signaling 7,* 1715-1727.
8. Berggren, M., Gallegos, A., Gasdaska, J. R., Gasdaska, P. Y., Warneke, J., and Powis, G. (1996) Thioredoxin and thioredoxin reductase gene expression in human tumors and cell lines, and the effects of serum stimulation and hypoxia. *Anticancer Res. 16,* 3459-3466.
9. Esworthy, R. S., Baker, M. A., and Chu, F. F. (1995) Expression of selenium-dependent glutathione peroxidase in human breast tumor cell lines. *Cancer Res. 55,* 957-962.
10. Nuray, N. N., Tandoğan, B., Türkoğlu, M. A., and Demirer, S. (2009) Is it Useful to Determine Glutathione Peroxidase and Thioredoxin Reductase Activities for Comparisons of Malign and Benign Breast Diseases? *Turk. J. Biochem. 34,* 187-194.
11. Holmgren, A. (1977) Bovine Thioredoxin System. Purification of thioredoxin reductase from calf liver and thymus and studies of its fuction in disulfide reduction. *J. Biol. Chem. 252,* 4600-4606.
12. May, J. M., Mendiratta, S., Hill, K. E., and Burk, R. F. (1997) Reduction of Dehydroascorbate to Ascorbate by the Selenoenzyme Thioredoxin Reductase. *J Biol. Chem. 272,* 22607-22610.
13. Prabhakar, R., Vreven, T., Morokuma, K., and Musaev, D. G. (2005) Elucidation of the mechanism of selenoprotein glutathione peroxidase (GPx)-catalyzed hydrogen peroxide reduction by two glutathione molecules: a density functional study. *Biochemistry 44,* 11864-11871.
14. Asahi, M., Fujii, J., Takao, T., Kuzuya, T., Hori, M., Shimonishi, Y., and Taniguchi, N. (1997) The oxidation of selenocysteine is involved in the inactivation of glutathione peroxidase by nitric oxide donor. *J Biol. Chem. 272,* 19152-19157.
15. Huber, R. E., and Criddle, R. S. (1967) Comparison of the chemical properties of selenocysteine and selenocystine with their sulfur analogs. *Arch. Biochem. Biophys. 122,* 164-173.

16. Witte, A. B., Anestal, K., Jerremalm, E., Ehrsson, H., and Arner, E. S. (2005) Inhibition of thioredoxin reductase but not of glutathione reductase by the major classes of alkylating and platinum-containing anticancer compounds. *Free Radical Biol. Med. 39,* 696-703.
17. Liu, X., and Sturla, S. J. (2009) Profiling patterns of glutathione reductase inhibition by the natural product illudin S and its acylfulvene analogues. *Mol. BioSyst. 5,* 1013-1024.
18. Anchel, M., Hervey, A., and Robbins, W. J. (1950) Antibiotic substances from Basidiomycetes+. VII. Clitocybe illudens. *Proc. Natl. Acad. Sci. U.S.A. 36,* 300-305.
19. McMorris, T. C., and Anchel, M. (1965) Fungal Metabolites. the Structures of the Novel Sesquiterpenoids Illudin-S and -M. *J. Am. Chem. Soc. 87,* 1594-1600.
20. McMorris, T. C., Kelner, M. J., Wang, W., Diaz, M. A., Estes, L. A., and Taetle, R. (1996) Acylfulvenes, a new class of potent antitumor agents. *Experientia 52,* 75-80.
21. McMorris, T. C., Kelner, M. J., Wang, W., Yu, J., Estes, L. A., and Taetle, R. (1996) (Hydroxymethyl)acylfulvene: an illudin derivative with superior antitumor properties. *J. Nat. Prod. 59,* 896-899.
22. Kelner, M. J., McMorris, T. C., and Taetle, R. (1990) Preclinical evaluation of illudins as anticancer agents: basis for selective cytotoxicity. *J. Natl. Cancer. Inst. 82,* 1562-1565.
23. Kelner, M. J., McMorris, T. C., Estes, L., Wang, W., Samson, K. M., and Taetle, R. (1996) Efficacy of HMAF (MGI-114) in the MV522 metastatic lung carcinoma xenograft model nonresponsive to traditional anticancer agents. *Invest. New Drugs 14,* 161-167.
24. MacDonald, J. R., Muscoplat, C. C., Dexter, D. L., Mangold, G. L., Chen, S. F., Kelner, M. J., McMorris, T. C., and Von Hoff, D. D. (1997) Preclinical antitumor activity of 6-hydroxymethylacylfulvene, a semisynthetic derivative of the mushroom toxin illudin S. *Cancer Res. 57,* 279-283.
25. Kelner, M. J., McMorris, T. C., Montoya, M. A., Estes, L., Uglik, S. F., Rutherford, M., Samson, K. M., Bagnell, R. D., and Taetle, R. (1999) Characterization of MGI 114 (HMAF) histiospecific toxicity in human tumor cell lines. *Cancer Chemother. Pharmacol. 44,* 235-240.
26. Herzig, M. C., Arnett, B., MacDonald, J. R., and Woynarowski, J. M. (1999) Drug uptake and cellular targets of hydroxymethylacylfulvene (HMAF). *Biochem. Pharmacol. 58,* 217-225.
27. Dick, R. A., Yu, X., and Kensler, T. W. (2004) NADPH alkenal/one oxidoreductase activity determines sensitivity of cancer cells to the chemotherapeutic alkylating agent irofulven. *Clin. Cancer Res. 10,* 1492-1499.
28. Gong, J., Vaidyanathan, V. G., Yu, X., Kensler, T. W., Peterson, L. A., and Sturla, S. J. (2007) Depurinating acylfulvene-DNA adducts: characterizing cellular chemical reactions of a selective antitumor agent. *J. Am. Chem. Soc. 129,* 2101-2111.
29. Jaspers, N. G., Raams, A., Kelner, M. J., Ng, J. M., Yamashita, Y. M., Takeda, S., McMorris, T. C., and Hoeijmakers, J. H. (2002) Anti-tumour compounds illudin S and Irofulven induce DNA lesions ignored by global repair and exclusively processed by transcription- and replication-coupled repair pathways. *DNA Repair 1,* 1027-1038.

30. Koeppel, F., Poindessous, V., Lazar, V., Raymond, E., Sarasin, A., and Larsen, A. K. (2004) Irofulven cytotoxicity depends on transcription-coupled nucleotide excision repair and is correlated with XPG expression in solid tumor cells. *Clin. Cancer Res. 10,* 5604-5613.
31. Amato, R. J., Perez, C., and Pagliaro, L. (2002) Irofulven, a novel inhibitor of DNA synthesis, in metastatic renal cell cancer. *Invest. New Drugs 20,* 413-417.
32. Neels, J. F., Gong, J., Yu, X., and Sturla, S. J. (2007) Quantitative correlation of drug bioactivation and deoxyadenosine alkylation by acylfulvene. *Chem. Res. Toxicol. 20,* 1513-1519.
33. Tanaka, K., Inoue, T., Tezuka, Y., and Kikuchi, T. (1996) Michael-type addition of illudin S, a toxic substance from Lampteromyces japonicus, with cysteine and cysteine-containing peptides in vitro. *Chem. Pharm. Bull. 44,* 273-279.
34. McMorris, T. C., and Yu, J. (1997) Reaction of antitumor hydroxymethylacylfulvene (HMAF) with thiols. *Tetrahedron 53,* 14579-14590.
35. McMorris, T. C., Yu, J., Ngo, H. T., Wang, H., and Kelner, M. J. (2000) Preparation and biological activity of amino acid and peptide conjugates of antitumor hydroxymethylacylfulvene. *J. Med. Chem. 43,* 3577-3580.
36. McCloud, T. G., Klueh, P. A., Pearl, K. C., Cartner, L. K., Mushik, G. M., and Poole, K. K. (1996) Isolation of illudin S from the mature basidiocarp of *Omphalotus illudens*, and isolation of illudin S and M from the fermentation broth of *Omphalotus olearis*. *Nat. Prod. Lett. 9,* 87-95.
37. Flohé, L., and Günzler, W. A. (1984) Assays of Glutathione Peroxidase. *Methods Enzymol. 105,* 114-121.
38. CellTiter 96® AQueous One Solution Cell Proliferation Assay. Promega, Ed. 2009; pp a-13.
39. See Appendix A for inhibition curves for treatment of Gpx with iodoacetamide.
40. See Appendix A for LC/MS spectra derived from AFs-treated Gpx.
41. Liu, X., Pietsch, K. E., and Sturla, S. J. (2011) Susceptibility of the antioxidant selenoenyzmes thioredoxin reductase and glutathione peroxidase to alkylation-mediated inhibition by anticancer acylfulvenes. *Chem. Res. Toxicol. 24,* 726-736.
42. Fang, J., Lu, J., and Holmgren, A. (2005) Thioredoxin reductase is irreversibly modified by curcumin: a novel molecular mechanism for its anticancer activity. *J Biol. Chem. 280,* 25284-25290.
43. Kim, J.-R., Yoon, H. W., Kwon, K.-S., Lee, S.-R., and Rhee, S. G. (2000) Identification of Proteins Containing Cysteine Residues That Are Sensitive to Oxidation by Hydrogen Peroxide at Neutral pH. *Anal. Biochem. 283,* 214-221.
44. Jan, Y.-H., Heck, D. E., Gray, J. P., Zheng, H., Casillas, R. P., Laskin, D. L., and Laskin, J. D. (2010) Selective Targeting of Selenocysteine in Thioredoxin Reductase by the Half Mustard 2-Chloroethyl Ethyl Sulfide in Lung Epithelial Cells. *Chem. Res. Toxicol. 23,* 1045-1053.
45. Gallegos, A., Berggren, M., Gasdaska, J. R., and Powis, G. (1997) Mechanisms of the regulation of thioredoxin reductase activity in cancer cells by the chemopreventive agent selenium. *Cancer Res. 57,* 4965-4970.
46. Zhang, J., Svehlikova, V., Bao, Y., Howie, A. F., Beckett, G. J., and Williamson, G. (2003) Synergy between sulforaphane and selenium in the induction of thioredoxin reductase 1 requires both transcriptional and translational modulation. *Carcinogenesis 24,* 497-503.
47. See Figure S5 in Supporting Information of Reference 41.

48. Yu, S. Y., Ao, P., Wang, L. M., Huang, S. L., Chen, H. C., Lu, X. P., and Liu, Q. Y. (1988) Biochemical and cellular aspects of the anticancer activity of selenium. *Biol. Trace Elem. Res. 15,* 243-255.
49. Novoselov, S. V., Calvisi, D. F., Labunskyy, V. M., Factor, V. M., Carlson, B. A., Fomenko, D. E., Moustafa, M. E., Hatfield, D. L., and Gladyshev, V. N. (2005) Selenoprotein deficiency and high levels of selenium compounds can effectively inhibit hepatocarcinogenesis in transgenic mice. *Oncogene 24,* 8003-8011.
50. Gundimeda, U., Schiffman, J. E., Gottlieb, S. N., Roth, B., and Gopalakrishna, R. (2009) Negation of the cancer-preventive actions of selenium by overexpression of protein kinase C{epsilon} and selenoprotein thioredoxin reductase. *Carcinogenesis 30,* 1553-1561.
51. Renko, K., Hofmann, P. J., Stoedter, M., Hollenbach, B., Behrends, T., Kohrle, J., Schweizer, U., and Schomburg, L. (2009) Down-regulation of the hepatic selenoprotein biosynthesis machinery impairs selenium metabolism during the acute phase response in mice. *FASEB J. 23,* 1758-1765.
52. Karunasinghe, N., Ferguson, L. R., Tuckey, J., and Masters, J. (2006) Hemolysate thioredoxin reductase and glutathione peroxidase activities correlate with serum selenium in a group of New Zealand men at high prostate cancer risk. *J. Nutr. 136,* 2232-2235.
53. Allmang, C., Wurth, L., and Krol, A. (2009) The selenium to selenoprotein pathway in eukaryotes: More molecular partners than anticipated. *Biochim. Biophys. Acta 1790,* 1415-1423.
54. Lu, J., and Holmgren, A. (2009) Selenoproteins. *J. Biol. Chem. 284,* 723-727.
55. Donovan, J., and Copeland, P. R. (2010) Threading the Needle: Getting Selenocysteine Into Proteins. *Antioxid. Redox Signaling 12,* 881-892.
56. Gong, J., Neels, J. F., Yu, X., Kensler, T. W., Peterson, L. A., and Sturla, S. J. (2006) Investigating the role of stereochemistry in the activity of anticancer acylfulvenes: synthesis, reductase-mediated bioactivation, and cellular toxicity. *J. Med. Chem. 49,* 2593-2599.
57. Woynarowska, B. A., Woynarowski, J. M., Herzig, M. C., Roberts, K., Higdon, A. L., and MacDonald, J. R. (2000) Differential cytotoxicity and induction of apoptosis in tumor and normal cells by hydroxymethylacylfulvene (HMAF). *Biochem. Pharmacol. 59,* 1217-1226.
58. Woynarowski, J. M., Napier, C., Koester, S. K., Chen, S. F., Troyer, D., Chapman, W., and MacDonald, J. R. (1997) Effects on DNA integrity and apoptosis induction by a novel antitumor sesquiterpene drug, 6-hydroxymethylacylfulvene (HMAF, MGI 114). *Biochem. Pharmacol. 54,* 1181-1193.
59. McMorris, T. C., Kelner, M. J., Wang, W., Moon, S., and Taetle, R. (1990) On the mechanism of toxicity of illudins: the role of glutathione. *Chem. Res. Toxicol. 3,* 574-579.
60. Arscott, L. D., Gromer, S., Schirmer, R. H., Becker, K., and Williams, C. H., Jr. (1997) The mechanism of thioredoxin reductase from human placenta is similar to the mechanisms of lipoamide dehydrogenase and glutathione reductase and is distinct from the mechanism of thioredoxin reductase from Escherichia coli. *Proc. Natl. Acad. Sci. U.S.A. 94,* 3621-3626.
61. Williams, C. H., Arscott, L. D., Muller, S., Lennon, B. W., Ludwig, M. L., Wang, P. F., Veine, D. M., Becker, K., and Schirmer, R. H. (2000) Thioredoxin reductase two modes of catalysis have evolved. *Eur. J. Biochem. 267,* 6110-6117.

62. Zhong, L., and Holmgren, A. (2000) Essential role of selenium in the catalytic activities of mammalian thioredoxin reductase revealed by characterization of recombinant enzymes with selenocysteine mutations. *J Biol. Chem. 275,* 18121-18128.
63. Hashemy, S. I., Ungerstedt, J. S., Zahedi Avval, F., and Holmgren, A. (2006) Motexafin gadolinium, a tumor-selective drug targeting thioredoxin reductase and ribonucleotide reductase. *J. Biol. Chem. 281,* 10691-10697.
64. Dal Piaz, F., Braca, A., Belisario, M. A., and De Tommasi, N. (2010) Thioredoxin System Modulation by Plant and Fungal Secondary Metabolites. *Curr. Med. Chem. 17,* 479-494.
65. Urig, S., and Becker, K. (2006) On the potential of thioredoxin reductase inhibitors for cancer therapy. *Semin. Cancer Biol. 16,* 452-465.
66. Bindoli, A., Rigobello, M. P., Scutari, G., Gabbiani, C., Casini, A., and Messori, L. (2009) Thioredoxin reductase: A target for gold compounds acting as potential anticancer drugs. *Coord. Chem. Rev. 253,* 1692-1707.
67. Tonissen, K. F., and Di Trapani, G. (2009) Thioredoxin system inhibitors as mediators of apoptosis for cancer therapy. *Mol. Nutr. Food Res. 53,* 87-103.
68. Ladenstein, R., Epp, O., Bartels, K., Jones, A., Huber, R., and Wendel, A. (1979) Structure analysis and molecular model of the selenoenzyme glutathione peroxidase at 2.8 A resolution. *J. Mol. Biol. 134,* 199-218.
69. Sun, Q. A., Wu, Y., Zappacosta, F., Jeang, K. T., Lee, B. J., Hatfield, D. L., and Gladyshev, V. N. (1999) Redox Regulation of Cell Signaling by Selenocysteine in Mammalian Thioredoxin Reductases. *J. Biol. Chem. 274,* 24522-24530.
70. Nordberg, J., Zhong, L., Holmgren, A., and Arner, E. S. (1998) Mammalian thioredoxin reductase is irreversibly inhibited by dinitrohalobenzenes by alkylation of both the redox active selenocysteine and its neighboring cysteine residue. *J. Biol. Chem. 273,* 10835-10842.
71. Arnér, E. S., Nakamura, H., Sasada, T., Yodoi, J., Holmgren, A., and Spyrou, G. (2001) Analysis of the inhibition of mammalian thioredoxin, thioredoxin reductase, and glutaredoxin by cis-diamminedichloroplatinum (II) and its major metabolite, the glutathione-platinum complex. *Free Radical Biol. Med. 31,* 1170-1178.
72. Anestål, K., and Arnér, E. S. J. (2003) Rapid Induction of Cell Death by Selenium-compromised Thioredoxin Reductase 1 but Not by the Fully Active Enzyme Containing Selenocysteine. *J. Biol. Chem. 278,* 15966-15972.
73. Anestål, K., Prast-Nielsen, S., Cenas, N., and Arnér, E. S. J. (2008) Cell Death by SecTRAPs: Thioredoxin Reductase as a Prooxidant Killer of Cells. *PLoS One 3,* e1846.
74. See Figure S1 in Supporting Information of Reference 41.
75. Cassidy, P. B., Edes, K., Nelson, C. C., Parsawar, K., Fitzpatrick, F. A., and Moos, P. J. (2006) Thioredoxin reductase is required for the inactivation of tumor suppressor p53 and for apoptosis induced by endogenous electrophiles. *Carcinogenesis 27,* 2538-2549.
76. Tamura, T., and Stadtman, T. C. (1996) A new selenoprotein from human lung adenocarcinoma cells: purification, properties, and thioredoxin reductase activity. *Proc. Natl. Acad. Sci. U.S.A. 93,* 1006-1011.
77. Hu, Y., Urig, S., Koncarevic, S., Wu, X., Fischer, M., Rahlfs, S., Mersch-Sundermann, V., and Becker, K. (2007) Glutathione- and thioredoxin-related

enzymes are modulated by sulfur-containing chemopreventive agents. *Biol. Chem. 388,* 1069-1081.

78. Vadgama, J. V., Wu, Y., Shen, D., Hsia, S., and Block, J. (2000) Effect of selenium in combination with Adriamycin or Taxol on several different cancer cells. *Anticancer Res. 20,* 1391-1414.
79. Fakih, M., Cao, S., Durrani, F. A., and Rustum, Y. M. (2005) Selenium protects against toxicity induced by anticancer drugs and augments antitumor activity: a highly selective, new, and novel approach for the treatment of solid tumors. *Clin. Colorectal Cancer 5*, 132-135.
80. Rudolf, E., Radocha, J., Cervinka, M., and Cerman, J. (2004) Combined effect of sodium selenite and campthotecin on cervical carcinoma cells. *Neoplasma 51,* 127-135.

Chapter Three:

Quantification of acylfulvene- and illudin S-DNA adducts in cells with variable bioactivation capacities[1]

[1] Portions reprinted with permission from Pietsch, K. E., Van Midwoud, P. M., Villalta, P. W., Sturla, S. J. (2013) Quantification of acylfulvene- and illudin S-DNA adducts in cells with variable bioactivation capacities. *Chem. Res. Toxicol. 26*, 146–155. Copyright 2013 American Chemical Society.

1. Introduction

Alkylating agents continue to be a useful and effective strategy for anticancer therapy, but tend to lack selectivity and result in unwanted side effects at off-site targets. One strategy to increase the selectivity of alkylating agents involves metabolic activation of a prodrug. A well-known example is mitomycin C, which is bioactivated by NAD(P)H:quinone oxidoreductase (NQO1), an enzyme that is overexpressed in colon and non-small cell lung cancer cells.[1] Other examples are the acylfulvenes (AFs), semisynthetic analogues of their more toxic natural product precursor illudin S (structures in Scheme 1). AFs are bioactivated by prostaglandin reductase 1 (PTGR1) to cytotoxic reactive intermediates that can react with nucleophilic biomolecules, including DNA. The bioactivation of AFs has been implicated in their selective toxicity in cancer cells versus normal cells, and cells are more sensitive to AFs when they have higher levels of PTGR1.[2–4] Although illudin S also can be reductively metabolized by PTGR1, illudin S displays poor selectivity for cancer cells versus normal cells,[5] and its cytotoxicity does not correlate with bioreduction.[2] The aim of this study was to understand how DNA alkylation may contribute to differential cytotoxicity profiles on the basis of drug chemical structure.

The cytotoxicities and alkylation properties of AFs and illudin S, and how they differ, may be attributed to the changes in their chemical structures (Scheme 1). Illudin S is comprised of a spirocyclopropyl-substituted fused 6,5-bicyclic ring system. AFs contain these same components but with additional unsaturation such that the five-membered ring is a fulvene, acylated by virtue of the carbonyl in the six-membered ring. Along with the parent unsubstituted AF, the AFs include many derivatives with additional substituents to the same ring system [including hydroxymethylacylfulvene (HMAF), which has been in human clinical trials[6]]. To varying extents, AF analogues share

cytotoxicity properties with the parent molecule AF, as well as potentially improved pharmacological properties.[7] DNA is a key cellular target for each of these compounds, and we have identified previously the major cellular drug-specific DNA adducts for the unsubstituted parent compound AF and demonstrated that adduct formation is positively correlated with PTGR1 levels.[8,9] However, there is no reported absolute quantification of AF-DNA adducts in cells, and the structures of illudin S-DNA adducts remain unknown.[10,11] DNA adduct characterization and quantification can be a basis for chemical biomarkers for understanding how toxin exposure leads to DNA damage, especially when their structures definitively link the damage to the toxin.[12–14]

In this study, we chemically identified and biologically tracked adducts arising from illudin S and AF in cancer cells as a function of cellular bioactivation capacity. With a quantitative isotope dilution mass spectrometry method for the major 3-AF-Ade adduct,[9] we measured levels of AF or illudin S adducts in cells. To assess the contribution of the enzyme PTGR1 to adduct levels, we engineered SW-480 colon cancer cells to overexpress PTGR1 by a stable transfection. The newly developed cells (PTGR1-480) provide a robust model for studying the impact of PTGR1 on toxicity and adduct formation. With the combination of analytical approaches and an engineered cell line, we addressed in this study the hypothesis that AF-mediated DNA alkylation levels in cells are influenced by bioactivation capacity, while adducts from the non-selective toxin illudin S arise non-discriminately.

2. Experimental procedures

2.1. Chemicals and enzymes

AF[3,15] and 3-AF-Ade-d_3[9] were prepared as previously described. Illudin S, isolated from *Omphalotus* species, was provided by MGI Pharma.[16] Water was purified with a Milli-Q Integral Water Purification System (Millipore Corporation, Billerica, MA). Rat liver cytosol was prepared as previously described and provided by Dr. Bruno Stieger (Klinische Pharmakologie and Toxikologie, UniversitätSpital Zürich).[17] NADPH was purchased from Calbiochem (San Diego, CA). Deoxyguanosine hydrate was purchased from Tokyo Chemical Industry (Tokyo, Japan). Alkaline phosphatase was purchased from Roche (Mannheim, Germany).

2.2. Instrumentation

Cytotoxicity measurements were made with a BioTek EL808 absorbance microplate reader (BioTek Instruments, Inc., Winooski, VT). The DNA concentration was measured using a NanoDrop™ 1000 spectrophotometer (Thermo Scientific, Waltham, MA). Quantitative LC-electrospray ionization (ESI)-MS^2 analysis was carried out on a Waters nanoAcquity Ultra Performance LC (Waters Corporation, Milford, MA) interfaced with a Thermo TSQ Vantage triple quadrupole mass spectrometer (Thermo Scientific). Qualitative LC-ESI-MS^n analysis was carried out on a Waters nanoAcquity Ultra Performance LC (Waters Corporation) interfaced with a Thermo LTQ Velos ion trap mass spectrometer (Thermo Scientific). Thermo Xcalibur software was used for mass spectrometry data acquisition and processing. Studies regarding the identity of the illudin S-Ade adduct were performed with material that was isolated by liquid chromatography performed on an Agilent Technologies 1200 Series HPLC (Agilent Technologies, Santa Clara, CA).

2.3. Reactions of calf thymus DNA (ctDNA) with illudin S and constant neutral loss scanning with triple stage mass spectrometry (CNL-MS^3) analysis

In a microcentrifuge tube (1.5 mL), illudin S (10 μL, 50 mM) was mixed with ctDNA (2 mg) in phosphate buffer (100 μL, 1.0 mM, pH 7.4). PTGR1 (4.2 μL, 1.7 mg/mL) and an NADPH-regenerating system comprised of glucose-6-phosphate dehydrogenase (1.2 μL, 4.1 U/μL), glucose-6-phosphate (100 μL, 28.2 mg/mL in water), and $NADP^+$ (100 μL, 38.3 mg/mL in water) were added. The mixture was diluted to a final volume of 1 mL with water, and samples were incubated at 37 ^oC for 24 h. DNA was precipitated by adding 3 mL of ice cold ethanol, centrifuging at 4000 rpm for 30 min, and removing supernatant. To the resulting DNA sample, 2 mL of 70% ethanol was added, followed by centrifugation at 4000 rpm for 20 min. The supernatant was removed and the remaining DNA pellet was dried under a stream of N_2. To hydrolyze the DNA, 0.83 mL Tris buffer (10 mM with 5 mM $MgCl_2$) and 86.2 μL deoxyribonuclease I from bovine pancreas (5 U/μL in Tris buffer) were added, and the mixture was allowed to incubate at 37 ^oC for 10 min. Phosphodiesterase I (18.4 μL, 0.001 U/μL in Tris buffer) and alkaline phosphatase (13.8 μL, 10 U/μL) were added and the mixture was allowed to incubate at 37 ^oC for 1 h. Aliquots were removed directly from this reaction mixture and analyzed with no further processing. The same procedure, but with AF or dimethyl sulfoxide (DMSO), was carried out as positive and negative controls, respectively.

CNL-MS^3 was performed on a Thermo LTQ Velos mass spectrometer by adapting a previously published analytical method.[18] Development of this method and analysis of samples was performed by Dr. Peter Villalta. MS ionization parameters were optimized by tuning with deoxyguanosine (dGuo). The ESI source was set in positive ion mode with the following parameters: S-lens RF level, 60%; capillary temperature, 275 ^oC; voltage, 5 kV; sheath gas pressure, 10; and auxiliary gas pressure, 5. Full scan event range was *m/z*

265–600. MS^2 scan event parameters included the following: activation type, collision-induced dissociation (CID); minimum signal required, 2000; isolation width, *m/z* 2.0; normalized collision energy, 35; activation Q, 0.25; and activation time, 10 ms. MS^3 scan event parameters were the same as those for MS^2, except the minimum signal required was 500. Alternating full-scan and data-dependent MS^2 scanning is performed with MS^2 fragmentation occurring on the top four most intense peaks observed in the preceding full-scan spectrum. Observation of a neutral loss of *m/z* 116 between the MS^2 parent and a fragment ion (provided it is one of the top three most intense with a signal ≥500) triggers an MS^3 scan event. Signals identified also in the negative control sample were excluded; these included, for example, DNA bases and base clusters. Dynamic exclusion was enabled with a repeat count of 1, an exclusion duration of 30 s, and an exclusion list size of 50. Chromatography was performed with a Phenomenex Synergi Polar RP 80 Å column (150×0.5 mm, 4 μm particle size) (Phenomenex, Torrance, CA). The ultra performance liquid chromatography (UPLC) flow rate was 10 μL/min and the mobile phases were 0.1% formic acid in water (v/v) (mobile phase A) and 0.1% formic acid in acetonitrile (v/v) (mobile phase B). The mobile phase gradient elution was as follows: 98% mobile phase A for 5 minutes, then decrease to 5% mobile phase A over 60 min, hold at 5% mobile phase A for 4 min, return to starting conditions over 1 min, and hold at starting conditions for 15 min (85 min total run time).

2.4. Reactions of nucleic acids with illudin S and qualitative analysis by LC-ESI-MS^2

In a microcentrifuge tube (1.5 mL), a mixture of illudin S (10 μL, 10 mM) and nucleoside [3.7 mmol deoxyadenosine (dAdo) or 10.2 mmol dGuo] or ctDNA (1 mg) was combined with 150 μL phosphate buffer (0.1 M, pH 7.4) and 20 μL $MgCl_2$ (50 mM). For

reactions carried out in the presence of enzymes, rat liver cytosol (300 μg) and NADPH (50 μL, 100 mM) were added. Reactions were diluted to a final volume of 0.5 mL by addition of water and incubated at 37 ^{o}C in a shaking heat block for 24 h. Following the incubation, samples were vortex mixed and heated at 90 ^{o}C for 1 h and then dried by rotary vacuum centrifugation. The resulting solids were washed with methanol (3×300 μL) and filtered with a 0.45 μm nylon syringe filter, which was then rinsed with 300 μL methanol. Methanol was evaporated by rotary vacuum centrifugation, and the resulting solids were dissolved in 20 μL 50% methanol/50% water (v/v). The resulting samples were analyzed by LC-ESI-MS^2 on a Thermo LTQ Velos mass spectrometer, with MS ionization parameters optimized by tuning with dAdo. The ESI source was set in positive ion mode with the following parameters: capillary temperature, 200 ^{o}C; voltage, 3.5 kV; sheath gas pressure, 10; auxiliary gas pressure, 5. Scan events included full-scan plus MS^2 of *m/z* 384.0, 400.0, 352.0, and 336.0. Scan event parameters for each mass monitored were set as follows: activation type, CID; normalized collision energy, 40; activation Q, 0.250; activation time, 10 ms; isolation width, *m/z* 1.0. Chromatography was performed with a Phenomenex Synergi Fusion column (150×0.5 mm, 4 μm particle size) (Phenomenex). The UPLC flow rate was 10 μL/min and the mobile phases were 0.1% formic acid in water (v/v) (mobile phase A) and 0.1% formic acid in acetonitrile (v/v) (mobile phase B). The mobile phase gradient elution was as follows: 100% A to 0% A over 30 min, hold at 0% A for 10 min, return to starting conditions over 2 min, and re-equilibrate for 15 min (57 min total run time).

2.5. Cell culture and transfection

SW-480 cells were provided by Dr. Giancarlo Marra (Institute of Molecular Cancer Research, University of Zurich). Cells were maintained in RPMI 1640 medium

with 10% fetal calf serum (v/v) and 1% pen/strep (v/v), and incubated at 37 ^{o}C in a humidified incubator containing 5% CO_2. Stable transfection of 2×10^5 SW-480 cells was performed in a six-well plate with 1 μg Myc-DDK tagged PTGR1 cDNA (OriGene Technologies, Rockville, MD) with Lipofectamine reagents (Invitrogen, Inc.) and selected with Geneticin (Invitrogen, Inc.).[2]

2.6. Immunoassay of PTGR1 levels in SW-480 cells

Cells were digested with trypsin (Promega, Madison, WI; enzyme:substrate ratio 1:20; 15 h, 37 °C) and homogenized with a sonication needle, and the resulting lysates (70 μg) were separated on NuPAGE® 4–12% Bis-Tris gel at 200 V for 45 min in 1X NuPAGE MES SDS running buffer (Invitrogen, Carlsbad, CA) and transferred to Amersham Hybond-P polyvinylidene fluoride (PVDF) membrane (GE Healthcare, Buckinghamshire, United Kingdom) at 30 V for 60 min in 1X NuPAGE® transfer buffer (Invitrogen). PVDF membranes were blocked with 5% (w/v) nonfat milk powder in Tris-buffered saline (TBS)/Tween 20 (1%, v/v) (blocking buffer) for 2 h at room temperature. The membrane was incubated with primary anti-PTGR1 antibody (rabbit polyclonal anti-PTGR1, Sigma, 1:500 dilution in blocking buffer) at 4 ^{o}C for 12 h and subsequently washed [1×25 mL blocking buffer for 10 min, 2×25 mL TBS/Tween 20 (1%, v/v) for 10 min]. The membrane was then incubated with secondary conjugated antibody (anti-rabbit IgG HRP, GE Healthcare, 1:5000 dilution in blocking buffer) at room temperature for 1 h, followed by the same washing steps described above. Proteins were visualized with a Pierce ECL Western Blotting Substrate (Thermo Scientific, Rockford, IL) by mixing the Peroxide Solution and Luminol Enhancer Solution in a 1:1 ratio and rinsing the mixture over the membrane for 1 min. The treated membrane was exposed to a film for 8 min and

[2] This experiment, performed by Dr. Paul van Midwoud and published previously, is included here for completeness.

developed. The protein bands were quantified with ImageJ software. Actin served as loading control (rabbit polyclonal anti-actin antibody, Sigma, 1:1000 dilution in blocking buffer).

2.7. Cell viability assay

Cells were seeded in a 96-well plate at a density of 2.5×10^3 cells/well and were allowed to attach overnight. Experiments were initiated by replacing the maintenance media with media containing AF (final concentration, 0.1% DMSO)[3] or illudin S (final concentration, l% DMSO) at indicated concentrations. [AF cytotoxicity data were the same, whether experiments were conducted with 0.1 or 1% DMSO (final concentration); however, illudin S cytotoxicity results were not reproducible with 0.1% DMSO. No changes in cell morphology or proliferation were observed for cells incubated with 1% DMSO as compared to cells incubated without DMSO.] Cell viability was measured 48 h later with the CellTiter 96 AQ_{ueous} One Solution Cell Proliferation Assay, which measures the metabolic capacity of viable cells as determined by the propensity to reduce the 3-(4,5-dimethylthiazol-2-yl)-5-(3-carboxymethoxyphenyl)-2-(4-sulfophenyl)-2*H*-tetrazolium (MTS) to the corresponding formazan product (Promega Corporation, Madison, WI). Absorbance at 490 nm was measured 4 h after adding 20 μL MTS solution to each well. Linear regression analysis and IC_{50} calculations were performed using Sigma Plot (version 12.2).

2.8. Isolation of DNA from drug-treated cells

Cells were seeded in six-well plates at a density of 1×10^5 cells/well and allowed to attach overnight. The media was replaced with 2 mL fresh media and 2 μL AF stock in

[3] These experiments, performed by Dr. Paul van Midwoud and published previously, are included here for completeness.

DMSO (final concentration, 0.1% DMSO)[4] or 2 mL fresh media and 20 μL illudin S stock in DMSO (final concentration, 1% DMSO). After incubation for the time indicated in the Results, cells were washed once with 1X PBS, and then, DNA was isolated with the Wizard SV Genomic DNA Purification System according to manufacturer's protocol (Promega). Thus, 500 μL lysis buffer was added to each well, and sample lysate was transferred to a Wizard SV minicolumn assembly. The assembly was centrifuged (13000*g*, 2 min) and filtrate in the collection tube was discarded. Wizard SV wash solution (650 μL) was added, the assembly was centrifuged (13000*g*, 1 min), and filtrate was discarded from the collection tube; this step was repeated for a total of four washes. Afterwards, the collection tube and the minicolumn assembly was centrifuged (13000*g*, 2 min) to dry the binding matrix, and the minicolumn was transferred to a new 1.5 mL tube containing 2 μL RNAse solution. Nuclease-free water (250 μL) was added to the minicolumn and after 2 min at room temperature, the assembly was centrifuged (13000*g*, 5 min), and then allowed to stand at room temperature for 10 min. The DNA concentration of the resulting solution was determined with a NanoDrop™ 1000 spectrophotometer (Thermo Scientific), and the solution was stored at 4 ^{o}C for up to four days.

2.9. Preparation of cellular DNA samples for adduct analysis

To the purified DNA solution, obtained as described above, was added an equal volume of water plus 3 μL 3-AF-Ade-d_3 [200 nM in 50% methanol/water (v/v)] as an internal standard. The resulting solution was heated at 90 ^{o}C for 1 h and then dried by rotary vacuum centrifugation. The resulting solids were washed with methanol (3×300

[4] These experiments, performed by Dr. Paul van Midwoud and published previously, are included here for completeness.

uL) and filtered with a 0.45 μm nylon syringe filter, which was then rinsed with 300 μL methanol. Methanol was evaporated by rotary vacuum centrifugation, and the resulting solids were dissolved in 20 μL 50% methanol/50% water (v/v) for quantitative LCMS analysis.

2.10. Quantitation of DNA adducts by LC-ESI-MS^2

Quantitative adduct measurements were performed by LC-ESI-MS^2 in SRM mode by a method adapted from the procedure of Neels *et al.*[9] MS ionization parameters were optimized by tuning with 1 μM AF-Ade solution. The ESI source was set in positive ion mode with the following parameters: capillary temperature, 300 ^{o}C; voltage, 3 kV; sheath gas pressure, 10; aux gas pressure, 5; Q2 CID gas pressure, 1.5 mTorr; collision gas, argon; scan width, *m/z* 0.100; scan time, 0.050 s; collision energy, 17 V; Q1 peak width, 0.70 amu; and Q3 peak width, 0.70 amu. Mass transitions monitored were *m/z* 336.2 to 201.1, *m/z* 339.2 to 204.1, and *m/z* 352.0 to 201.0. For analysis of illudin S-treated samples, *m/z* 384.2 to 201.1, *m/z* 384.2 to 336.2, *m/z* 400.2 to 201.1, and *m/z* 400.2 to 352.0 were also monitored. Chromatography was performed with a Phenomenex Synergi Polar-RP 80 Å column (150×0.5 mm, 4 μm particle size) (Phenomenex). The UPLC flow rate was 10 μL/min and the mobile phases were 3% acetonitrile and 0.1 % formic acid in water (v/v) (mobile phase A) and 0.1% formic acid in acetonitrile (v/v) (mobile phase B). The mobile phase gradient elution was as follows: 100% mobile phase A to 0% mobile phase A over 20 minutes, hold at 0% mobile phase A for 10 minutes, return to starting conditions over 2 minutes, and re-equilibrate for 8 minutes (40 min total run time).

2.11. Statistical evaluation

All data are expressed as means ± 1 SD. For the IC_{50} values and DNA adduct levels, results were analyzed by Dr. Paul van Midwoud for significant differences by Student's *t* test, with $p < 0.05$ considered significantly different.

3. Results

3.1. Formation and identification of illudin S-DNA adducts

As a fast approach to identify unknown illudin S-DNA adducts, we performed mass spectral analysis by data-dependent scanning for loss of 116 amu (deoxyribose) as a diagnostic of the presence of a DNA adduct. The method that we used is adapted from a previously described CNL-MS^3 strategy.[18] Thus, illudin S was allowed to react with ctDNA in the presence of PTGR1/NADPH, and the resulting mixture was analyzed by

Scheme 1. AF- and illudin S-DNA adduct structures and corresponding *m/z* values: (A) AF-DNA adducts identified in previous studies and (B) Anticipated illudin S-DNA adducts.

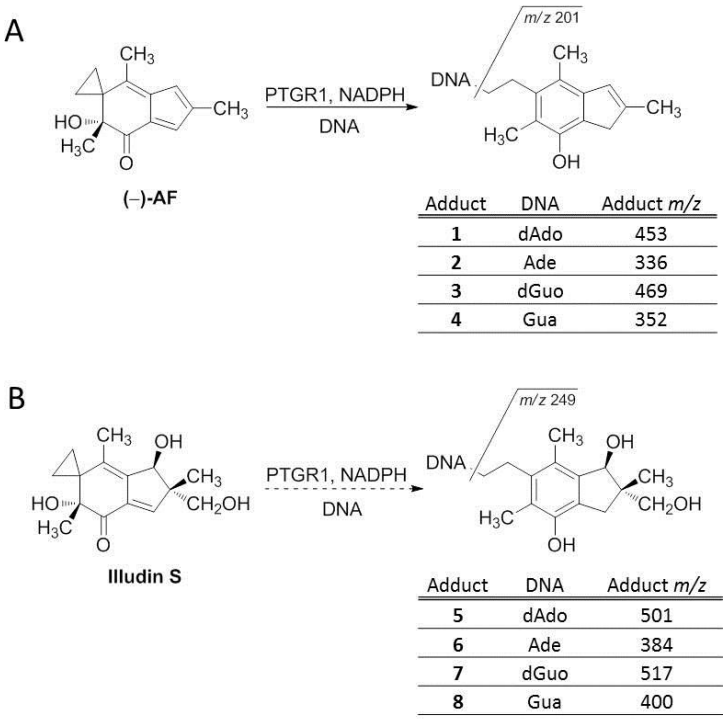

Adduct	DNA	Adduct *m/z*
1	dAdo	453
2	Ade	336
3	dGuo	469
4	Gua	352

Adduct	DNA	Adduct *m/z*
5	dAdo	501
6	Ade	384
7	dGuo	517
8	Gua	400

mass spectrometry in the CNL-MS^3 scan mode by Dr. Peter Villalta. On the basis of *m/z* values and fragmentation patterns analogous to known AF-DNA adducts (Scheme 1A), we anticipated that illudin S might react with DNA in a similar fashion and that the presence of mass fragments with *m/z* 249 would arise from bioactivated illudin S (Scheme 1B). We detected a mass fragment *m/z* 249, but interestingly, we also detected fragments *m/z* 336 and 201, which correspond to the AF-Ade DNA adduct **2** (Figure 1).

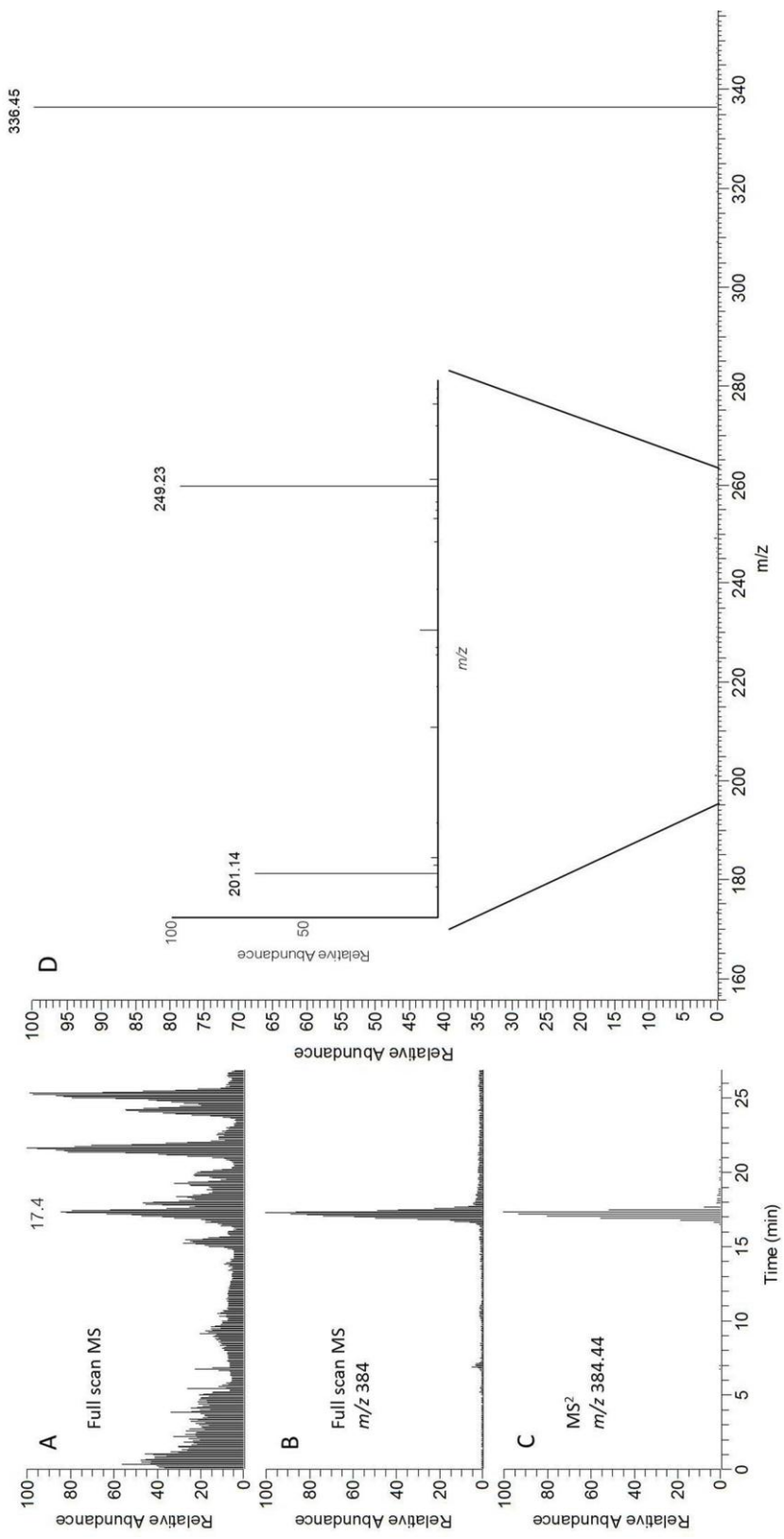

Figure 1. CNL-MS^3 data-dependent analysis of products of reactions of ctDNA with illudin S in the presence of PTGR1 and NADPH. Data are normalized to the base peak in each spectra, and the relative intensity is given as a normalized level (NL). (A) Full-scan MS (NL 1.55E6). (B) Full-scan MS of *m/z* 384 (NL 9.88E5). (C) Triggered MS^2 of *m/z* 384.44 (NL 1.25E6). (D) Mass spectra of peak in panel C with major fragment *m/z* 336 and minor fragments *m/z* 249 and 201 (inset).

On the basis of these data regarding the presence and potential identity of illudin S adducts as being derived from the reaction with dAdo, having the same fragmentation pattern as AF adducts, and being susceptible to depurination, we performed additional experiments in which we reacted illudin S with dAdo and ctDNA. After reaction, adduct depurination was induced by neutral thermal hydrolysis (NTH), and resulting samples were analyzed with an ion trap mass spectrometer, wherein we tested for the presence of mass fragments that we had observed in the CNL-MS^3 experiments described above. We obtained evidence for a compound that eluted at 8.6 min and gave rise to two different MS peaks: *m/z* 384, which would correspond with the illudin S-Ade adduct **6**, and *m/z* 336, which would correspond with the AF-Ade adduct **2**. Furthermore, fragmentation of both yielded the corresponding indene moieties (*m/z* 249 or 201, respectively), also at the same retention time. The retention time (t_R) of the peak corresponding to **2** did not, however, match that of the authentic 3-AF-Ade standard, which suggested that the AF adducts (like **2**) detected in illudin S-treated samples arose from illudin S adducts (like **6**) and appeared to be products of a reaction taking place in the source of the mass spectrometer. Attempts to isolate quantities of the illudin S adducts suitable for more complete characterization were not successful; however, in subsequent cell-based studies, nano-ESI-MS^3 analysis (performed by Dr. Cédric Bovet) of pooled cell lysates (from 27 samples, each sample collected from one well of a six well plate) from illudin S-treated

HT-29 cells further confirmed the LC-MS behavior of the adduct and its presence in both cell-free and cell-based systems.[19]

3.2. Transfection and characterization of PTGR1-overexpressing cells

Previous experiments regarding the relationship of AF toxicity with PTGR1 expression relied on cells transiently transfected with a PTGR1-encoding vector; however, due to high interexperiment variability in transfection efficiency and resulting PTGR1 levels, data from different studies cannot be compared reliably, and precise experimental situations cannot be reproduced.[2–4] To address such shortcomings of the transient transfection system and provide a more robust model for the present and for future work, we developed and utilized a stably transfected cell line that overexpresses PTGR1 relative to its isogenic parent. Thus, SW-480 cells were transfected with Myc-DDK-tagged PTGR1 cDNA and selected with Geneticin. PTGR1 levels in three different passages of the newly engineered transfected PTGR1-480 versus SW-480 cells were measured by Western blot and mass spectrometry (targeted SRM). Western blot analysis revealed two bands of interest: endogenously expressed PTGR1 (37 kDa) and Myc-DDK tagged-PTGR1 expressed in PTGR1-480 cells (40 kDa, Figure 2). The Myc-DDK tag (3 kDa) is fused to the C-terminus of the enzyme in PTGR1-480 cells; no tagged enzyme was present in SW-480 cells. We assume that these non-identical enzymes have similar catalytic efficiencies, although this has not been explicitly tested with isolated tagged enzyme. The overexpression of PTGR1 in PTGR1-480 cells is further supported by targeted SRM analysis for PTGR1, performed by Dr. Paul van Midwoud, which showed a 17-fold induction of the enzyme relative to SW-480 cells (Table 1). To ensure that other reductase enzymes were not overexpressed in PTGR1-480 cells, peptides corresponding to thioredoxin reductase (TrxR1) and NQO1 were also monitored, and there were no differences.

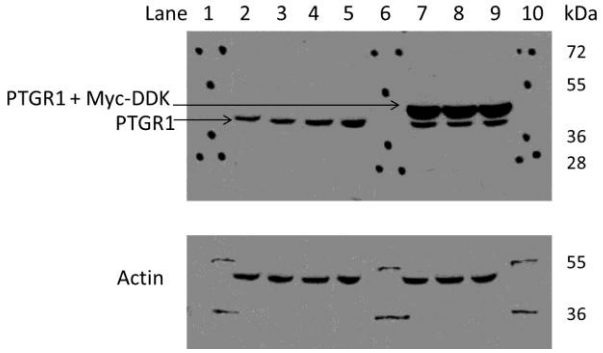

Figure 2. Western blot analysis of PTGR1 levels in SW-480 and PTGR1-480 cells. Lanes 1, 6, and 10, marker; lanes 2–4, SW-480 cells; lane 5, SW-837 cells (positive control); lanes 7–9, PTGR1-480 cells. All lanes loaded with 70 μg protein, except lane 4 (62 μg).

Table 1. SRM protein measurements in SW-480 and PTGR1-480 cells.

Protein[a]	**Fold expression**[b]
PTGR1	17 ± 2
TrxR1	1.1 ± 0.2
NQO1	1.3 ± 0.3

[a]TrxR1, thioredoxin reductase 1; NQO1, NAD(P)H quinone reductase 1. [b]Fold expression in PTGR1-480 cells is relative to SW-480 cells. Average of two replicates from three passages.

3.3. Cytotoxicity

To test the relative susceptibility of PTGR1-480 versus SW-480 cells toward AF or illudin S, cell viabilities were evaluated after 48 h treatment. In the case of AF, we found that PTGR1-480 cells were 3-fold more sensitive to the drug compared to SW-480 cells (IC_{50} values of 104 ± 22 nM and 301 ± 14 nM, respectively, n = 4, p = 0.002, Figure 3A). For illudin S, however, cell viability in PTGR1-480 versus SW-480 cells was diminished, and both situations were more similar (IC_{50} values of 10 ± 1 nM and 14 ± 1 nM, respectively, n = 3, p = 0.08, Figure 3B).

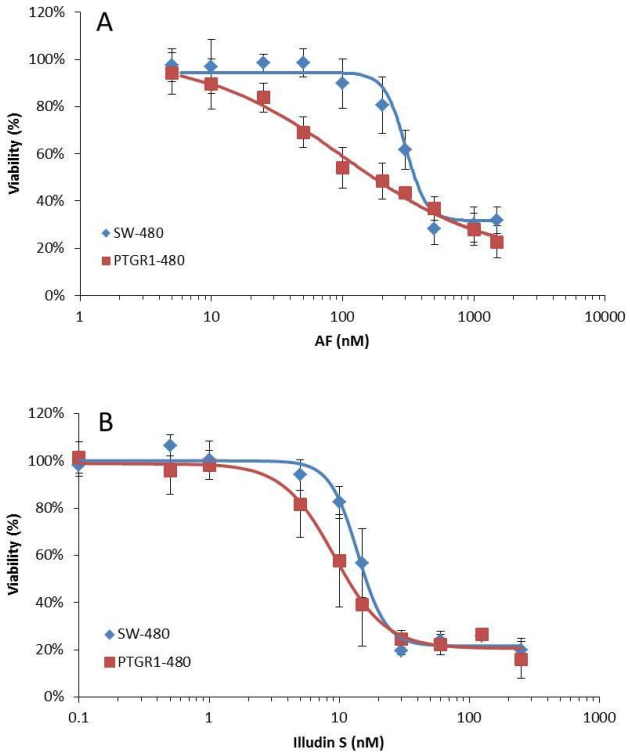

Figure 3. Cell viability of drug-treated SW-480 and PTGR1-480 cells (48 h treatment time). (A) AF-treated cells (n = 4). (B) Illudin S-treated cells (n = 3).

3.4. Quantitation of AF- and illudin S-DNA adduct formation in cells

DNA adduct formation in PTGR1-480 versus SW-480 cells treated with either AF or illudin S was evaluated quantitatively by stable isotope dilution mass spectrometry. We established and applied a general SRM-based analysis method to measure adducts in all four cases. The method involved monitoring fragmentation of AF-Ade (**2**, *m/z* 336) and AF-Gua (**4**, *m/z* 352) adducts to the AF indene moiety (*m/z* 201). In the case of cells being treated with illudin S rather than AF, and on the basis of the results described above for the behavior of illudin S-derived adducts, the same AF adduct mass transitions were used as a diagnostic of illudin S-derived adducts, in combination with additional ions corresponding to conversion of the illudin S adduct to the AF adduct. We used 3-AF-Ade, stable isotope-labeled with three deuterium atoms and as previously reported,[9] to semiquantify illudin S-Ade adducts.

AF-DNA adducts were measured in AF-treated PTGR1-480 and SW-480 cells as a function of concentration and treatment time. Cells were treated with varying concentrations of AF ranging from 50 to 1500 nM (0.5–15-fold IC_{50} for PTGR1-480; 0.17–5-fold IC_{50} for SW-480). In both cell types, there was a dose-dependent increase in AF-Ade (14–355 adducts/10^7 nucleotides in SW-480 cells and 21–700 adducts/10^7 nucleotides in PTGR1-480 cells), and levels in transfected cells were up to 2-fold higher than in control cells (Figure 4A). The rate of AF adduct formation and their persistence were also evaluated for 500 nM AF (1.7-fold IC_{50} in SW-480 cells; 4.8-fold IC_{50} in PTGR1-480 cells) as a function of time (Figure 5A). For AF-Ade, there were 4-fold more adducts in PTGR1-480 cells as compared to control cells at the 4 and 8 h treatment times. This difference diminished, however, to 1.7-fold by 72 h. In both cell types, the quantity of adducts gradually increased as a function of treatment time, with the greatest number

of adducts being measured at 72 h (136 and 227 adducts/10^7 nucleotides for SW-480 and PTGR1-480 cells, respectively).

On the basis of the semiquantitative strategy described above, we estimated differences in DNA adduct formation in illudin S-treated PTGR1-480 versus SW-480 cells after treatment with varying concentrations of illudin S ranging from 5 to 100 nM (0.5–10-fold IC_{50}). Like the AF-treated cells, we observed a dose-dependent response in adduct formation. However, the results from SW-480 and PTGR1-480 cells were not significantly different (Figure 4B). The rate of illudin S adduct formation was evaluated over the same five time points as for AF and with 20 nM illudin S (1.7-fold IC_{50}, Figure 5B). In both cases, there was large interexperiment variability in adduct levels for the two short time points (4 and 8 h), but overall, it appeared that PTGR1-480 cells had 2.4-fold more adducts than SW-480 at the early time point (4 h) and less than half at the latest time point (72 h).

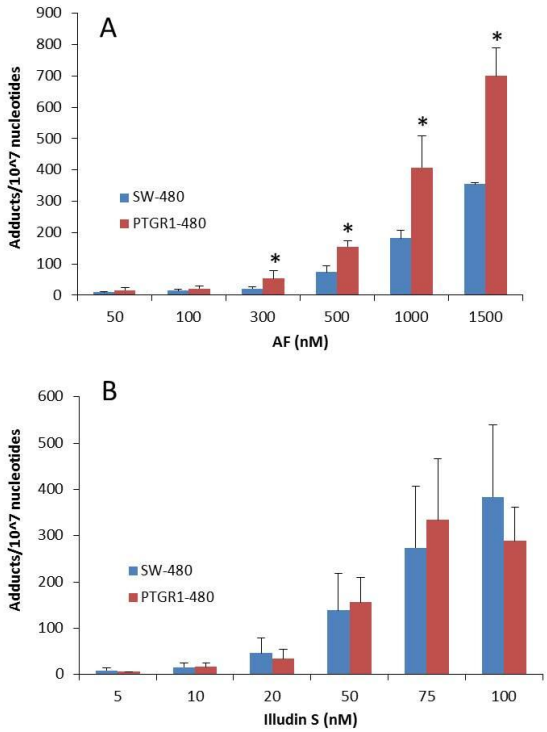

Figure 4. Concentration-dependent formation of Ade-adducts in drug-treated SW-480 (blue/left) and PTGR1-480 cells (red/right) (24 h treatment time). (A) 3-AF-Ade DNA adducts (n = 4). (B) Illudin S-Ade DNA adducts (n = 3). Asterisks denote statistically significant differences between levels in SW-480 vs. PTGR1-480 cells ($p < 0.05$).

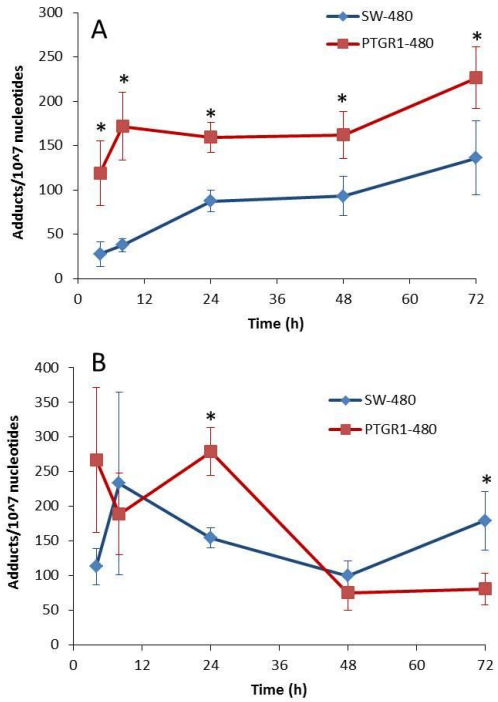

Figure 5. Time-dependent formation of AF- or illudin S-derived Ade adducts in drug-treated SW-480 and PTGR1-480 cells. (A) 3-AF-Ade, cells treated with 500 nM AF (n = 3). (B) Illudin-S-Ade, cells treated with 20 nM illudin S (n = 3). Asterisks denote statistically significant differences between levels in SW-480 vs. PTGR1-480 cells ($p < 0.05$).

4. Discussion

Various biochemical factors have been addressed with respect to the impact of AF and illudin S cytotoxicity, including cellular uptake, metabolism, and DNA repair capacity. For AF, reductive bioactivation and subsequent DNA adduct formation have emerged as important controlling factors; however, these conclusions have been made with available data regarding only relative quantities of AF-DNA adducts in cells transiently transfected to express PTGR1.[8] Furthermore, the correlation between PTGR1, adduct formation, and cytotoxicity is hypothesized to not hold true for illudin S.[2] This assumption, however, has not been explicitly tested, nor has it been determined whether

elevated adduct formation is a contributing factor in the greater cytotoxicity of illudin S versus AF. Establishing such relationships would be important for better understanding how differences in illudin S and AF structures and reactivities contribute to their differential performance as chemotherapy drugs; however, previous limitations in addressing these questions relate to the lack of availability of stable PTGR1-overexpressing cell lines and of analytical strategies for measuring illudin S-derived DNA adducts. In this study, we engineered SW-480 cells to overexpress PTGR1 and derived a mass spectrometric approach for evaluating illudin S adducts, and we used these tools to compare AF and illudin S cytotoxicity and DNA adduct levels on the basis of cellular PTGR1 levels.

Mass spectrometric analysis of illudin S-treated ctDNA, obtained by data-dependent CNL, provided initial evidence that mass fragments from illudin S-derived DNA adducts are the same as AF-derived fragments. This situation was further confirmed by standard MS^2 analysis of these samples and of the product of the reaction of illudin S with dAdo. It remains possible that adducts with other nucleobases and/or other chemical structures form. On the basis of fragmentation and adduct t_R, it appears that illudin S-derived adducts convert to AF type adducts in the mass spectrometer source. We propose that this can occur by a retro-Prins reaction (Scheme 2). This model is supported by two previous studies in which illudin S-cysteine adducts and illudin S analyzed by ESI and

Scheme 2. Proposed mechanism for formation of the illudin S-Ade adduct (*m/z* 384) transitions to *m/z* 336 and 201.

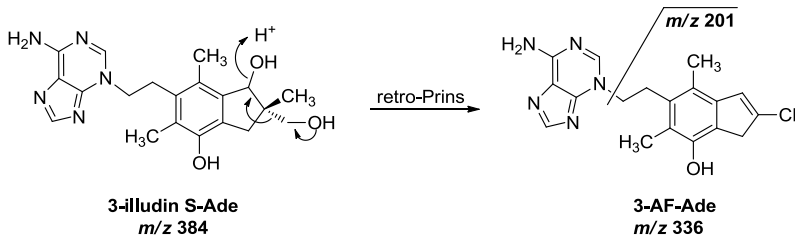

atmospheric pressure chemical ionization (APCI) tandem mass spectrometry, respectively, gave rise to a fragment corresponding to the mass of AF (*m/z* 217).[20,21] Furthermore, the t_R of illudin S-derived adducts did not match that of authentic 3-AF-Ade, allowing us to dismiss the possibility that illudin S is converted to AF before reacting with DNA. The hypothesized conversion of illudin S-Ade (**6**, *m/z* 384) to AF-Ade (**2**, *m/z* 336) appears to be more facile than fragmentation to the illudin S indene moiety (Scheme 1B, *m/z* 249), as no *m/z* 249 peak suitably resolved to allow accurate quantitative measurement was observed under the conditions tested. The products of cell-free reactions of illudin S and ctDNA or dAdo coeluted with the products from illudin S-treated cells.[22]

It has been demonstrated in previous studies that cells with elevated levels of PTGR1 are more sensitive to AFs.[2–4] We have determined previously how varying levels of PTGR1 influence AF-DNA adduct formation in a cell-free system[9] and compared relative AF-DNA adduct levels in cells.[8] All of these previous experiments were carried out with transiently transfected cells. The stable transfection of SW-480 cells, accomplished in this study, provides a robust platform for studying the influence of PTGR1 levels on cytotoxicity and DNA adduct formation. Because the two types of cells are the same in all aspects (including DNA repair, etc.) we can be confident that upon treatment with AF or illudin S, any observable differences are attributable to the different bioactivation capacities.

Between the two cell lines tested in this study, there was a 3-fold difference in sensitivity to AF in PTGR1-480 cells compared to SW-480 cells (IC_{50} values of 104 nM versus 301 nM, respectively). This difference in IC_{50} values was statistically significant ($p = 0.002$); however, the shapes of the toxicity curves also differed. Thus, for PTGR1-480 cells, toxic influences of AF were observed with as low as 10 nM drug, while for SW-480

cells, no response was observed until they were treated with 100 nM drug. Similar curve-shape changes have been observed previously for cells in which bioactivation capacity is stimulated pharmacologically.[23] On the other hand, for illudin S-treated cells, IC_{50} values were not significantly different (p = 0.08) at 10 versus 14 nM for PTGR1-480 and SW-480 cells, respectively. Finally, illudin S was 21-fold more toxic than AF in SW-480 cells. There is no previously published cytotoxicity data for these compounds in SW-480 cells, but for comparison, illudin S is 2–56-fold more toxic than AF in a variety of cancer cell lines, as assessed with a 2 h colony-forming assay.[24,25]

For both AF- and illudin S-treated PTGR1-480 and SW-480 cells, there was a dose-dependent formation of DNA adducts. At equivalent drug concentrations, illudin S-Ade adducts outnumber AF-Ade adducts around 10-to-1 [e.g., at 50 nM, 139–156 illudin S-Ade adducts (**6**) versus 9–16 AF-Ade adducts (**2**) per 10^7 nucleotides]. Interestingly, when adduct levels are normalized on the basis of IC_{50} values for each cell type, the adduct quantities are the same (Figure 6). For example, the number of Ade adducts that

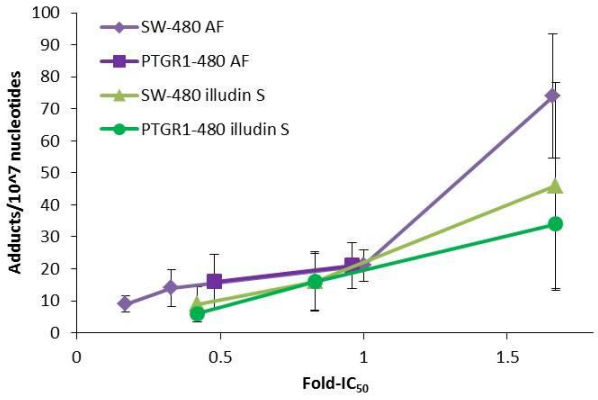

Figure 6. Ade adduct formation by AF and illudin S in SW-480 and PTGR1-480 cells as a function of fold-IC_{50}.

formed, upon treatment with a drug concentration equal to the IC_{50} for the drug-cell combination of interest, were as follows: For AF, in SW-480 cells treated with 300 nM drug, 21 adducts/10^7 nucleotides formed, and in PTGR1-480 cells treated with 100 nM

drug (an equitoxic dose to 300 nM in SW-480 cells), again 21 adducts/10^7 nucleotides formed. For illudin S, in both SW-480 and PTGR1-480 cells treated with 10 nM drug, 16 adducts/10^7 nucleotides formed. This observation is supported by a previous study that showed, on the basis of overall radiolabeling distributions, equal incorporation of AF and illudin S into genomic DNA at equitoxic concentrations.[24] Also, previous DNA binding studies in which cisplatin and illudin S,[10] as well as illudin S, AF, and HMAF,[26] were compared, it was shown that the number of adducts required to kill 50% of cells by each drug is the same. These data suggest that adducts resulting from each drug are equally lethal, but the amount of illudin S required to produce the same adduct levels as for AF is much lower. That is, on a dose-per-dose basis, illudin S is more efficient at alkylating DNA.

Finally, additional information established in this study is that this efficiency in illudin S-mediated DNA alkylation does not depend on bioactivation capacity; that is, unlike AF, bioactivation is not a major toxicity-limiting factor. The accumulation of illudin S- or AF-DNA adducts in cells up to 72 h was in the same range (approximately 50–250 adducts/10^7 nucleotides), but the time-course profiles were different (Figure 5). While AF-Ade adducts were constant from 4–48 h, the number of illudin S-Ade adducts decreased at 48 h. A possible rationale for these differences in the AF versus illudin S profile behavior is differences in the rate of adduct depurination or repair. AF and illudin S adducts both appear to be repaired by the same DNA repair pathway,[10,24] but there could be a difference in how quickly the corresponding adducts are recognized or processed by these pathways.

The *m/z* values for the identified illudin S adduct and its subsequent fragments suggest that bioactivation is necessary for illudin S to react with DNA. The observation of this bioactivation requirement is further supported by previous studies indicating that

illudins do not react with nitrogen or oxygen nucleophiles or DNA directly.[27,28] Our results are in agreement with a previous study that has demonstrated that PTGR1 levels do not influence illudin S cytotoxicity,[2] and our data further extend this observation to include that higher PTGR1 levels do not translate to higher amounts of DNA alkylation by bioactivated illudin S. These data may be rationalized on the basis of an emerging model for AF and illudin S cytotoxicity that considers drug uptake into the cell, bioactivation by PTGR1 in the cytosol, translocation of the reactive intermediate to the nucleus, and reactivity of the intermediate with DNA (Figure 7).

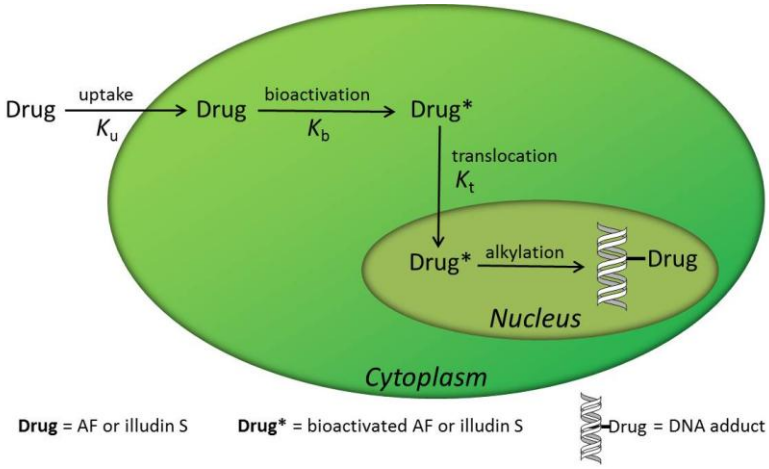

Figure 7. Model illustrating the steps required to form a DNA adduct from a bioactivated drug. This model is used to explain how different levels of PTGR1 do not influence illudin S-DNA adduct levels.

With respect to drug updake in the cell, relative rates for illudin S and AF depend on cell type, and in general, illudin S uptake is positively correlated with cytotoxicity, but for AF, both uptake and bioactivation are implicated in dictating toxicity.[6,24,25] With respect to internal dose amongst sensitive HL60 leukemia and MV522 lung cancer cells, a higher number of AF molecules (up to 40-fold more as compared to illudin S) may be required to kill the same percentage of cells as illudin S, and this corresponds to a higher IC_{50} for AF versus illudin S (up to 60-fold higher).[24,25] With respect to relative IC_{50}

values, we have observed in this study a similar relationship, including a 21-fold IC_{50} reduction for illudin S versus AF toxicity in SW-480 cells, suggesting here that K_u(illudin S) > K_u(AF) (Figure 7).

With respect to the contribution of the bioactivation term in this model (Figure 7), it is established that illudin S is metabolized by rat PTGR1 faster than is HMAF.[2] When incubated with rat liver cytosol, illudin S was metabolized faster than AF.[29] In further studies, we have characterized illudin S and AF metabolism by rat and human variants of PTGR1, further supporting that K_b(illudin S) > K_b(AF).

There remains limited information available regarding relative rates for translocation to the nucleus (K_t) (Figure 7). This process, together with the final step of DNA alkylation, depends on the stability and reactivity of the reactive intermediates formed by the action of PTGR1. While there is no data regarding K_t(illudin S^*) versus K_t(AF^*), it has been suggested that illudin S^* may be less stable than AF^*.[6] Knowing that illudin S quickly reacts to form hydroxylated and chlorinated ring-opened metabolites upon incubation with rat 9000*g* supernatant,[30] it is plausible that the reactive intermediate may be quenched before reaching DNA in the nucleus. The reactive intermediate of AF, on the other hand, may be stabilized by its aromatic fulvene,[6] which would be supported by our data regarding the ability of a chemically activated analog AF to reach the nucleus and form DNA adducts in cells.[3] The process of crossing the nuclear membrane is not well studied in this case, but if transporters are involved, structural differences in AF^* and illudin S^* may influence translocation. These observations suggest the following relationship for translocation of AF^* and illudin S^* to the nucleus: K_t(illudin S^*) ≤ K_t(AF^*).

We may further consider the data obtained in this study in the context of the model described above and depicted in Figure 7. A plausible scenario is that illudin S

may enter the cell more efficiently than AF and react with PTGR1 faster than AF. As compared to AF, more bioactivated illudin S may be generated, therefore, but the lower stability of illudin S^* may lead to more decomposition within the cytosol and a diminished yield of illudin S-DNA adducts as compared to the case of AF. In illudin S-treated PTGR1-480 cells, we assume that uptake is unchanged from SW-480 cells, but PTGR1 availability and PTGR1-mediated activation appear not to be rate-limiting in this case. Therefore, the excess PTGR1 (as compared to SW-480 cells) is not utilized and has no functional influence. In the case of AF, on the other hand, the additional PTGR1 in PTGR1-480 cells has a real impact because PTGR1-mediated activation becomes rate limiting, and additional bioactivation capacity translates to higher AF-DNA adduct formation and higher sensitivity in transfected cells.

5. Conclusion

In this study, we identified illudin S-DNA adducts resulting from reactions with Ade and quantified them, along with AF-DNA adducts in SW-480 and PTGR1-480 cells engineered to overexpress PTGR1, an enzyme implicated in the bioactivation of these drugs. The concentration- and time-dependent formation of genomic DNA adducts of AF or illudin S was determined, and differences in the two cell types mirrored cytotoxicity results: for AF, PTGR1-480 cells were more sensitive than SW-480 cells, and more AF-Ade adducts were measured in PTGR1-480 cells as compared to SW-480; for illudin S, cytotoxicity was similar in both cell types, as well as illudin S-Ade adduct levels. On the basis of mass spectral data, it appears that bioactivation is required for illudin S to react with DNA, but unlike AF, there is no positive correlation between PTGR1 levels and illudin S adduct levels. These new data, integrated with the current status of knowledge concerning illudin S and AF, are used to formulate a model that rationalizes the

differential cytotoxicity outcomes and selectivities for these structurally related cytotoxic molecules.

References

1. Cummings, J., Spanswick, V. J., Tomasz, M., and Smyth, J. F. (1998) Enzymology of Mitomycin C Metabolic Activation in Tumor Tissue. *Biochem. Pharmacol. 56,* 405-414.
2. Dick, R. A., Yu, X., and Kensler, T. W. (2004) NADPH alkenal/one oxidoreductase activity determines sensitivity of cancer cells to the chemotherapeutic alkylating agent irofulven. *Clin. Cancer Res. 10,* 1492-1499.
3. Pietsch, K. E., Neels, J. F., Yu, X., Gong, J., and Sturla, S. J. (2011) Chemical and Enzymatic Reductive Activation of Acylfulvene to Isomeric Cytotoxic Reactive Intermediates. *Chem. Res. Toxicol. 24,* 2044-2054.
4. Gong, J., Neels, J. F., Yu, X., Kensler, T. W., Peterson, L. A., and Sturla, S. J. (2006) Investigating the role of stereochemistry in the activity of anticancer acylfulvenes: synthesis, reductase-mediated bioactivation, and cellular toxicity. *J. Med. Chem. 49,* 2593-2599.
5. Kelner, M. J., McMorris, T. C., Beck, W. T., Zamora, J. M., and Taetle, R. (1987) Preclinical evaluation of illudins as anticancer agents. *Cancer Res. 47,* 3186-3189.
6. Tanasova, M., and Sturla, S. J. (2012) Chemistry and Biology of Acylfulvenes: Sesquiterpene-Derived Antitumor Agents. *Chem. Rev. 112,* 3578-3610.
7. McMorris, T. C., Chimmani, R., Alisala, K., Staake, M. D., Banda, G., and Kelner, M. J. (2010) Structure-activity studies of urea, carbamate, and sulfonamide derivatives of acylfulvene. *J. Med. Chem. 53,* 1109-1116.
8. Gong, J., Vaidyanathan, V. G., Yu, X., Kensler, T. W., Peterson, L. A., and Sturla, S. J. (2007) Depurinating acylfulvene-DNA adducts: characterizing cellular chemical reactions of a selective antitumor agent. *J. Am. Chem. Soc. 129,* 2101-2111.
9. Neels, J. F., Gong, J., Yu, X., and Sturla, S. J. (2007) Quantitative correlation of drug bioactivation and deoxyadenosine alkylation by acylfulvene. *Chem. Res. Toxicol. 20,* 1513-1519.
10. Kelner, M. J., McMorris, T. C., Estes, L., Rutherford, M., Montoya, M., Goldstein, J., Samson, K., Starr, R., and Taetle, R. (1994) Characterization of illudin S sensitivity in DNA repair-deficient Chinese hamster cells. Unusually high sensitivity of ERCC2 and ERCC3 DNA helicase-deficient mutants in comparison to other chemotherapeutic agents. *Biochem. Pharmacol. 48,* 403-409.
11. Jaspers, N. G., Raams, A., Kelner, M. J., Ng, J. M., Yamashita, Y. M., Takeda, S., McMorris, T. C., and Hoeijmakers, J. H. (2002) Anti-tumour compounds illudin S and Irofulven induce DNA lesions ignored by global repair and exclusively processed by transcription- and replication-coupled repair pathways. *DNA Repair 1,* 1027-1038.
12. Groopman, J. D., and Kensler, T. W. (1993) Molecular biomarkers for human chemical carcinogen exposures. *Chemical Research in Toxicology 6,* 764-770.
13. Qu, S.-X., Bai, C.-L., and Stacey, N. H. (1997) Determination of bulky DNA adducts in biomonitoring of carcinogenic chemical exposures: features and comparison of current techniques. *Biomarkers 2,* 3-16.
14. Swenberg, J. A., Fryar-Tita, E., Jeong, Y.-C., Boysen, G., Starr, T., Walker, V. E., and Albertini, R. J. (2008) Biomarkers in toxicology and risk assessment: informing critical dose-response relationships. *Chem. Res. Toxicol. 21,* 253-265.

15. McMorris, T. C., Kelner, M. J., Wang, W., Diaz, M. A., Estes, L. A., and Taetle, R. (1996) Acylfulvenes, a new class of potent antitumor agents. *Experientia 52*, 75-80.
16. McCloud, T. G., Klueh, P. A., Pearl, K. C., Cartner, L. K., Mushik, G. M., and Poole, K. K. (1996) Isolation of illudin S from the mature basidiocarp of *Omphalotus illudens*, and isolation of illudin S and M from the fermentation broth of *Omphalotus olearis*. *Nat. Prod. Lett. 9*, 87-95.
17. Meier, P. J., Sztul, E. S., Reuben, A., and Boyer, J. L. (1984) Structural and functional polarity of canalicular and basolateral plasma membrane vesicles isolated in high yield from rat liver. *J. Cell Biol. 98*, 991-1000.
18. Bessette, E. E., Goodenough, A. K., Langouët, S., Yasa, I., Kozekov, I. D., Spivack, S. D., and Turesky, R. J. (2009) Screening for DNA Adducts by Data-Dependent Constant Neutral Loss-Triple Stage Mass Spectrometry with a Linear Quadrupole Ion Trap Mass Spectrometer. *Anal. Chem. 81*, 809-819.
19. See Appendix B for nano-ESI-MS^3 spectra of illudin S-Ade adduct isolated from HT-29 cells.
20. Tanaka, K., Inoue, T., Tezuka, Y., and Kikuchi, T. (1996) Michael-type addition of illudin S, a toxic substance from Lampteromyces japonicus, with cysteine and cysteine-containing peptides in vitro. *Chem. Pharm. Bull. 44*, 273-279.
21. Kirchmair, M., Poder, R., and Huber, C. G. (1999) Identification of illudins in Omphalotus nidiformis and Omphalotus olivascens var. indigo by column liquid chromatography-atmospheric pressure chemical ionization tandem mass spectrometry. *J. Chromatogr. A. 832*, 247-252.
22. See Appendix B for co-injections of cellular DNA and dAdo treated with illudin S.
23. Yu, X., Erzinger, M. E., Pietsch, K. E., Cervoni-Curet, F. N., Whang, J., Niederhuber, J., and Sturla, S. J. (2012) Up-regulation of human prostaglandin reductase 1 improves the efficacy of hydroxymethylacylfulvene, an antitumor chemotherapeutic agent. *J. Pharmacol. Exp. Ther. 343*, 426-433.
24. Kelner, M. J., McMorris, T. C., Montoya, M. A., Estes, L., Uglik, S. F., Rutherford, M., Samson, K. M., Bagnell, R. D., and Taetle, R. (1998) Characterization of acylfulvene histiospecific toxicity in human tumor cell lines. *Cancer Chemother. Pharmacol. 41*, 237-242.
25. Kelner, M. J., McMorris, T. C., Montoya, M. A., Estes, L., Rutherford, M., Samson, K. M., and Taetle, R. (1997) Characterization of cellular accumulation and toxicity of illudin S in sensitive and nonsensitive tumor cells. *Cancer Chemother. Pharmacol. 40*, 65-71.
26. Kelner, M. J., McMorris, T. C., Montoya, M. A., Estes, L., Uglik, S. F., Rutherford, M., Samson, K. M., Bagnell, R. D., and Taetle, R. (1999) Characterization of MGI 114 (HMAF) histiospecific toxicity in human tumor cell lines. *Cancer Chemother. Pharmacol. 44*, 235-240.
27. McMorris, T. C., Kelner, M. J., Wang, W., Moon, S., and Taetle, R. (1990) On the mechanism of toxicity of illudins: the role of glutathione. *Chem. Res. Toxicol. 3*, 574-579.
28. Kelner, M. J., McMorris, T. C., and Taetle, R. Unpublished results.
29. McMorris, T. C., Elayadi, A. N., Yu, J., and Kelner, M. J. (1999) Metabolism of antitumor acylfulvene by rat liver cytosol. *Biochem. Pharmacol. 57*, 83-88.
30. Tanaka, K., Inoue, T., Kadota, S., and Kikuchi, T. (1990) Metabolism of illudin S, a toxic principle of Lampteromyces japonicus, by rat liver. I. Isolation and

identification of cyclopropane ring-cleavage metabolites. *Xenobiotica 20*, 671-681.

Chapter Four:

Strategies for evaluating the formation and persistence of abasic sites in cells treated with illudin S or AF

1. Introduction

The abasic site (also known as the apurinic/apyrimidinic or AP site) is one of the most frequent forms of DNA damage, resulting from loss of a nucleobase via cleavage of its *N*-glycosyl bond, and is estimated to approach levels of 10,000 lesions per human cell per day.[1] DNA alkylation promotes the rate of abasic site formation by 6 orders of magnitude,[2] and abasic site formation resulting from DNA adduct depurination is often invoked to explain toxicity for a wide variety of chemicals.[2] The resulting abasic site can

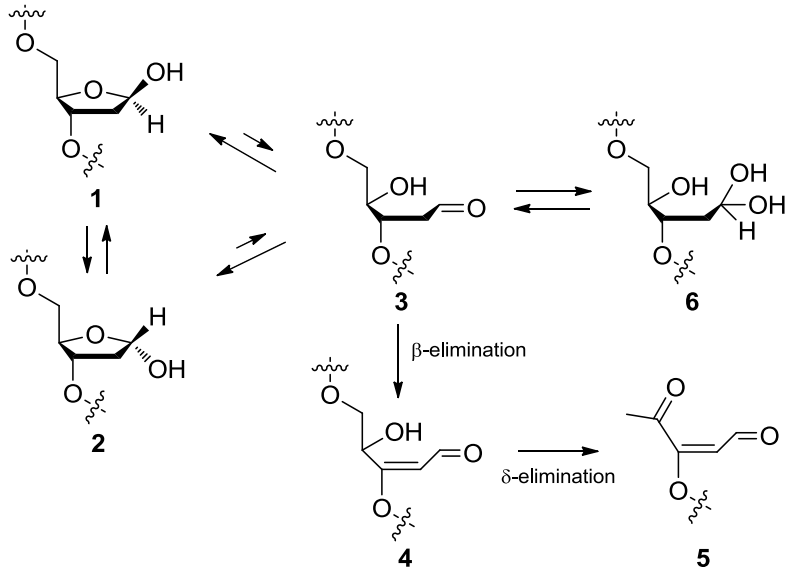

Scheme 1. DNA abasic site represented in its equilibrating closed (**1**, **2**) and open (**3–5**) conformations and further relevant transformations.

take on a number of forms (Scheme 1). The most common conformation is the closed ring structure (Scheme 1, **1** and **2**).[3,4] Unrepaired abasic sites may block DNA replication, lead to mutations, and threaten cell viability.[3] The repair of abasic sites in mammalian cells is carried out primarily by enzymes involved in base excision repair (BER), as the abasic site is an intermediate in this pathway, but repair can also be assisted by nucleotide

excision repair (NER)[5, 6] and recombination, and are tolerated by translesion DNA synthesis (TLS).[7]

Due to the importance of cellular impacts resulting from processes such as DNA alkylation, mutagenesis and BER, together with their potential connection to the formation of abasic sites in cells, there is ongoing interest in corresponding detection and quantitation strategies. An indirect method to evaluate abasic site formations involves measuring strand breaks that result from intact abasic sites via hydrolysis of phosphodiester bonds adjacent to abasic sites.[8] Following this early work, strategies that relied on covalent labels for abasic sites soon emerged (Chart 1). ^{14}C-labeled methoxyamine[9] was one of the first, later followed by the popular aldehyde reactive probe (ARP), react with the ring-opened aldehyde conformation of the abasic site (**3**–**5**).[10–12] *O*-4-nitrobenzylhydroxylamine (NBHA) has also been used to label abasic sites and was originally applied for generating a monoclonal antibody against the labeled DNA.[13] Later,

Chart 1. Structures of common abasic site labels.

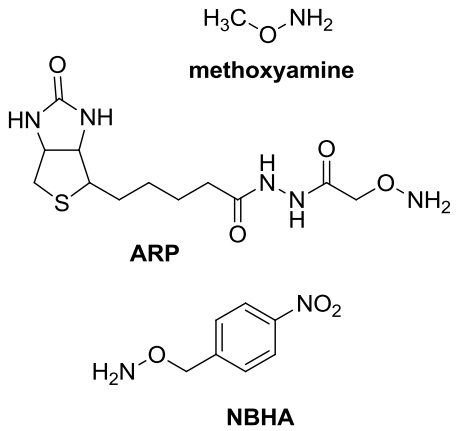

Roberts, *et al.* employed the alkoxylamine NBHA and developed a quantitative mass spectrometry method to measure NBHA-labeled abasic sites.[14] This strategy was validated with a uracil-containing oligonucleotide (uracil glycosylase removes uracil to produce abasic sites) and applied to calf thymus DNA (ctDNA) heated in the presence of

acid to induce abasic site formation with a limit of quantitation of 3 abasic sites/10^7 bases. The adaptation of this approach to the analysis of abasic sites in more complex systems, such as cellular DNA, however, has never been reported. There is available a commercial kit for abasic site detection, and recently this strategy has been applied to quantify abasic sites resulting from the antitumor antibiotic leinamycin in MiaPaCa pancreatic cancer cells.[15] As its general strategy, this kit employs the ARP probe to label abasic sites in isolated cellular DNA with a biotin tag. After fixing the ARP-labeled DNA to a 96-well plate, detection involves a colorimetric biotin-avidin-peroxidase assay.[16]

In the case of acylfulvene (AF), the major AF-DNA adducts 3-AF-Ade and 7-AF-Gua,[17] as well as the recently identified illudin S-DNA adduct (see Chapter 3), depurinate. The half-life of 3-AF-Ado in ctDNA was measured to be 8.5 h, and for 7-AF-Guo and 7-AF-Gua, it was less than 2 h.[17] The process of depurination has not been characterized in cells, however, and it therefore remains unclear whether toxic responses to AF are initiated by primary adducts, abasic sites, or their relative contributions. An important gap in knowledge for further understanding AF toxicity concerns the rates of AF- and illudin S-DNA adduct depurination and abasic site formation and persistence in cells. Therefore, a goal motivating the work performed in this study centered on identifying a suitable strategy for evaluating the rate of accumulation of abasic sites in drug-treated cells.

On the basis of published information regarding methods for detecting abasic sites, we have explored the potential for applying the commercially available kit produced by Dojindo Molecular Technologies Inc. and an extension of the Roberts *et al.* mass spectrometry strategy for the analysis of AF- and illudin S-treated cells. We invested significant effort in applying the Dojindo kit for our measuring abasic sites in AF-treated cells. However technical issues, potentially related to various components of the kit or in

obtaining DNA samples suitable for use with the kit, have triggered extensive and ongoing investigation of our samples by the commercial supplier Dojindo. Overall, we have failed to detect abasic sites in drug-treated DNA samples by this approach. As a complementary strategy, the Roberts *et al.* method is attractive because it is a relatively straight forward approach that relies on mass spectrometry, an area of our analytical expertise. It is anticipated that the means for sample preparation and analysis will be more suitable for tailoring this method to more complex systems. In this study, we therefore took initial steps needed for future realization of the extension and application of the Roberts *et al.* NBHA method[14] to quantify abasic sites in AF- and illudin S-treated cancer cells (strategy shown in Scheme 2A), and would use our previously developed isotope dilution method[18] described in Chapter 3 to measure the rate of AF- and illudin S-DNA adduct depurination.

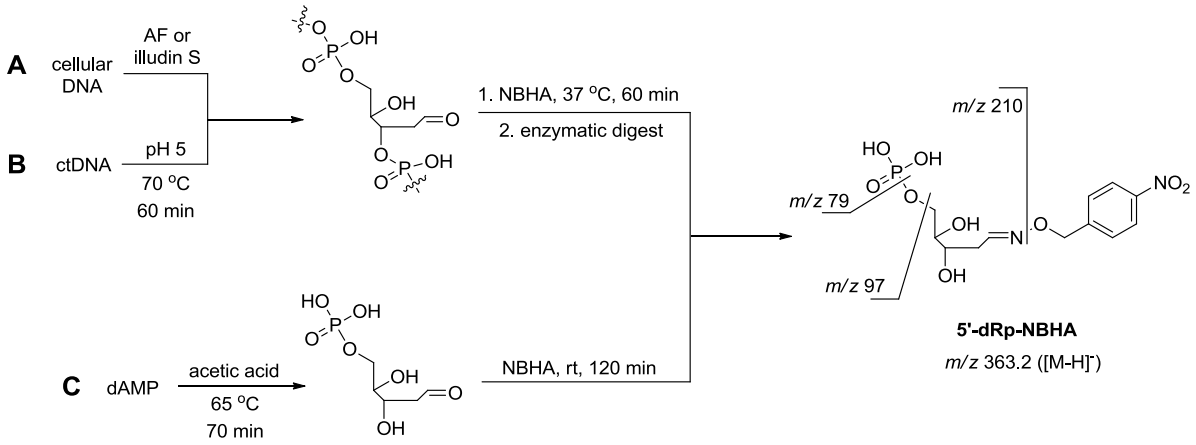

Scheme 2. NBHA-labeling strategy for quantifying abasic sites by LC-ESI-MS^2. (A) Proposed application of method to AF- or illudin S-treated cells. (B) Preparation of ctDNA labeled with NBHA. (C) Preparation of 5'-dRp-NBHA, the standard, from dAMP.

2. Experimental procedures

2.1. Chemicals and enyzmes

Water was purified with a Milli-Q Integral Water Purification System (Millipore Corporation, Billerica, MA). All other reagents and enyzmes were purchased from Sigma (St. Louis, Missouri).

2.2. Instrumentation

DNA concentration was measured using a NanoDrop™ 1000 spectrophotometer (Thermo Scientific, Waltham, MA) or a Varian Cary UV 100 UV/visible spectrophotometer (Varian, Inc., Palo Alto, CA). LC-ESI-MS/MS analysis was carried out on a Waters nanoAcquity Ultra Performance LC interfaced with a Thermo TSQ Vantage triple quadrupole mass spectrometer.

2.3. Preparation of 5'-deoxyribose monophosphate-NBHA (5'-dRp-NBHA, NBHA-labeled abasic site standard)

Following the procedure described by Roberts *et al.* with the following minor modifications,[14] 100 mg deoxyadenosine monophosphate (dAMP) was dissolved in 10 mL water and 173 μL acetic acid. This solution was heated at 65 ^{o}C for 70 min to induce hydrolysis. After cooling, 3.8 mg NBHA was added (1.8 mM final concentration), tube was covered with foil, and put on a shaker table at room temperature for 24.5 h. Sample was centrifuged to remove insoluble components, but none were seen. SPE purification was performed with Waters Sep-Pak® Vac tC18 1 cc cartridges (50 mg sorbent), but the published procedure specifies 3 cc cartridges. The described elution procedure for the 3 cc cartridges was used and is as follows: condition cartridge with 2 mL methanol, then 2 mL of 2 mM NaH_2PO_4 (pH 4.5), and load 1 mL of the hydrolysis supernatant to the conditioned cartridge. 1 mL aliquots of 2 mM NaH_2PO_4 and methanol (in order of addition: 100% NaH_2PO_4, 75% NaH_2PO_4/25% methanol, 50% NaH_2PO_4/50% methanol,

25% NaH_2PO_4/75% methanol, 100% methanol) were applied to create a gradient for eluting the product. 0.5 mL fractions (2 fractions per gradient step, 10 total fractions) were collected and subsequently dried by rotary centrifugation. Samples were dissolved in 20 μL 50% 2.5 mM ammonium acetate/50% 2.5 mM ammonium acetate in acetonitrile and subjected to LC-ESI-MS^2 analysis.

2.4. Preparation of NBHA-labeled AP sites from ctDNA

Following the procedure described by Roberts *et al.* with the following minor modifications,[14] 5 mg ctDNA was dissolved in 5 mL citrate buffer (10 mM trisodium citrate, 10 mM NaH_2PO_4, 10 mM NaCl, pH 4.5) and incubated at 70 ^oC for 60 min to induce 7 AP sites/10^4 nucleotides.[19] The reaction was stopped by chilling the mixture on ice, followed by addition of 100 μL 5 M NaCl. AP DNA was precipitated with 10 mL cold ethanol, washed with cold 70% ethanol (3×5 mL), and the AP DNA pellet was dried under a stream of N_2.

The AP-DNA pellet was re-dissolved in 2.5 mL Tris-HCl buffer (10 mM, adjusted to pH 7.2 with NaOH), followed by addition of 2 mM NBHA (in 10 mM Tris-HCl buffer, pH 7.2). This solution was incubated at 37 ^oC for 60 min to label AP sites with NBHA. The reaction was stopped by chilling on ice, followed by addition of 100 μL 5 M NaCl. NBHA-labeled AP DNA was precipitated with 10 mL cold ethanol and washed with cold 70% ethanol (3×5 mL). The NBHA-labeled AP DNA pellet was dried under a stream of N_2, re-dissolved in 5 mL Tris-HCl buffer (10 mM, pH 7.2), and the DNA concentration was measured on the basis of UV absorbance.

To the re-dissolved AP-DNA pellet, 500 μL 100 mM $MgCl_2$ was added, followed by 50 μL deoxyribonuclease I (10 mg/mL in 0.9% NaCl). The mixture was incubated at

37 ^{o}C for 1.5 h. 75 μL nuclease P1 (1 mg/mL in 1 mM $ZnCl_2$) was then added, followed by incubation at 37 ^{o}C for 3 h. 10 μL of phosphodiesterase I (1 U/mL in DNA- and RNA-free water) was added last, and the mixture was incubated for 37 ^{o}C for 13 h. The incubation as stopped by rapid chilling on ice, then centrifuged (4000 RPM, 10 min) to precipitate protein. SPE purification was performed with Waters Sep-Pak® Vac tC18 1 cc cartridges per the elution gradient described above. Resulting fractions were dried by rotary evaporation, dissolved in 20 μL 50% 2.5 mM ammonium acetate/50% 2.5 mM ammonium acetate in acetonitrile and subjected to LC-ESI-MS^2 analysis.

2.5. UPLC-ESI-MS^2 analysis of NBHA-labeled samples

Samples were analyzed by LC-ESI-MS^2 with MS ionization parameters optimized by tuning with deoxyguanosine (dGuo) (100 pmol/μL in 50% 2.5 mM ammonium acetate in water/50% 2.5 mM ammonium acetate in acetonitrile). The electrospray (ESI) source was set in negative ion mode with the following parameters: capillary temperature, 200 ^{o}C; voltage, 3 kV; sheath gas pressure, 10; vaporizer temperature, 30 ^{o}C; Q2 CID gas pressure, 1.5 mTorr; collision gas, argon; S-lens RF level, 67%. Full scan event range was *m/z* 50–500. Full product scan event of parent mass *m/z* 363.2 (range *m/z* 50–400) included the following parameters: collision energy, 21 V; scan time, 1 s; Q1 and Q3 peak widths, 0.7 amu. Data for three selected reaction monitoring (SRM) events were acquired. These corresponded to the transitions *m/z* 363.2 to 97.0, *m/z* 363.2 to 79.0, and *m/z* 363.2 to 210.0 (acquisition parameters: scan width, *m/z* 0.5; scan time, 1 s; collision energy, 10 V, Q1 and Q3 peak widths, 0.7 amu). Chromatography was performed with a Phenomenex Synergi Fusion-RP 80 Å column (150×0.5 mm, 4 μm particle size). The ultra performance liquid chromatography (UPLC) flow rate was 10 μL/min and the mobile phases were 2.5 mM ammonium acetate in water (mobile phase A) and 2.5 mM

ammonium acetate in acetonitrile (mobile phase B). The mobile phase gradient elution was as follows: hold at 100% A for 1 min, decrease to 0% A over 9 min, hold for 2 min, return to starting conditions over 2 min, and re-equilibrate for 11 min (25 min total run time).

3. Preliminary results

3.1. Synthesis of 5'-dRp-NBHA

The molecular equivalent of an NBHA-labeled abasic site (5'-dRp-NBHA), required as an analytical standard, was synthesized from dAMP (Scheme 2C). The fragmentation pattern shown in Figure 1 is in agreement with the published spectra (fragmentation shown in Scheme 2), confirming the identity of the compound. With respect to its isolation and analysis, however, there was an apparent pervasive presence of the compound in most of the fractions obtained from SPE purification throughout the intended chromatographic process and poor peak shape and a different retention time (relative to published data) for the analyte when detected by HPLC. Two potentially contributing factors are differences in SPE cartridge size and UPLC chromatography conditions between our experiments and the published method, and these aspects require further refinement.[20]

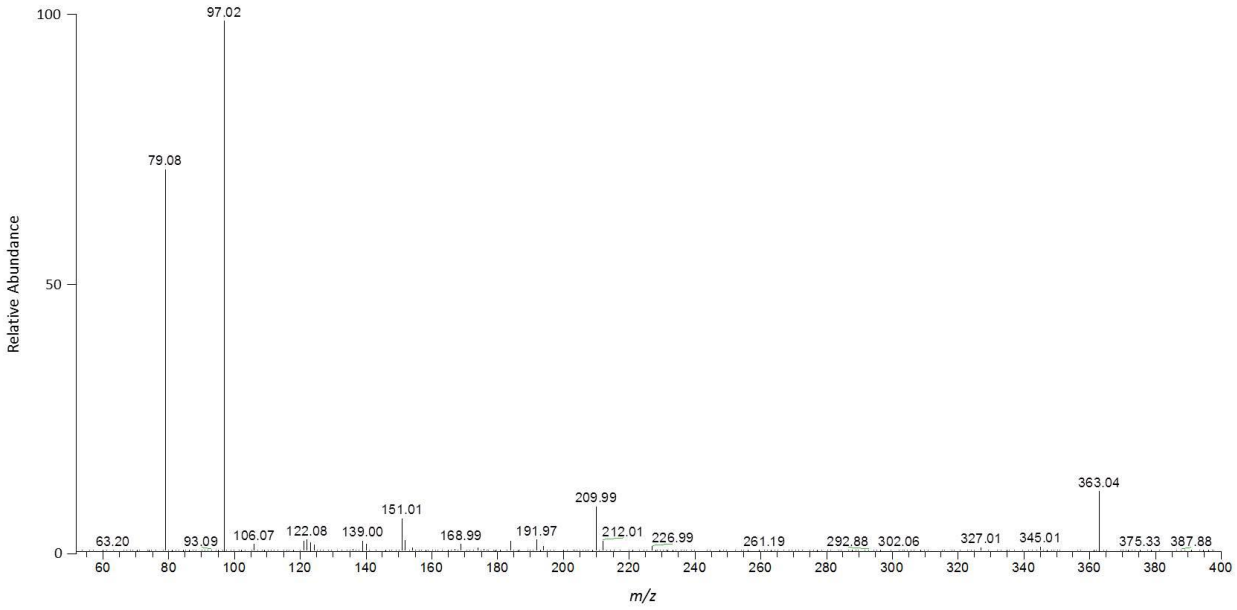

Figure 1. Full scan MS^2 product spectra of *m/z* 363.2, parent mass of 5'-dRp-NBHA standard.

3.2. Detection of 5'-dRp-NBHA from acid/heat treated ctDNA

Evidence for the formation of abasic sites in acid-treated ctDNA was obtained by labeling with NBHA and confirming the presence of 5'-dRp-NBHA in these samples. ctDNA was heated at 70 ^{o}C at pH 5 for 65 min, followed by labeling with NBHA and enzymatic digestion (Scheme 2B). Enzymatic digestion involved separate, subsequent incubations with deoxyribonuclease I, nuclease P1, and phosphodiesterase I.[21] Analysis by LC-ESI-MS^2, and identification of mass fragments corresponding to 5'-dRp-NBHA, was performed to confirm that abasic site formation in ctDNA could be detected on the basis of NBHA labeling.

4. Discussion and outlook

Preliminary results discussed here demonstrate that the 5'-dRp-NBHA was successfully synthesized, and that abasic sites generated from the acid- and heat-treatment of ctDNA could be detected on the basis of NBHA-labeling. For ctDNA, generated abasic sites were labeled with NBHA, digested to 5'-dRp-NBHA, and detected by LC-ESI-MS^2. These data provide the first information needed to pursue further studies aiming to validate the analytical method for cell-based studies, and eventually to measure abasic sites in AF- and illudin S-treated cells. The data provided here offer a qualitative demonstration of abasic site detection, and the next necessary step should involve adapting a quantitative approach. These next steps will rely on use of a ^{13}C-labeled 5'-dRp-NBHA standard that will allow optimization of pending technical aspects of work-up and chromatography, as well as quantitation by isotope dilution mass spectrometry. To extend this method for analyzing cellular DNA, critical aspects to address will include masking background abasic site lesions prior to drug treatment, retaining DNA integrity in the isolation process and additional masking of artifactual abasic sites induced during sample preparation. A convenient approach for measuring abasic sites in cells would be valuable for better understanding the role of depurination in the toxicity of AF, as well as other DNA-alkylating drugs or carcinogens that are prone to depurination.

Extension of the analytical method described here to drug-treated cells would be a significant step and provide a useful analytical approach for us and others interested in quantifying this type of DNA lesion in treated-cells. Relevant to the research presented in this thesis, such an approach could be used to quantify abasic site formation as a function of drug concentration and exposure time for AF or illudin S. Such studies will involve determining the persistence of drug-induced elevation in abasic site levels by quantifying

DNA sampled from cells exposed to the drug. These data will be interpreted on the basis of contributing rates of adduct depurination, AF- or illudin-S nucleoside adduct repair, and abasic site repair. Understanding how these processes contribute to the overall abasic site burden in the cell require comparing results on the basis of repair capacity of the cell lines under interrogation. Data from our lab and others suggest that the transcription-coupled NER (TC-NER) pathway is important in processing AF- or illudin S-induced DNA adducts.[22,23] On the other hand, BER is primarily implicated in in the repair of abasic sites, but NER assists as well.[5,6] As a convenient model, HT-29 colon cancer cells would be used to establish the method in cells, followed by experiments with SW-480 colon cancer cells engineered to overexpress PTGR1 (PTGR1-480) described in Chapter 3. Based on the findings in Chapter 3, it is hypothesized that there would be a higher level of abasic site formation in PTGR1-480 cells treated with AF compared to SW-480 cells, and the amount of abasic sites resulting from illudin S-treated PTGR1-480 and SW-480 would be the same. Finally, it would be important to perform related experiments with cells deficient in NER enzymes, for example, cells derived from terminal patients suffering from xeroderma pigmentosum (XP).[22] If TC-NER was not functioning in a cell treated with illudin S or AF, abasic site persistence would be expected to greater than for control cells with no repair deficiencies. Completion of these studies would ultimately allow us to relate depurination kinetics, abasic site persistence, and rate of DNA repair in AF- and illudin S-treated cells, and would enhance our understanding of how each of these factors contribute to drug toxicity.

References

1. Lindahl, T. (1993) Instability and decay of the primary structure of DNA. *Nature 362,* 709-715.
2. Loeb, L. A., and Preston, B. D. (1986) Mutagenesis by apurinic/apyrimidinic sites. *Annu.Rev. Genet. 20,* 201-230.
3. Lowry, D., and Wilson III, D., Recognition and repair of abasic sites. In *DNA Damage Recognition*, CRC Press: 2005.
4. Lhomme, J., Constant, J.-F., and Demeunynck, M. (1999) Abasic DNA structure, reactivity, and recognition. *Biopolymers 52,* 65-83.
5. Lin, J.-J., and Sancar, A. (1989) A new mechanism for repairing oxidative damage to DNA: (A)BC excinuclease removes AP sites and thymine glycols from DNA. *Biochemistry 28,* 7979-7984.
6. Kim, N., and Jinks-Robertson, S. (2010) Abasic sites in the transcribed strand of yeast DNA are removed by transcription-coupled nucleotide excision repair. *Mol. Cell. Biol. 30,* 3206-3215.
7. Otterlei, M., Kavli, B., Standal, R., Skjelbred, C., Bharati, S., and Krokan, H. E. (2000) Repair of chromosomal abasic sites *in vivo* involves at least three different repair pathways. *EMBO J. 19,* 5542-5551.
8. Crine, P., and Verly, W. G. (1976) Determination of single-strand breaks in DNA using neutral sucrose gradients. *Anal. Biochem. 75,* 583-595.
9. Talpaert-Borlé, M., and Liuzzi, M. (1983) Reaction of apurinic/apyrimidinic sites with [^{14}C]methoxyamine, a method for the quantitative assay of AP sites in DNA. *Biochem. Biophys. Acta 740,* 410-416.
10. Kubo, K., Ide, H., Wallace, S. S., and Kow, Y. W. (1992) A novel sensitive and specific assay for abasic sites, the most commonly produced DNA lesion. *Biochemistry 31,* 3703-3708.
11. Nakamura, J., Walker, V. E., Upton, P. B., Chiang, S.-Y., Kow, Y. W., and Swenberg, J. A. (1998) Highly sensitive apurinic/apyrimidinic site assay can detect spontaneous and chemically induced depurination under physiological conditions. *Cancer Res. 58,* 222-225.
12. Atamna, H., Cheung, I., and Ames, B. N. (2000) A method for detecting abasic sites in living cells: Age-dependent changes in base excision repair. *Proc. Nat. Acad. Sci. U.S.A. 97,* 686-691.
13. Chen, B. X., Kubo, K., Ide, H., Erlanger, B. F., Wallace, S. S., and Kow, Y. W. (1992) Properties of a monoclonal antibody for the detection of abasic sites, a common DNA lesion. *Mutat. Res., DNA Repair 273,* 253-261.
14. Roberts, K. P., Sobrino, J. A., Payton, J., Mason, L. B., and Turesky, R. J. (2006) Determination of apurinic/apyrimidinic lesions in DNA with high-performance liquid chromatography and tandem mass spectrometry. *Chem. Res. Toxicol. 19,* 300-309.
15. Viswesh, V., Gates, K., and Sun, D. (2010) Characterization of DNA damage induced by a natural product antitumor antibiotic leinamycin in human cancer cells. *Chem. Res. Toxicol. 23,* 99-107.
16. DNA Damage Quantification Kit (DK02-12), technical manual. Dojindo Molecular Technologies Inc., 2012.
17. Gong, J., Vaidyanathan, V. G., Yu, X., Kensler, T. W., Peterson, L. A., and Sturla, S. J. (2007) Depurinating acylfulvene-DNA adducts: characterizing cellular

chemical reactions of a selective antitumor agent. *J. Am. Chem. Soc. 129*, 2101-2111.
18. Neels, J. F., Gong, J., Yu, X., and Sturla, S. J. (2007) Quantitative correlation of drug bioactivation and deoxyadenosine alkylation by acylfulvene. *Chem. Res. Toxicol. 20*, 1513-1519.
19. Ide, H., Akamatsu, K., Kimura, Y., Michiue, K., Makino, K., Asaeda, A., Takamori, Y., and Kubo, K. (1993) Synthesis and damage specificity of a novel probe for the detection of abasic sites in DNA. *Biochemistry 32*, 8276-8283.
20. Synergi product overview. http://www.phenomenex.com/Products/HPLCDetail/Synergi/Polar-RP?returnURL=/Products/Search/HPLC (accessed October 16, 2012).
21. Relative to the published procedure (reference 14) less phosphodiesterase I (40-fold) was used in this experiment.
22. Jaspers, N. G., Raams, A., Kelner, M. J., Ng, J. M., Yamashita, Y. M., Takeda, S., McMorris, T. C., and Hoeijmakers, J. H. (2002) Anti-tumour compounds illudin S and Irofulven induce DNA lesions ignored by global repair and exclusively processed by transcription- and replication-coupled repair pathways. *DNA Repair (Amst) 1*, 1027-1038.
23. Tanasova, M., Otto, C., and Sturla, S. J. (2012) Unpublished results.

Chapter 5: Summary and outlook

The studies presented in this thesis investigate the reactivity of illudin S and AFs with critical cellular biomolecules and how these interactions translate to selective toxicity. Chapter 2 focuses on inhibition of selenocysteine-containing redox proteins by illudin S and AF. Chapter 3 investigates the role of PTGR1 levels on DNA adduct formation and cytotoxicity. In Chapter 4, a proposal for the potential importance of abasic sites in illudin S and AF toxicity is presented, along with preliminary results for quantifying abasic sites by mass spectrometry. Significant advances in understanding AFs mechanism of action have been made, but there are still various interesting questions and new research directions that are evident from the results of this work.

Illudin S and AFs have a similar profile for inhibiting TrxR vs. GR (HMAF > AF > illudin S), and alkylate both active site residues, however, the related enzyme Gpx is not inhibited. It is speculated that active site availability may account for this difference in inhibition. Future directions would involve examining at how sterics and electronics (Se vs. S) influence active site residue alkylation patterns (and subsequently, enzyme inhibition) in redox-regulating proteins like GR, Gpx, Trx, and TrxR. The notion of shared patterns of inhibition amongst these different redox proteins for a number of compounds is put forth in the Chapter 2 discussion, and as mentioned there, it is unknown if selectively targeting one or both active site residues results in different biological outcomes. Assessing a series of known inhibitors across this panel of cysteine- and selenocysteine-containing enzymes on the basis of the enzyme assays developed here may shed light on a potential relationship between alkylation and downstream cellular outcomes resulting from enzyme inhibition. These would further contribute to understanding of the role of redox protein inhibition in selective toxicity.

Levels of AF- and illudin S-DNA adducts in cells that stably overexpress PTGR1 vs. their wild-type counterparts are a key piece of information regarding the role of PTGR1 in AF- and illudin S- toxicity on the basis of DNA alkylation. While bioactivation of illudin S by PTGR1 is required for alkylation, there is no correlation between PTGR1 and illudin S cytotoxicity and DNA adduct levels. The CNL-MS^3 strategy described in Chapter 3 could be utilized to identify other unknown illudin S- and AF-DNA adducts that may be involved in the selective toxicity of AFs and/or extensive toxicity of illudin S.

We pursued a means for quantifying abasic sites, with the future potential to apply this strategy to evaluating abasic sites in cells, on the basis of an aldehyde-reactive alkoxyamino label termed NBHA. By this approach, NBHA-tagged abasic sites (5'-dRp-NBHA) are measured, and we have demonstrated that such adducts could be detected by mass spectrometry. Several future challenges and possibilities for applying the method for quantifying abasic sites in cells have been described in Chapter 4. To examine how DNA adduct depurination and resulting abasic adduct formation, persistence, and repair contribute to cytotoxicity profiles of AF and illudin S, the NBHA labeling method, along with the isotope dilution mass spectrometry method utilized in Chapter 3 for the quantitation of depurinating AF- and illudin S-DNA adducts, are envisioned to be executed (Scheme 1). Experiments would first be carried out with ctDNA, and later, cell-based experiments to determine the same parameters along with the extent of abasic site persistence and repair.

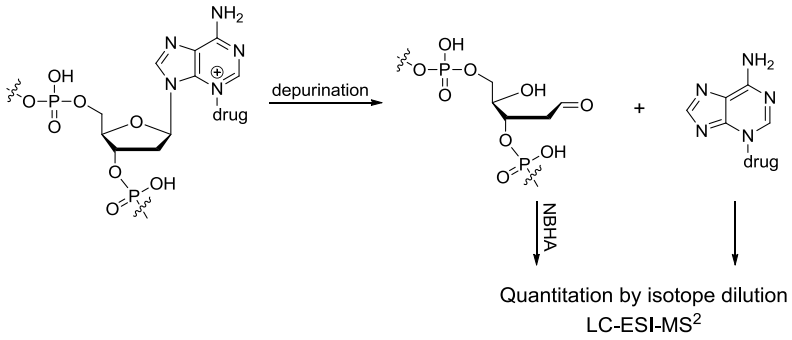

Scheme 1. Parallel approach for quantifying depurinated DNA adducts and resulting abasic sites from drug-treated DNA using two separate LC-ESI-MS^2 methods. Example shown here is for deoxyadenosine alkylated at the 3 position.

This thesis investigates how structural differences between illudin S and AFs translate to varying cytotoxic outcomes. Bioactivation requirements and the resulting alkylation of redox proteins and DNA were determined. Covalent modification of TrxR active site residues does not require bioactivation by PTGR1, and conversely, alkylation of Gpx is not possible, possibly due to a less accessible active site compared to TrxR. Formation of DNA adducts by AF or illudin S requires bioactivation, however, PTGR1 levels influence only AF-DNA adduct formation. Overall, different biological outcomes from illudin S and AFs examined here contribute to our understanding of mechanisms of their selective toxicity.

Appendix A: Chapter 2 supporting information

Inhibition curves for treatment of Gpx with iodoacetamide. Gpx (0.4 pmol) was allowed to react with iodoacetamide (1.87 mM) for 40 min in a total volume of 0.5 mL phosphate buffer (0.1 M, 1 mM EDTA, pH 7.0) at 37 ^{o}C. Average IC_{50} for two trials is 2.4 ± 0.1 mM.

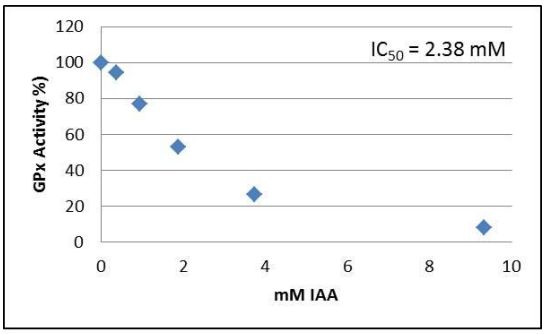

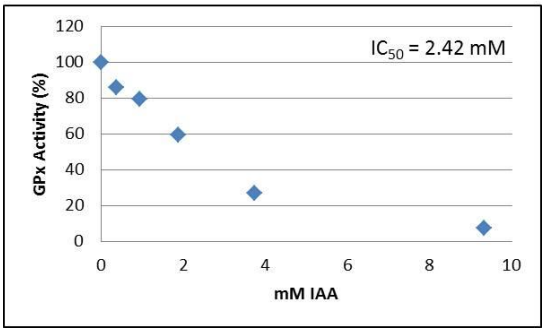

LC/MS spectra derived from AFs-treated Gpx. Gpx (1.6 nmol) was allowed to react with AFs (1.25 mM) in a total volume of 1 mL TE buffer. Gpx samples were then concentrated and unbound compound removed before LC/MS analysis.

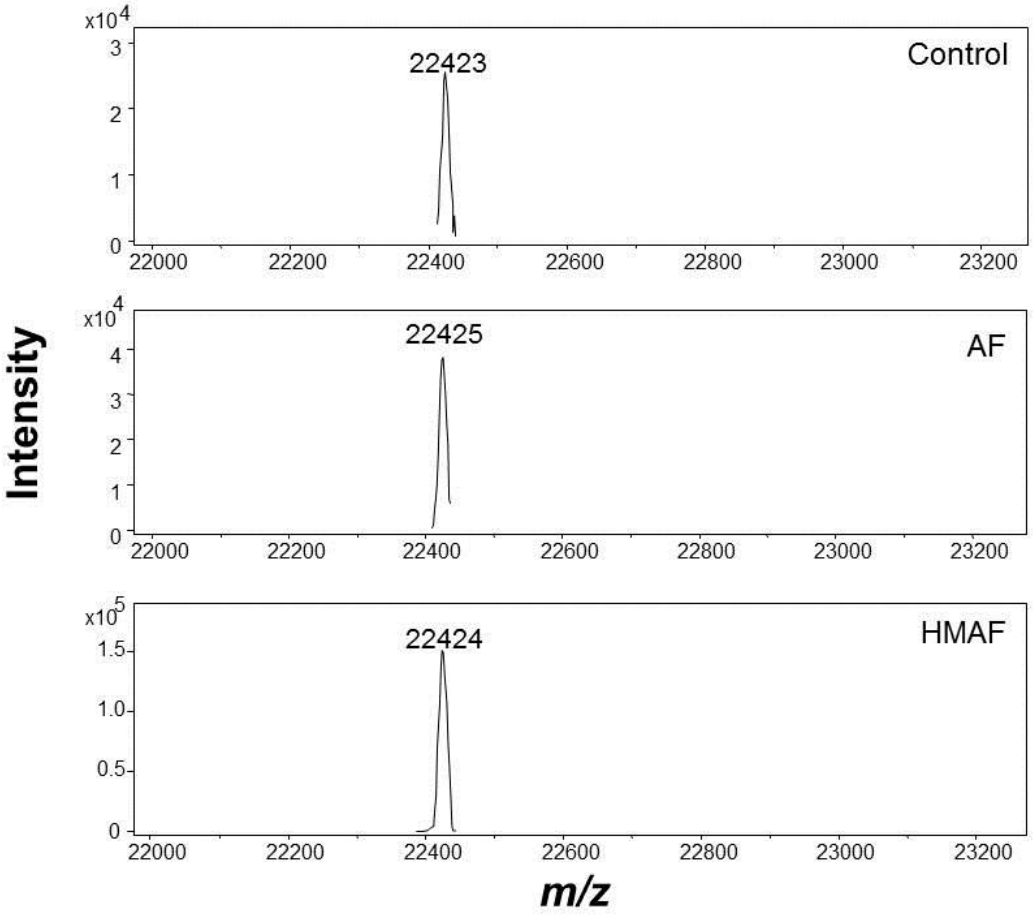

Appendix B: Chapter 3 supporting information

Co-injection of cellular DNA and dAdo treated with illudin S. Cellular DNA was isolated from HT-29 cells treated with 1 μM illudin S for 24 h. dAdo was treated with illudin S in the presence of RLC and NADPH. The mass transition for AF-Ade is shown in panels A–C, and the mass transition for illudin S-Ade is shown in panels D–F. Data is normalized to the base peak in each spectra and relative intensity is given as a normalized level (NL) value. (A) Co-injection of cellular DNA and dAdo incubations, NL 1.40E7. (B) Cellular DNA incubation, NL 2.64E5. (C) dAdo incubation, NL 8.28E6. (D) Co-injection of cellular DNA and dAdo incubation, NL 4.62E7. (E) Cellular DNA incubation, NL 1.45E6. (F) dAdo incubation, NL 4.96E7.

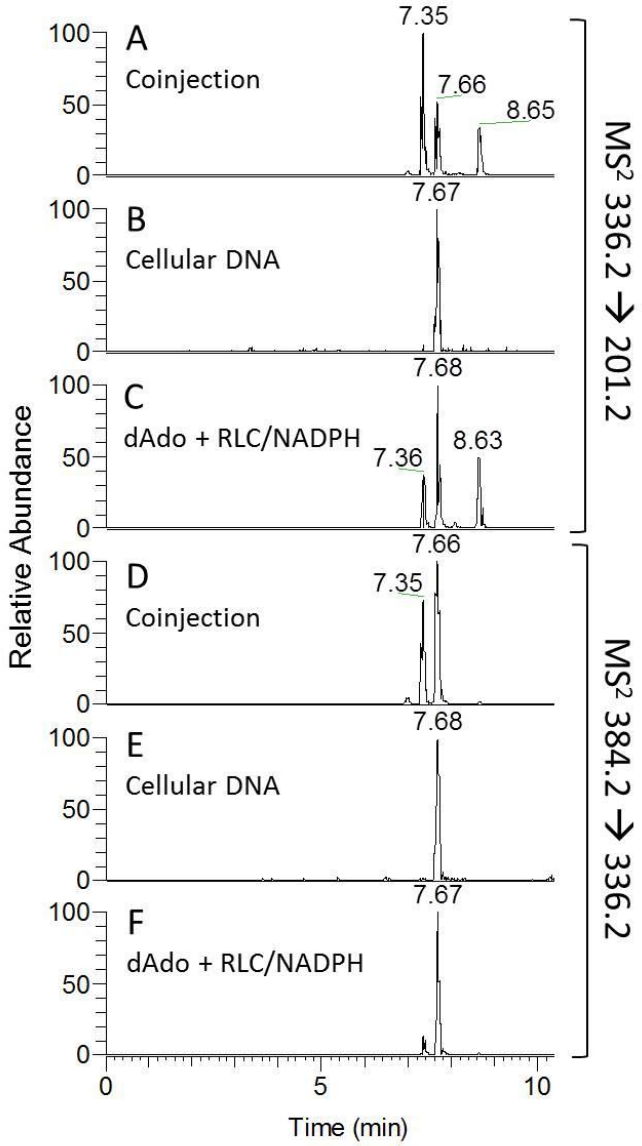

Experimental details for the isolation and nano-ESI-MS^3 analysis of Illudin-Ade from treated cells. HT-29 cells, provided by Professor Christophe Lacroix (Laboratory of Food Biotechnology, ETH Zurich), were originally obtained from the German Cell Culture Collection (Braunschweig, Germany). Cells were treated with varying concentrations of illudin for different time periods. Genomic cellular DNA was isolated with the Wizard® SV Genomic DNA Purification System and prepared for analysis as described in the experimental section. The resulting sample was analyzed by HPLC with a Phenomenex Synergi Polar-RP 80 Å column (250×4.60 mm, 4 μm particle size). The HPLC flow rate was 1.5 mL/min and the mobile phases were 3% acetonitrile and 0.1 % formic acid in water (v/v) (mobile phase A) and 0.1% formic acid in acetonitrile (v/v) (mobile phase B). The mobile phase gradient elution is as follows: 100% mobile phase A to 88% mobile phase A over 12 min, to 40% mobile phase A for 8 min, and hold at 40% for 0.5 min. Mobile phase A decreased to 0% over 1.5 min, and then return to starting conditions over 2 min and re-equilibrate for 10 min (34 min total run time). Fractions were collected from 1–25 min (1 fraction per 0.9 min, 27 total fractions), dried by rotary centrifugation, and reconstituted in 10 μL 50% methanol/50% water (v/v). Each fraction was analyzed (5 μL injection) by the quantitative SRM method described in the experimental section. Fractions collected over 1–2.8 min were combined and further analyzed by Dr. Cédric Bovet using nano-ESI-MS^3.

The nano-ESI source was set in positive ion mode with the following parameters: capillary temperature, 275 ^{o}C; voltage, 1.3 kV. MS^2 and MS^3 scan event parameters included: activation type, CID; minimum signal required, 500; isolation width, *m/z* 1.0; normalized collision energy, 35 V; activation Q, 0.25; activation time, 10 ms. MS^2 was performed on the most intense ion from the full scan, and MS^3 was carried out on the

most intense ion from the MS^2 scan event. Dynamic exclusion was enabled with a repeat count of 1, an exclusion duration of 20 s, and an exclusion list size of 200. Fractions collected over 1–2.8 min (from HT-29 cell sample preparation described above) were trapped on a Waters Symmetry C18 column (180 μm×20 mm, 5 μm particle size) at a flow rate of 5 μL/min for 3 min and separated on a 75 μm fused silica emitter packed with 80 mm Magic C18 AQ 3 um (Michrom Bioresources, USA) at a flow rate of 300 nL/min. Mobile phases A and B were 3% (v/v) acetonitrile and acetonitrile acidified with 0.1% (v/v) formic acid, respectively. The mobile phase gradient elution was as follows: 100% to 70% mobile phase A over 60 min, decrease to 55% mobile phase A over 10 min, decrease to 10% mobile phase A for 1 min and hold for 4 min, return to starting conditions over 1 minute, and hold at starting conditions for 14 min (90 min total run time).

Nano-ESI-MS^3 analysis of combined cellular DNA isolated from illudin-treated HT-29 cells. (A) Extracted ion chromatograph for *m/z* 384 from full scan. Arrow indicates peak corresponding to mass spectra in (B). (B) Mass spectra for peak in (A) at 20.09–21.11 min. The full scan spectra is in the top panel, MS^2 *m/z* 384.27 in the middle panel, and MS^3 *m/z* 384.27 → 336.34 in the bottom panel.